1963

Infrared spectra of N-monoaryl amides

Edgar William Day Jr.
Iowa State University

INFRARED SPECTRA OF N-MONOARYL AMIDES

by

Edgar William Day, Jr.

A Dissertation Submitted to the
Graduate Faculty in Partial Fulfillment of
The Requirements for the Degree of
DOCTOR OF PHILOSOPHY

Major Subject: Analytical Chemistry

Approved:

Signature was redacted for privacy.

In Charge of Major Work

Signature was redacted for privacy.

Head of Major Department

Signature was redacted for privacy.

Dean of Graduate College

Iowa State University
Of Science and Technology
Ames, Iowa

1963

TABLE OF CONTENTS

INTRODUCTION

The infrared spectra of monosubstituted amides have been extensively studied since the amide group, -CONH-, occurs in many biological materials and synthetic polymers. The majority of the work, however, has been confined to simple aliphatic amides and very little spectral information is available on aromatic secondary amides. Even in the aliphatic compounds, there is considerable disagreement as to the nature of the vibrations giving rise to absorptions characteristic of the amide group.

In the present investigation complete infrared spectral data were obtained for a number of substituted acetanilides. In addition, where possible, characteristic absorptions were assigned and structure interpretations made from the observed spectra. Deuterium and ^{15}N substitution in specific portions of the molecule aided in the characterization of vibrational modes involving significant hydrogen or nitrogen motion.

ORIGIN AND SIGNIFICANCE OF GROUP FREQUENCIES

Origin and Methods of Studying Infrared Spectra

Infrared spectra have their origin in transitions between rotational and vibrational levels in the ground electronic state of the molecule. Absorptions due to pure rotational transitions occur only in the far infrared though rotational fine structure is often observed in the infrared spectra of vapors. Vibrational transitions can most easily be discussed on the basis of a harmonic oscillator model. With such a model, Hooke's Law can be expected to hold at least approximately and the frequency of the vibrations of two atoms connected by a chemical bond is given by

$$\nu(cm^{-1}) = \frac{1}{2\pi c}\left(\frac{k}{\mu}\right)^{1/2}$$

where c is the velocity of light, k the force constant of the bond and μ the reduced mass of the two atoms. The expression for the reduced mass is

$$\mu = \frac{Mm}{M + m}$$

where M and m are the masses of the atoms involved in the vibration.

In complex molecules, the use of Hooke's Law cannot yield precise results since it neglects the effects of neighboring atoms as well as the anharmonicity resulting from a finite displacement of the atoms during the vibration. However, the concept permits the classification of absorption bands appearing in different spectral regions and gives some qualitative basis for predicting the direction of frequency shifts accompanying changes in masses of the atoms and relative bond strengths.

From the theory of molecular vibrations, non-linear molecules should possess 3n-6 fundamental vibrational modes, where n is the number of atoms in the molecule. Those vibrations which produce a change in the dipole moment of the molecule are "infrared active", while if no dipole moment change is produced, the vibration is "infrared inactive". Symmetry considerations provide a convenient and easy means of determining the general character of the vibrational modes of a molecule and the "activity" of those modes. It suffices to say here that in molecules of little or no symmetry, each of the vibrational modes is infrared active and thus gives rise to an infrared absorption band. In addition, absorptions due to whole number multiples and combinations of the fundamental bands could also be present. For example, acetanilide, which contains 19 atoms, will have 51 fundamental vibrations, all infrared active. Adding in the

combination and overtone bands the result is a spectrum of extreme complexity. Likewise, even minor changes in the structure of a molecule can have a profound effect on the spectrum. It is for this reason that the infrared vibrational spectrum has become one of the most characteristic physical properties of an organic compound.

There are several factors that have helped simplify the interpretation of the spectra of complex molecules, but the most prominent is probably the concept of group frequencies. It is now evident that compounds containing certain functional groups consistently give rise to absorptions in relatively narrow spectral regions. For example, molecules containing the carbonyl group possess an intense absorption in the 1600-1900 cm^{-1} region while the NH group consistently gives rise to absorptions in the 3100-3500 cm^{-1} region.

Most functional groups give rise to more than one absorption which can be used to identify or characterize the group. Atomic motions perpendicular to the bonds are permissible as well as stretching motions. Such vibrations are referred to as bending or deformation modes. For a given bond, the stretching vibration occurs at a higher frequency than a bending mode, since there is greater distortion of the electron distribution in the bond as it lengthens and contracts. The bond length is not appreciably changed during a bending vibration and thus less energy is

required.

There are two general methods of studying group frequencies in order to assign the vibrations involved. In the first method, infrared spectra are obtained for a large number of different compounds which contain the same functional group. These spectra are compared in order to determine a spectral region in which a band of similar intensity and shape occurs in all cases. A frequency range is then quoted for the common functional group. However, difficulties are sometimes encountered when all the compounds contain two or more common functional groups. In such cases, both groups may give rise to absorption bands in the same spectral region. For example, in substituted anilines, strong absorptions are observed near 1600 cm^{-1}. However, both the phenyl ring and the NH_2 group absorb strongly in this region and difficulty is experienced in making unequivocal assignments.

The second general method involves the use of isotopic substitution in the molecules. Such substitutions have little effect on the electronic distribution or the force constant of the bonds involved. As was seen earlier, however, the frequency of a vibration is strongly dependent upon the mass of the atoms as well as the force constant. Thus, isotopic substitution will cause the absorption frequencies of the substituted group to shift and permit positive identification of their absorption frequencies. In practice a

combination of these two general methods is often used to identify a frequency range for a given functional group.

Not only is the fact that a band shifts on isotopic substitution important, but the magnitude of the shift can also yield useful information. Assuming Hooke's law holds for a diatomic group and that the force constants are the same for the two isotopic species, the frequency ratio of a diatomic vibration will be given by

$$\frac{\nu}{\nu_i} = \left(\frac{\mu_i}{\mu}\right)^{1/2}$$

where the subscript i refers to the isotopically substituted molecule. Substituting the relation for the reduced mass into this equation yields

$$\frac{\nu}{\nu_i} = \left[\frac{M_i}{M}\left(\frac{M + m}{M_i + m}\right)\right]^{1/2}$$

Thus, by measuring an isotopic shift it is possible to determine whether a given vibration is restricted to the given group or if other factors are also operative. These factors will be discussed in more detail later.

Infrared dichroism is another technique which is of some value in making vibrational assignments on complex molecules. If a parallel beam of plain polarized infrared radiation is passed through an oriented crystal, the intensity of a given

absorption band will be at a maximum when the dipole moment of transition (usually termed transition moment) associated with the vibration is parallel to the electric vector of the radiation. If the light vector is perpendicular to the direction of dipole change, the absorption will be absent. More often, the absorbing group lies at a skew angle to the infrared beam and thus the intensity of the band varies with rotation of the electric vector but does not disappear. From the direction of maximum absorption it is possible to at least ascertain whether or not a given vibration is a possible assignment for the band. Usually the transition moments of several vibrations occur in approximately the same direction. Consequently, it is often necessary to use the other methods mentioned above to interpret fully the results of this type of study.

The concept of absorption bands arising solely from vibrations of functional groups is, of course, an over simplification. A given functional group will be found to absorb in a relatively small frequency range but the precise frequency in each compound is dictated by many factors. Some of these factors will be discussed in a general sense in the next part followed by a more specific discussion on the amide or peptide linkage.

General Factors Affecting Group Frequencies

The effects of change of state

At present, the factors which cause frequency shifts on changing the state of aggregation are only qualitatively understood. Thus, the increased association which occurs in passing from the vapor to the liquid to the solid state generally results in lower stretching frequencies and higher bending frequencies. Such shifts are generally small unless strong hydrogen bonds are formed. For example, it might be expected that the highly polarized carbonyl group would be strongly affected by the state of aggregation of the compound. However, the total shift on passing from the vapor to the solid state is usually of the order of 25 cm^{-1} unless hydrogen bonding is present in which case shifts of about 40-50 cm^{-1} are observed.

Frequency shifts caused by crystal packing are even less understood. In a rigid crystal, strong intermolecular forces are present and the group vibrations are affected by the nature of the unit cell. In some cases, in-phase and out-of-phase vibrations of the same group in two different molecules are set up, resulting in a splitting of the original single band. Similarly, different polymorphic forms may give rise to slightly different absorption frequencies for the same vibration. This is particularly true in the low frequency

region where the vibrations generally arise from skeletal modes of relatively large groups. A different type of crystal effect can occur with samples examined in the form of pressed alkali halide disks. Interactions have been observed between vibrations of the sample and vibrations of the alkali halide lattice. The degree of grinding of the sample and salt has also been noted to affect certain absorption bands.

Solvent effects

Unless hydrogen bonding is involved, only small frequency shifts are observed on passing from one solvent to another. For example, the carbonyl stretching frequency of a given compound in different non-polar solvents only varies a few wave numbers. However on changing the solvent from carbon tetrachloride to chloroform, shifts of 10-20 cm^{-1} are often observed. The absorption frequencies of essentially unpolarized bonds, such as C-C, are virtually independent of the solvent.

The causes of such shifts are imperfectly understood. For non-polar solvents, there seems to be a relationship between the size of the shift and the dielectric constant of the solvent, the higher frequencies occurring in the higher dielectric media. In polar solvents there is no apparent general relationship probably because of the existence of

solute-solvent interactions. Such interactions may result from specific association of a polar atom of the solvent with a group in the solute molecule or from general solvation of the solute molecules. At any rate, lower stretching frequencies are generally observed in polar solvents.

Hydrogen bonding

Hydrogen bonding is a special case of the molecular association mentioned above. However, this effect is quite large and merits some special attention.

The principal shifts occur in the stretching and bending frequencies of X-H bonds. The effect on the proton acceptor group is generally small, though if resonance stabilization is present, the effect could be large. Stretching frequencies are always lowered on hydrogen bonding since the electron density within the X-H bond has been decreased. This yields a lower force constant and therefore a lower stretching frequency. Bending frequencies, however, are shifted higher since the hydrogen bond tends to restrict motions at right angles to the bond.

Since stronger hydrogen bonds yield greater frequency shifts from the absorptions arising from unassociated molecules, infrared spectra have been used to estimate the strengths of hydrogen bonds and thus the distance between the atoms connected by the hydrogen bond. Non-linear

hydrogen bonds are generally found to be weaker than linear bonds since the shifts are smaller and the absorptions less intense. Intramolecular hydrogen bonds are nearly always non-linear.

Absorptions arising from hydrogen bonded species are generally quite broad and have a greater integrated intensity than the corresponding free absorptions. Often, too, there are sub-maxima present on the main absorption. These phenomena have been widely studied but no single theory has been proposed to fully account for them.

Electrical effects

Electrical effects are those factors which internally affect the electron distribution of the vibrating group. The inductive and mesomeric effects act along the bonds of the molecules while field effects result from non-bonded interactions.

If a change is made in the electronegativity of a substituent of a vibrating bond, the polarity, and therefore the frequency of the bond will be altered. This is the inductive effect. It is independent of the molecular geometry and depends only upon the electronegativities of the substituent atoms or upon the effective electronegativities of the substituent groups. For example, the carbonyl bond in acetone has some polar character and the oxygen atom carries some

negative charge. The electron cloud within the bond is apparently displaced from the geometric bond center towards the oxygen atom. If one of the methyl groups of acetone is now replaced by a highly electronegative substituent, such as chlorine, the electron cloud will be pulled back a little nearer the geometric center. Hence, the polar character is diminished and the carbonyl stretching frequency rises. If the methyl group is replaced by a more electropositive group, the vibrational frequency decreases. Such behavior suggests that frequency shifts from inductive effects alone should be related to the electronegativities of the substituents. It has been possible in a few simple cases to determine a linear relationship between absorption frequencies and Pauling electronegativities. With substituents, however, in which mesomerism is likely to be appreciable, the relation fails.

Mesomerism occurs in molecules having conjugated multiple bonds or in systems in which an atom with available lone-pair electrons is directly attached to a multiple bond. Generally speaking, resonance will cause a decrease in the bond orders of multiple bonds resulting in lower frequencies for the vibrations of these bonds. At the same time, single bond frequencies will generally increase. Mesomeric effects cannot be isolated from the inductive effects of the same substituent so both effects must be considered simultaneously.

Field effects arise from the close approach of charged

groups within a given molecule, due to the spatial arrangement of the atoms in the molecule. For example, in α-halogenated carbonyl compounds, the negatively charged halogen atom can be positioned fairly close to the easily polarized oxygen atom of the carbonyl group. Such a near approach results in mutual repulsion of the electrons from the atoms into their respective bonds. Thus higher frequencies are observed for both the C=O and C-Cl stretching frequencies than would have been predicted by considering only the inductive effect of the chlorine atom.

Mass and coupling effects

Mass effects are not easily studied since replacing one atom by another usually introduces other factors such as electrical effects. However, isotopic substitution permits the study of mass effects without significantly altering the force constants or electron distributions of the bonds. For example, replacement of hydrogen by deuterium in X-H bonds results in large frequency shifts due to the change in mass. Using the formula for calculating frequency ratios presented on page 6, the ratio of hydrogen to deuterium frequencies should approximate the square root of two. Thus, if a ratio of 1.3-1.4 is observed, the absorption in the undeuterated species can be safely assigned to an X-H mode.

However, many X-H absorptions do not shift by the

predicted amount. Such an observation indicates that either the X-H or the X-D mode is involved in vibrational coupling. This is frequently observed for bending modes. For example, in allene, the CH_2 stretching bands show a shift of 1.34 on deuteration (45) but the CH_2 deformation shifts by only 1.12. Moreover, the supposed C-C stretching frequencies, which should be only slightly affected, show shifts even larger than the CH_2 deformation bands. Thus, there is apparently an interaction between the two modes. When these interactions are studied theoretically, it is found that the vibrations are indeed "mixed", sometimes in the deuterium compound, sometimes in the normal compound and sometimes in both. It is therefore not proper to assign such absorptions to pure group vibrations, such as $\delta(CH_2)$* or ν(C-C), since the absorption actually involves both vibrations.

Such coupling of modes does not prevent them from being useful in correlation and structure work. A prime example of this is the case of the amide II and III bands which are characteristic of open-chained secondary amides. Both bands arise from vibrations involving both δ(NH) and ν(C-N) and possibly other modes. However, within the constant

---

*The use of Greek letters to describe vibrations is common in works of this nature. In this symbolism, ν represents a stretching vibration, δ an in-plane deformation, γ an out-of-plane deformation, τ a torsional mode and r a rocking vibration.

environment of the molecules, the degree of coupling is reasonably constant and characteristic frequencies result.

There are four requirements for strong coupling to occur between vibrational modes. (1) The vibrating atoms must be close to one another in the molecule; (2) the group frequencies should be approximately equal; (3) there must be strong forces between the vibrating groups and (4) the vibrations must lie in the same symmetry class. This fourth requirement is extremely important for such highly symmetrical molecules as benzene, acetylene and carbon tetrachloride but is easily satisfied for molecules with very low symmetry. In such cases, interactions are more generally permitted.

The -CONH- Group

Theoretically, secondary amides can exist in either the keto or the enol form. Each would be stabilized by resonance with a dipolar form.

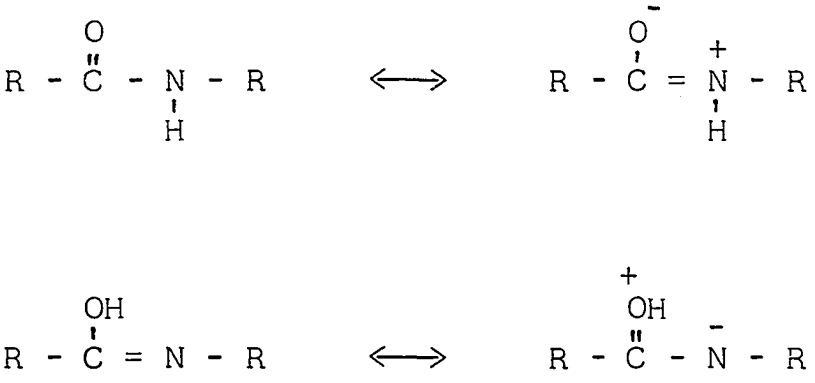

Indeed, certain early workers did postulate the existence of an enol form for simple amides, but later X-ray measurements indicated that the occurrence of the enol form is very unlikely. The fact that no infrared absorption exists which can reasonably be assigned to an OH mode is also indicative of the absence of the enol form. Thus, the ketonic structure is now universally accepted for secondary amides.

Since the amide linkage is stabilized by resonance, the four atoms in the group are probably co-planar. The presence of partial double bond character in the C-N bond restricts rotation about this bond permitting the possible existence of structural isomers of the cis-trans type. Thus, the oxygen and hydrogen atoms could be positioned

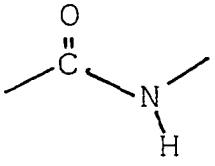

trans

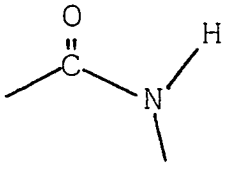

cis

on the same or on opposite sides of the C-N bond. It will be seen later that these two isomers can give rise to equivalent vibrations of slightly different frequencies.

The vibrational modes expected for the amide group are the NH stretching (ν(NH)), the NH in-plane (δ(NH)), and out-of-plane (γ(NH)) bending, the carbonyl stretching (ν(C=O)), the C-N stretching (ν(C-N)) and the OCN in-plane (δ(O=C-N)) and out-of-plane (γ(O=C-N)) bending modes. The descriptions of these vibrations are somewhat arbitrary since mixing of vibrations is well known in amides. However, for the purpose of discussion, these names do provide a convenient means of identifying the predominant motions.

The physical state in which an infrared spectrum is obtained is probably more important for amides than for most types of organic molecules. For example, the NH stretching bands lie 100-150 cm^{-1} lower in the solid state than in solution. Similarly, the carbonyl stretching frequency in the solid state is usually about 40 cm^{-1} lower than the corresponding solution frequency. These large frequency changes

are generally ascribed to the formation of relatively strong hydrogen bonds of the -N-H---O=C type. It is also interesting to note that there is a considerable difference between the behavior of OH and NH groups with changes of state. With increasing concentration in solution, the NH stretching bands move gradually to lower frequencies as opposed to the larger and more discrete shifts of OH absorptions. This has led various workers to suggest mechanisms other than hydrogen bonding for the association which occurs in amides. Cannon (11), for example, has suggested that dipole-dipole interactions of the $^{-}OCN^{+}$ groups account for the relatively large shift in ν(C=O) on association. Such an alignment of dipoles does not permit hydrogen bonding and the relatively small shift of the free NH stretching bands, as compared to OH, on association is due to a pure coulombic attraction between the amide hydrogen and oxygen atoms.

The amide linkage is a conjugated system and anything that changes the relative contributions of resonance structures will have some effect of the group frequencies. The carbonyl stretching frequencies of simple secondary amides are appreciably lower than those of normal ketones. This must be due to resonance with the dipolar form shown on page 15b. Replacement of an N-alkyl substituent with a N-aryl group causes a decrease in the polarity of the carbonyl bond since both the phenyl ring and the carbonyl group compete

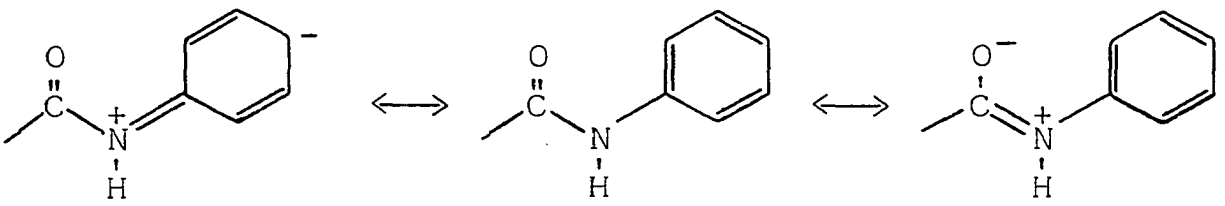

for the nitrogen labile electrons. Thus, the carbonyl stretching frequencies in N-monoaryl amides are higher than in N-monoalkyl amides. Substituting various functional groups onto the phenyl ring causes further displacements of the characteristic amide group frequencies.

Substitution of an aromatic nucleus onto the amide nitrogen, however, also introduces steric factors which must be considered. X-ray crystallographic studies (8) have shown that if acetanilide were a planar molecule the hydrogen atom on C_6 and the oxygen atom would be impossibly close. The

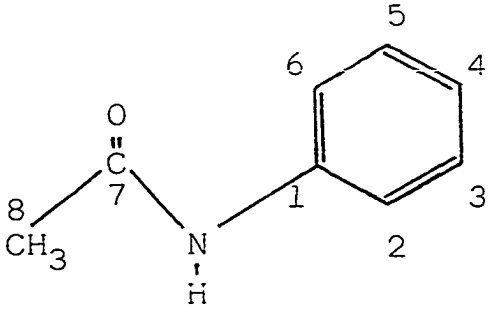

situation is relieved in three ways. (1) The C_6 and H_6 atoms are depressed out of the plane of the phenyl ring, (2) the angle at C_1NC_7 is increased from 120° to about 129°, and (3) the acetyl group is rotated about the C_1N bond. The

calculations of Brown and Corbridge (8) actually showed that the plane through N, C_7, O, and C_8 intersects at an angle of 37°54' with the plane through C_1, C_2, C_3, C_4, C_5, and N.

This close approach of the oxygen atom and H_6 suggests that steric factors may be quite important for acetanilides, especially the ortho-substituted derivatives. For such compounds, the two ortho positions are probably not equivalent and structure A is probably preferred in most cases. If the

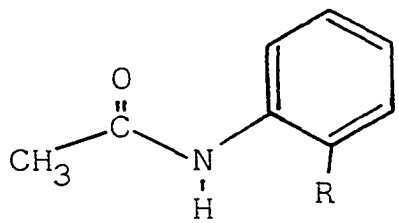

(A)

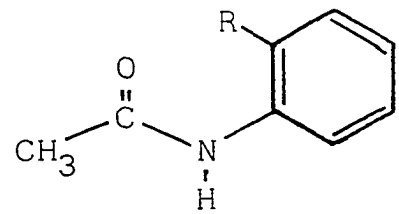

(B)

molecules do exist in the B form, the carbonyl group is undoubtedly forced further out of the plane of the phenyl ring. This would destroy the increased resonance stabilization supplied by the ring and might give rise to slightly different group frequencies.

It is obvious from structure A that the nature of the R group will have a marked influence on those infrared absorptions arising from the NH bond. Strongly electronegative groups will have an attractive influence on the hydrogen atom and tend to lower the NH stretching frequencies. Indeed,

intramolecular hydrogen bonding may even occur as in the case of o-nitroacetanilide. Contrarily, certain groups like the methyl group could have a repulsive influence, thus shortening the NH bond and increasing its stretching frequencies. These effects would be similar to the dipole interactions discussed previously for α-halogen ketones.

The effect of deuteration on X-H absorptions as discussed previously applies equally well to N-H absorptions, but it seems pertinent to mention the effects of another isotope, nitrogen-15. Since most of the atomic motion involved in an X-H vibration occurs in the hydrogen atom, nitrogen-15 substitution will have very little effect on such vibrations. Indeed, using the formula presented on page 6, the ratio of a nitrogen-15 absorption frequency to that of the normal species should be only 1.002. However, in a vibration involving the C-N bond, both atoms contribute approximately the same amplitude to the vibration and a larger effect should be observed. Theoretically, the ratio $\nu(C-^{14}N) / \nu(C-^{15}N)$ should be 1.015 if there is no coupling present. These absorptions generally occur in the spectral region where vibrational coupling is common, however, and the theoretical shift is seldom observed. The size of the shift, though, still yields useful information concerning the nature of the vibrational mode.

EXPERIMENTAL

Preparation of Materials

A list of the compounds studied in this investigation is presented in Table 1 along with their observed melting points. A number of compounds were deuterated and this is also indicated in the table. The melting points of isotopic derivatives were not recorded.

Table 1. Melting points and deuterium derivatives prepared of the N-monoaryl amides studied

Compound	Melting point (°C)		Deuterium derivatives prepared
	lit.[a]	obs.	
Acetanilide	114	114	yes
Benzanilide	163	163 - 164	yes
Hexananilide	95	97	yes
p-Aminoacetanilide	162 - 163	164 - 165	yes
p-Bromoacetanilide	168	168 - 169	no
p-Chloroacetanilide	178	179	yes
p-Hydroxyacetanilide	168	168 - 169	no

[a]These melting points were obtained from various handbooks and dictionaries of organic compounds.

Table 1. (Continued)

Compound	Melting point (°C)		Deuterium derivatives prepared
	lit.[a]	obs.	
p-Iodoacetanilide	184	184 - 185	no
p-Methoxyacetanilide	130 - 132	130 - 131	yes
p-Methylacetanilide	146 - 147	150 - 151	yes
p-Nitroacetanilide	215	215	yes
m-Aminoacetanilide	87 - 89	88 - 89	no
m-Bromoacetanilide	87½	86½- 87	no
m-Chloroacetanilide	72½	73 - 74	yes
m-Hydroxyacetanilide	148 - 149	147 - 148	no
m-Methylacetanilide	65½	67 - 68	yes
m-Nitroacetanilide	154 - 156	151 - 152	yes
o-Bromoacetanilide	99	102 - 103	no
o-Chloroacetanilide	87 - 88	87 - 88	yes
o-Fluoroacetanilide	80	78 - 79	no
o-Hydroxyacetanilide	209	209½	no
o-Methoxyacetanilide	87 - 88	87 - 88	yes
o-Methylacetanilide	110	110 - 111	yes
o-Nitroacetanilide	93	93	yes
2,6-Dibromoacetanilide	210	205 - 206	yes
2,6-Dimethylacetanilide	177	180 - 181	no

The procedures used in preparing some of these materials are described below. Those not discussed were purchased from either Distillation Products Industries, Rochester, New York, or K and K Laboratories, Inc., Jamaica, New York. All compounds obtained commercially were recrystallized prior to spectroscopic investigation. Dilute ethanol was the solvent most often used for recrystallization. The source of nitrogen-15 was isotopically labeled ammonium sulfate containing greater than 97 atomic percent of nitrogen-15. The amines, acids, and acid chlorides used in the preparations below were generally products of one of the chemical suppliers mentioned above. The hexananilide-^{15}N and benzanilide-^{15}N used was the same material prepared by Gray (28).

Acetanilide-^{15}N

Acetanilide-^{15}N was prepared by the same method as Gray (28) except that liquid bromine was used instead of chlorine in the Hofmann degradation of benzamide-^{15}N.

o-Nitroacetanilide-^{15}N and p-nitroacetanilide-^{15}N

When acetanilide is nitrated with nitric acid, the nature of the solvent has a profound effect on the relative amounts of the ortho and para isomers formed. If acetic or sulfuric acid is used as the solvent, nitration takes place almost exclusively at the para position, but if the nitration

is carried out in acetic anhydride, the ortho isomer predominates (2). Since the ortho isomer was of primary interest, acetic anhydride was chosen as the solvent. The experimental procedure employed was in part similar to that suggested by Arnall and Lewis (2).

One-half gram of acetanilide-^{15}N was dissolved in 9.0 ml of pure acetic anhydride and 0.23 ml of concentrated nitric acid was dissolved in 1.0 ml of the same solvent. The two solutions were mixed and allowed to stand at room temperature for three hours. At the end of this period, 20 ml of water was added and the mixture warmed slightly until it became homogeneous. Then cold concentrated sodium hydroxide solution was added with cooling and stirring. After several milliliters were added, a yellow fluffy precipitate formed which was filtered by suction. More alkali was added to the filtrate and more solid formed. When the solution was just barely acidic, it was filtered again, the residue being combined with that obtained above. The combined solids were air-dried. Then about 10 ml of water was added and the mixture was heated to 80°C. At this temperature, o-nitroacetanilide is water soluble but the para isomer is not. The mixture was filtered while hot and the filtrate was cooled. The yellow-orange needles of o-nitroacet-^{15}N-anilide were filtered and the filtrate was concentrated to obtain a second crop of crystals. The yield was about 50%.

The residue from the hot aqueous solution above was added to a dilute hydrochloric acid solution to remove any anilines present and filtered. The residual orange solid was recrystallized from a large quantity of water and dried at 140°. The yield of p-nitroacet-^{15}N-anilide was about 6%.

o-Chloroacetanilide-^{15}N

This material was prepared by the same procedure used for acetanilide-^{15}N. The o-chlorobenzoyl chloride used was prepared by reflexing o-chlorobenzoic acid with thionyl chloride, the excess chlorinating agent being removed by fractional distillation.

o- and m-Bromoacetanilide

These compounds were prepared by acetylating the corresponding amines according to standard procedures (65).

m-Hydroxyacetanilide

The procedure used was that described by Ikuta (34). A 10% excess of acetic anhydride was added to one gram of m-aminophenol. Dissolution occurred immediately but after a few minutes, colorless needles formed. The crystals were collected, recrystallized from water and dried at 110°C. The yield of pure material was about 80%.

2,6-Dibromoacetanilide

The method of preparing this material was devised from the suggestions of Smith and Orton (66). One gram of 2,6-dibromoaniline was dissolved with vigorous agitation in about 10 ml of acetic anhydride. Four drops of concentrated sulfuric acid were added with continuous stirring. A white solid formed immediately. The mixture was allowed to stand at room temperature for two hours after which it was poured into 100 ml of water and warmed slightly to hydrolyze the excess acetic anhydride. The anilide was removed by filtration, recrystallized from dilute ethanol and dried at 140°C. The yield was about 60%.

Liberation of m-aminoacetanilide from its hydrochloride

m-Aminoacetanilide hydrochloride was a commercially available product while the free amine was not. The amine was liberated from its hydrochloride salt by modifying the procedure of Jacobs and Heidelberger (35). Concentrated sodium hydroxide solution was added to a water slurry of the hydrochloride. On heating, a red-brown oil formed on top of the solution which hardened on cooling. The aqueous layer was decanted and the residual mass was washed quickly with a little water. The solid oil was then dissolved in hot benzene. The hot benzene solution was decanted from a few

dark droplets which had settled to the bottom of the beaker. On cooling, a fluffy white precipitate formed, which was filtered, recrystallized from benzene and air-dried.

Preparation of deuterium-containing derivatives

Deuteration in this investigation was accomplished by exchanging the anilide in a dioxane-deuterium oxide solution. The deuterium oxide was obtained from the Liquid Carbonic Division of the General Dynamics Corporation, San Carlos, California and contained 99.5% D_2O. About 0.5-1.0 gm of the anilide was dissolved in 1-5 ml of purified dioxane. About 1-2 ml of deuterium oxide was added and the solution was allowed to stand for at least 12 hours. The excess liquid was evaporated under a vacuum and the solid was freeze dried. The same procedure was then repeated. Five such exchanges were generally sufficient to obtain greater than 90% deuteration. The ortho-substituted acetanilides were more difficult to deuterate and often no more than 85% exchange could be accomplished even after several addition exchanges. All deuterated materials were handled in an atmosphere of dry nitrogen to prevent back-exchange with atmospheric water vapor which occurs rather rapidly.

The dioxane was purified prior to use to remove the water, acetal and aldehyde present in the commercial product. The dioxane was refluxed over sodium metal for two days. A

gummy red-brown solid which formed was removed by filtration and the dioxane was stored over sodium metal.

Spectroscopic Investigation

All infrared spectra were recorded on a Beckmann IR-7 prism-grating Spectrophotometer. For the 4000-600 cm^{-1} region, sodium chloride optics were used. An interchange equipped with a cesium iodide prism was used to record the 700-200 cm^{-1} spectral region. The factory calibration was periodically checked against atmospheric water and carbon dioxide bands.

Solid state spectra were obtained by pressing a mixture of finely ground sample and powdered potassium bromide to form a small disk. Normally about 1-3 mg of sample added to about 300 mg of potassium bromide was sufficient to produce a satisfactory spectrum. The spectra shown in Figures 1-26 were obtained from such disks. These disks were also used in the low frequency region. Potassium bromide, however, absorbs below 275 cm^{-1} so no useful data were obtained below this frequency.

In order to obtain data on the compounds in the unassociated state the spectra of most of the compounds were also run in carbon tetrachloride and dibromomethane solutions. In some cases chloroform was used as a solvent. However, it was

found that the deuterated amides exchanged very rapidly with chloroform and thus the usefulness of this solvent was limited.

For the undeuterated compounds, no prior purification of the solvents was deemed necessary. However, before running spectra of the deuterated species in solution, the solvents were dried with and stored over anhydrous sodium sulfate.

The anilides studied exhibited vastly different solubilities in dibromomethane and carbon tetrachloride. Most were sufficiently soluble in dibromomethane to obtain a good spectrum in either 0.1 or 0.2 mm cells. Notable exceptions were the hydroxyacetanilides, p-amino- and p-nitroacetanilide, which yielded only weak spectra even with saturated solutions in 0.8 mm cells. In carbon tetrachloride, only the ortho-substituted acetanilides and m-chloro- and m-methylacetanilide were sufficiently soluble to give good spectra in cells of short path-length. Only very weak spectra were obtained from saturated carbon tetrachloride solutions of the para-substituted acetanilides in 0.8 mm cells and the hydroxy-acetanilides, p-amino, p-nitro- and 2,6-dimethylacetanilide, were almost completely insoluble in carbon tetrachloride.

The observed solid state and solution absorption frequencies of the compounds studied are listed in the Appendix. The frequencies are given to the nearest wave number and are estimated to be accurate to ± 3 wavenumbers above 2000 cm^{-1}

and to ±2 wavenumbers below 2000 cm^{-1}. Two or more spectra were obtained for all the compounds under the same conditions and the average frequencies are reported. All frequencies and intensities below 650 cm^{-1} were taken from spectra recorded with the instrument equipped with cesium iodide optics.

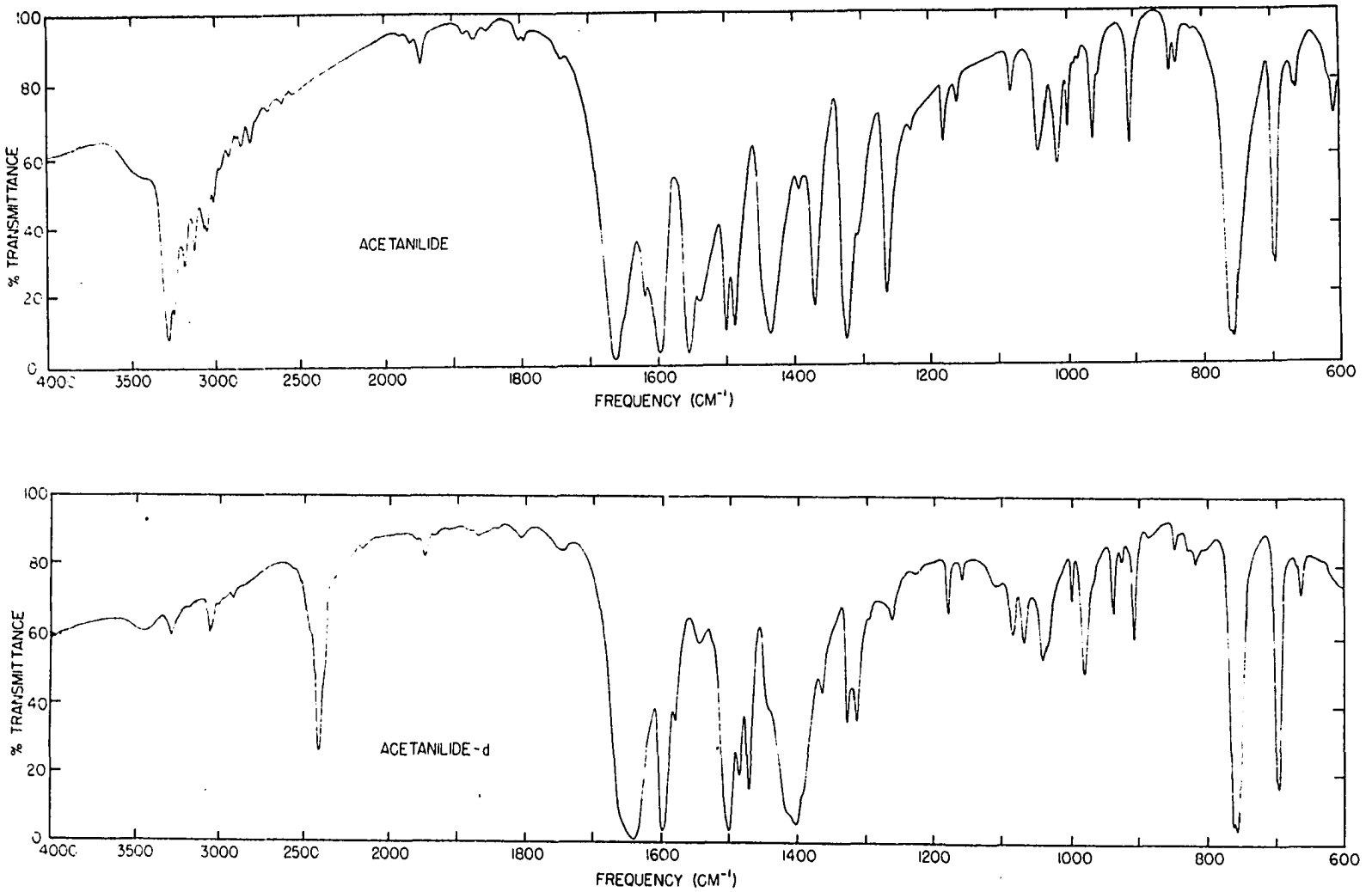

Figure 1. Potassium bromide disk spectra of acetanilide and deuterated acetanilide

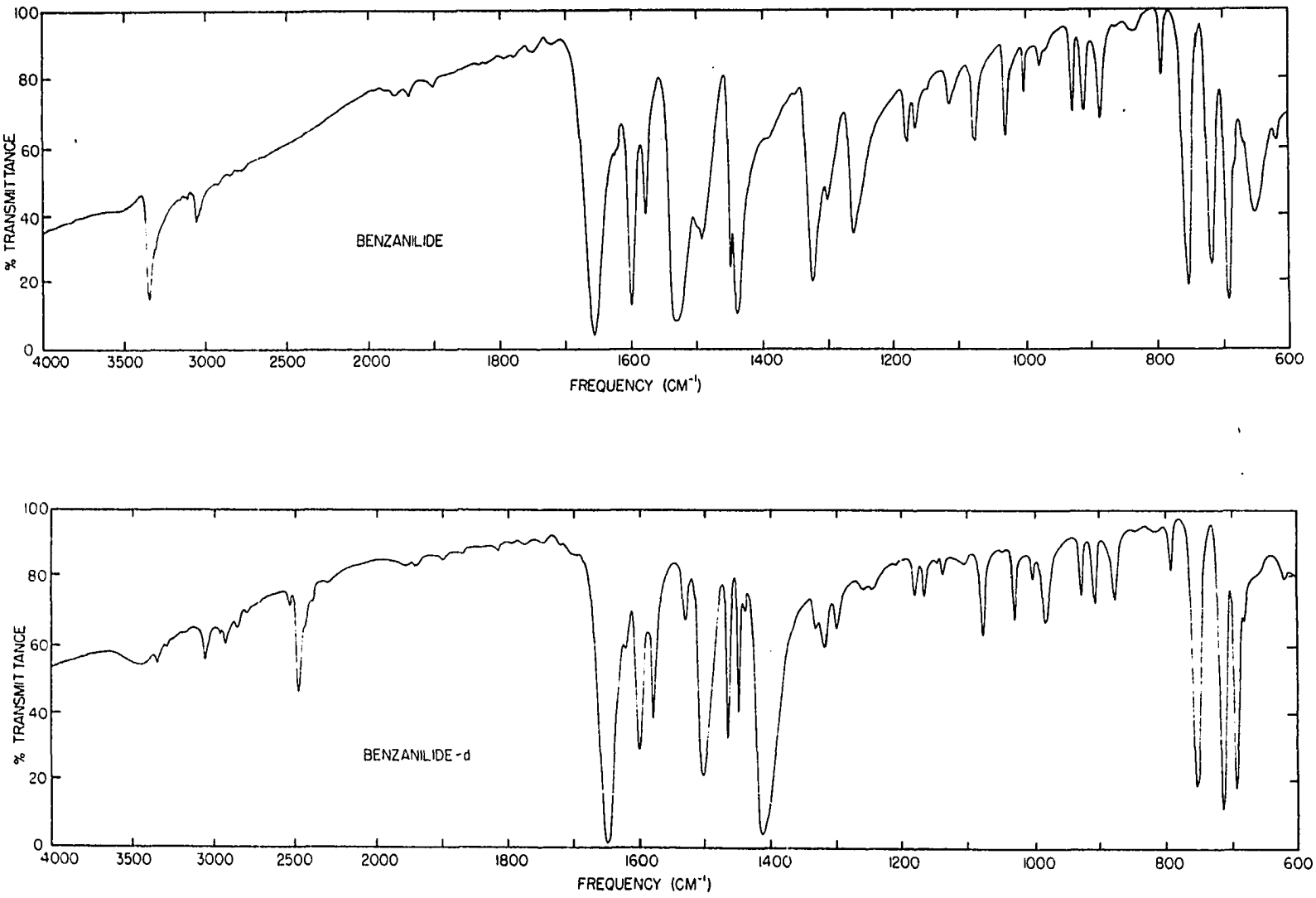

Figure 2. Potassium bromide disk spectra of benzanilide and deuterated benzanilide

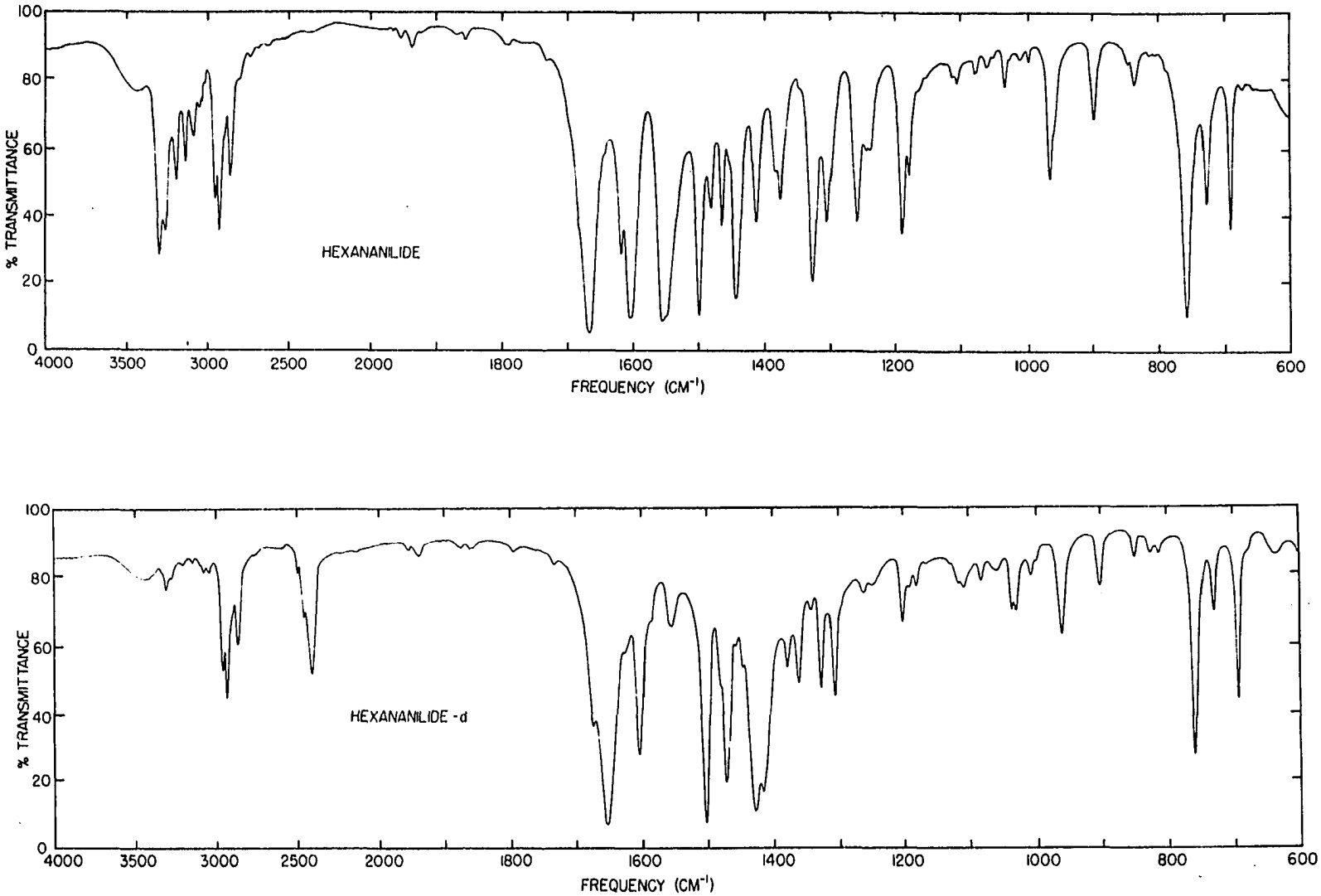

Figure 3. Potassium bromide disk spectra of hexananilide and deuterated hexananilide

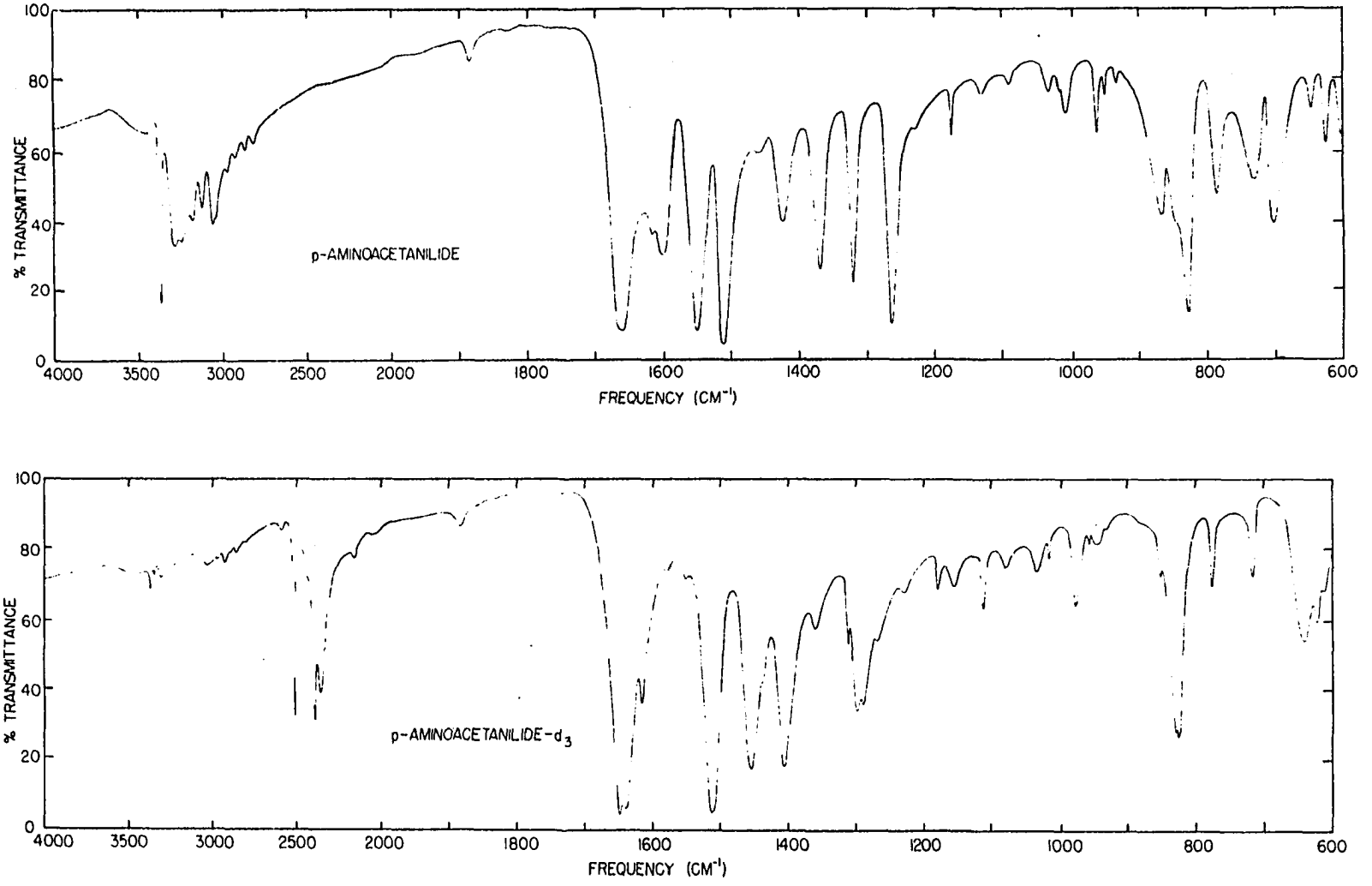

Figure 4. Potassium bromide disk spectra of p-aminoacetanilide and deuterated p-aminoacetanilide

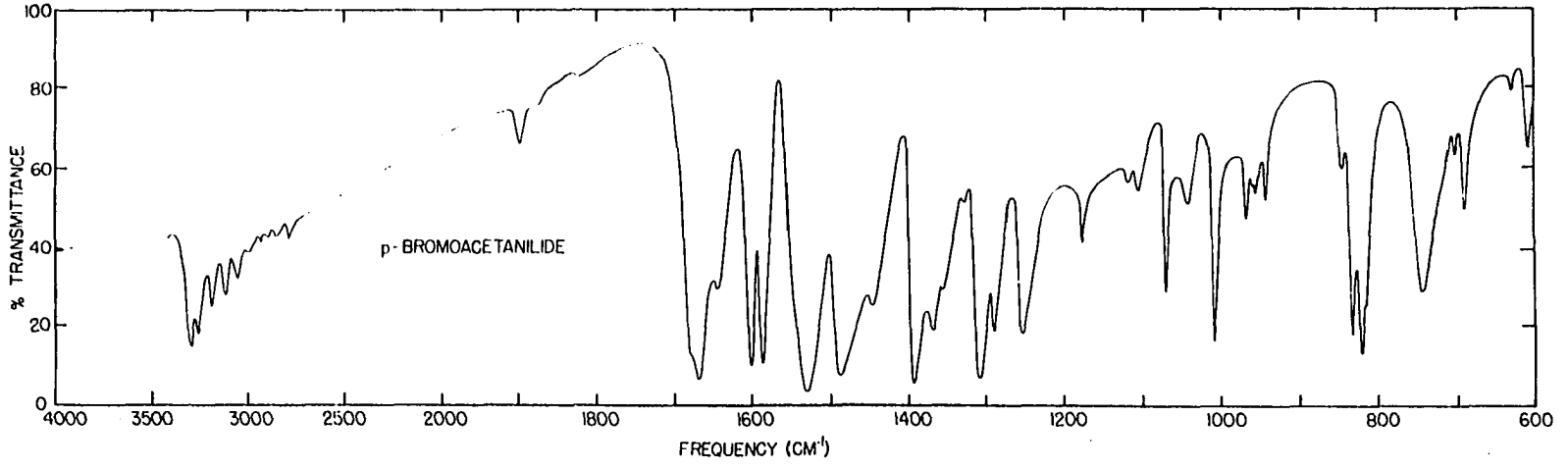

Figure 5. Potassium bromide disk spectrum of p-bromoacetanilide

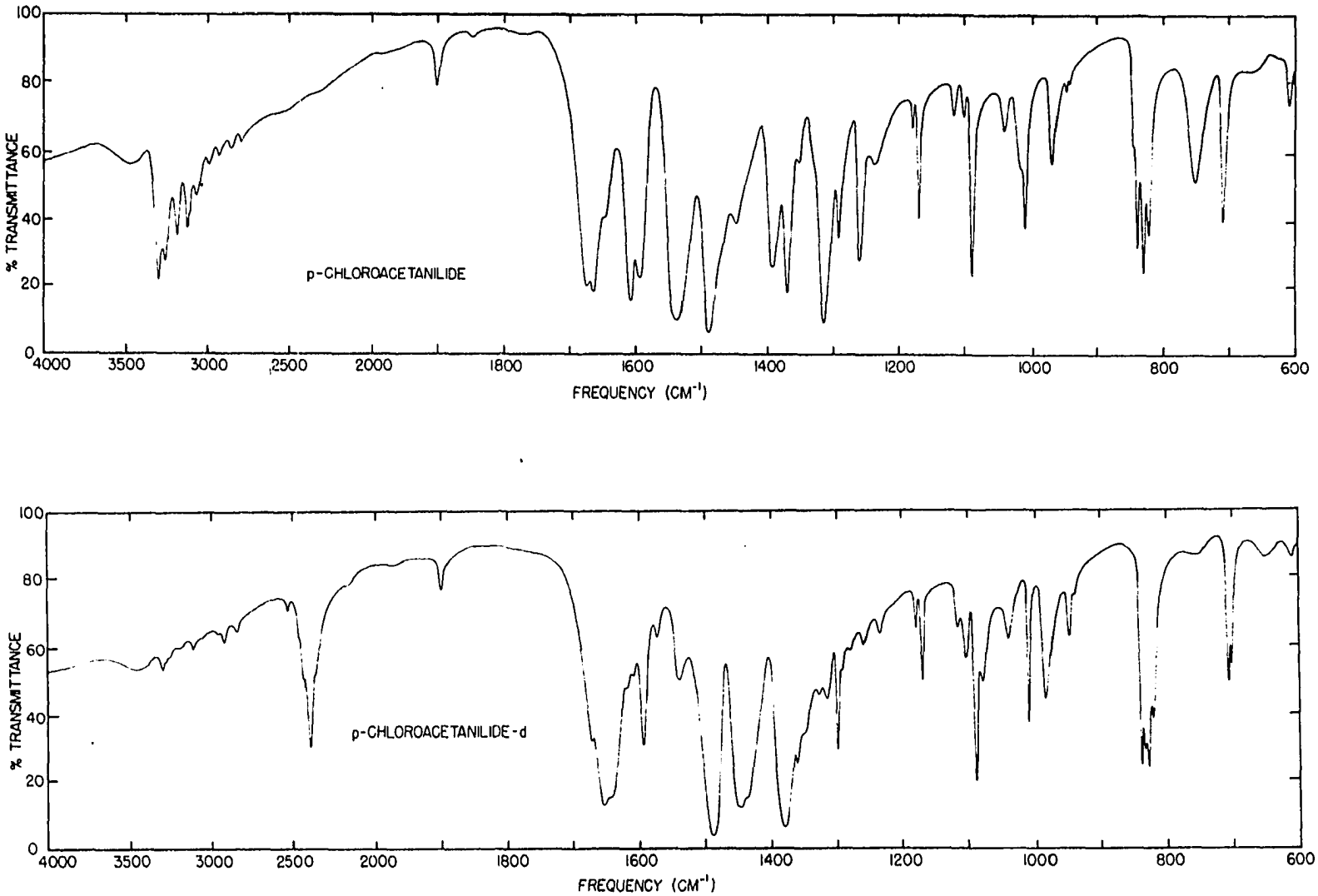

Figure 6. Potassium bromide disk spectra of p-chloroacetanilide and deuterated p-chloroacetanilide

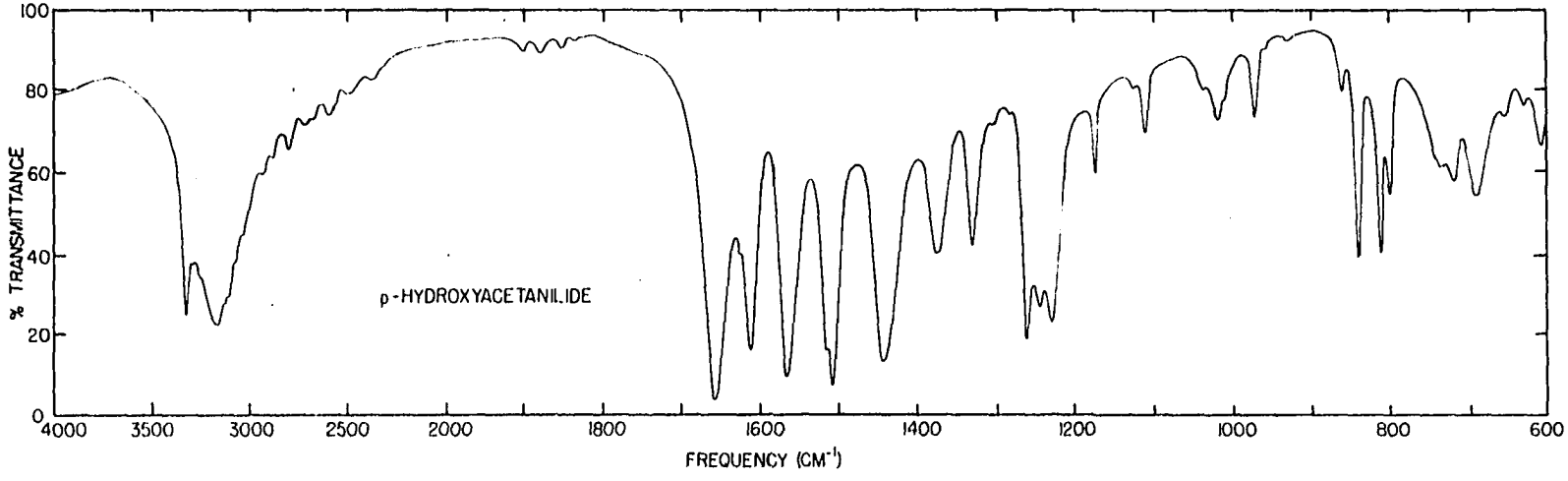

Figure 7. Potassium bromide disk spectrum of p-hydroxyacetanilide

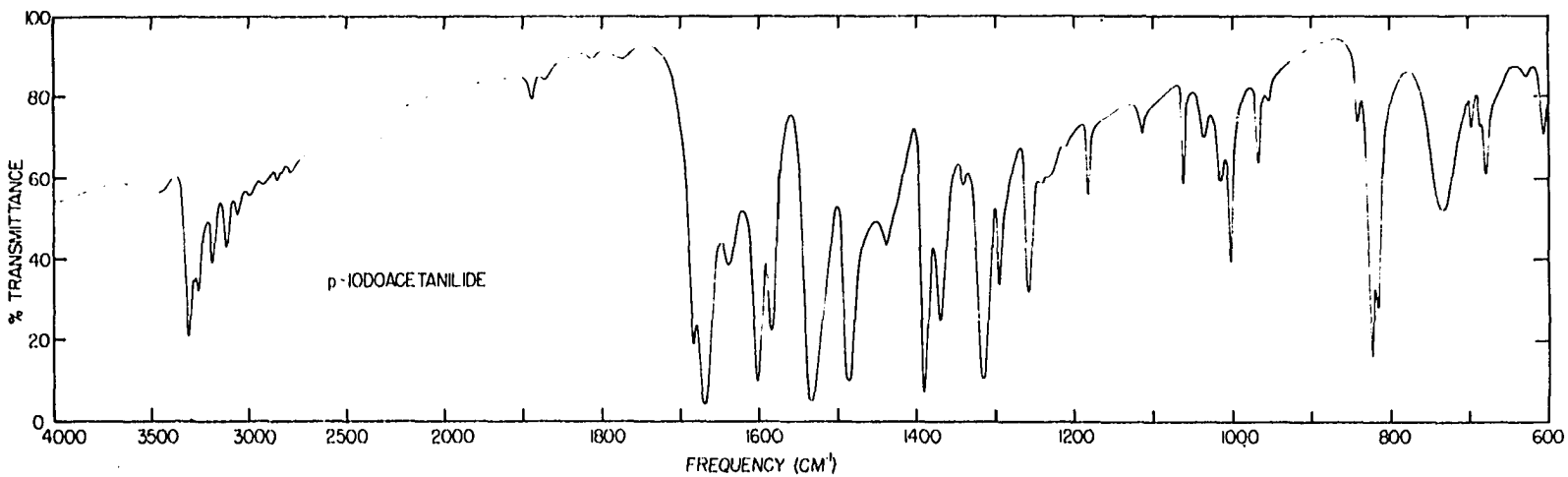

Figure 8. Potassium bromide disk spectrum of p-iodoacetanilide

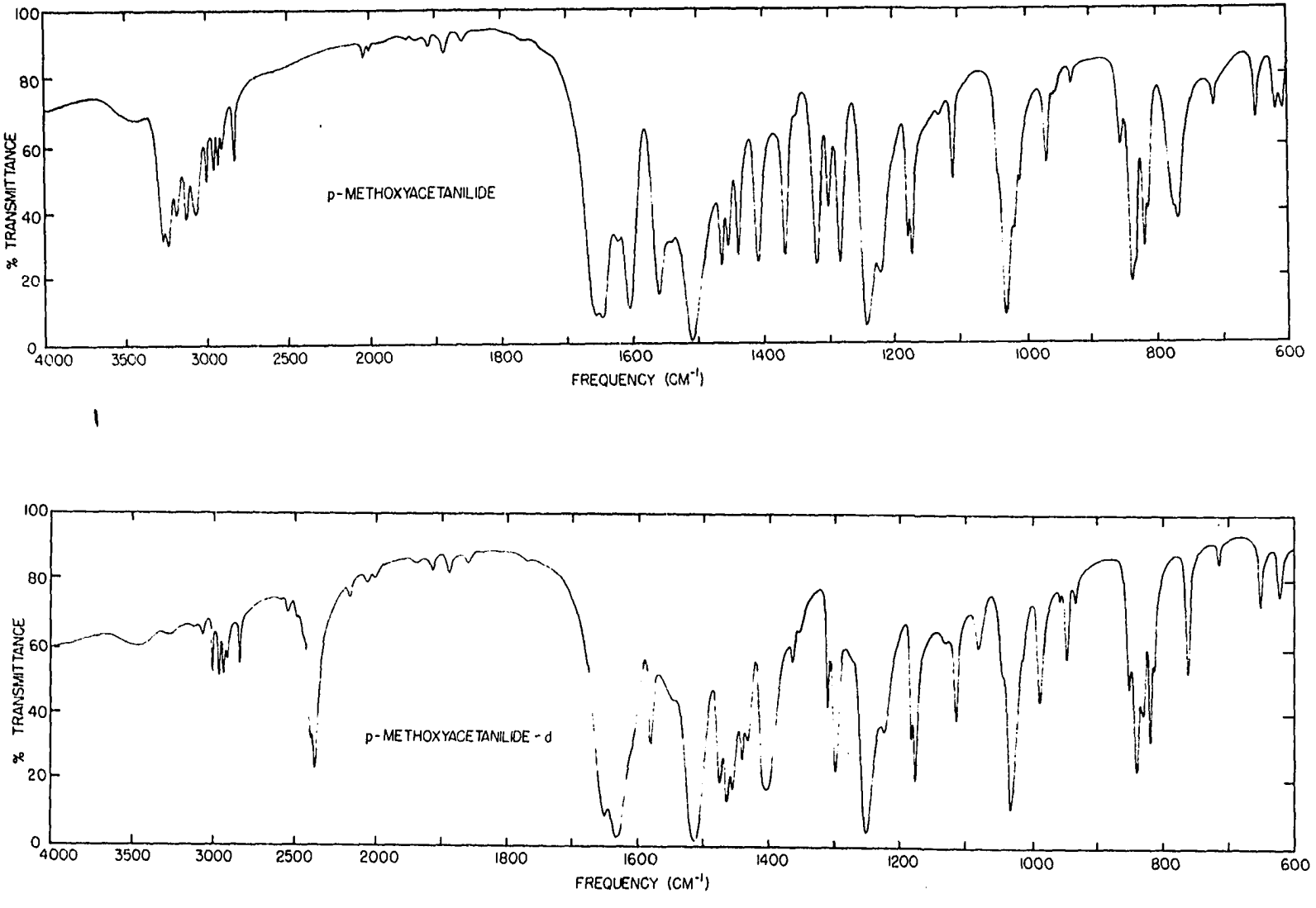

Figure 9. Potassium bromide disk spectra of p-methoxyacetanilide and deuterated p-methoxyacetanilide

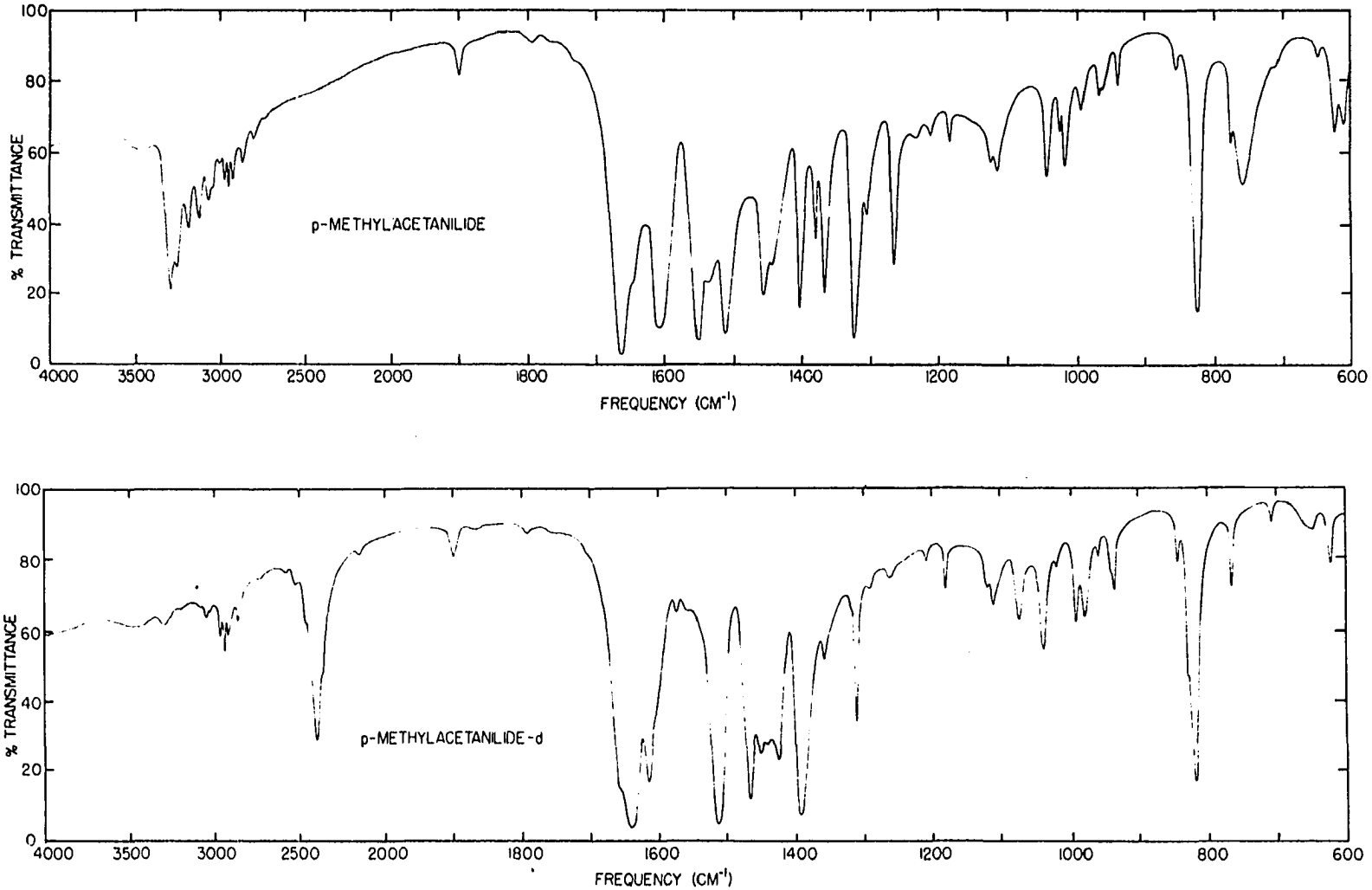

Figure 10. Potassium bromide disk spectra of p-methylacetanilide and deuterated p-methylacetanilide

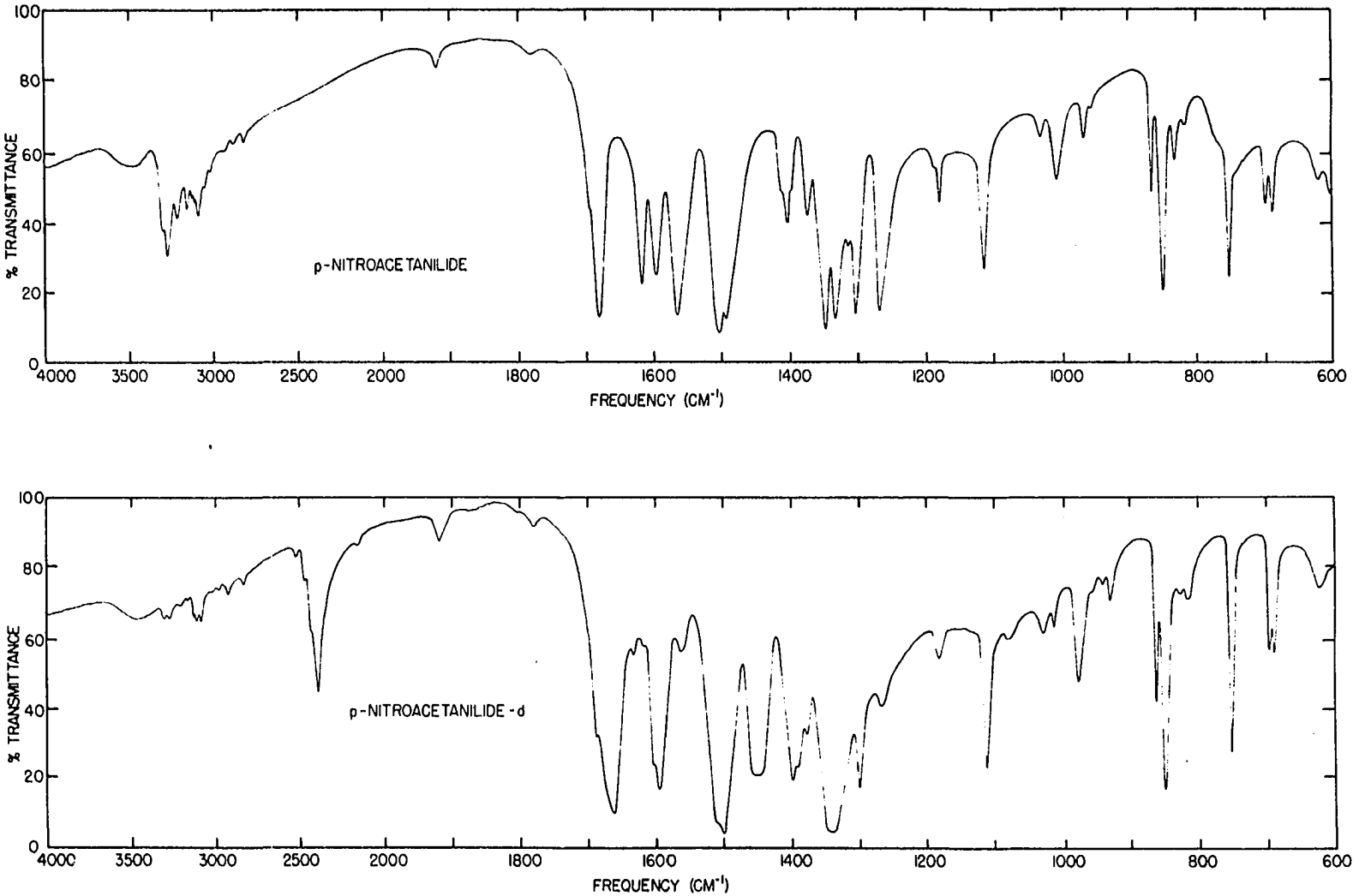

Figure 11. Potassium bromide disk spectra of p-nitroacetanilide and deuterated p-nitroacetanilide

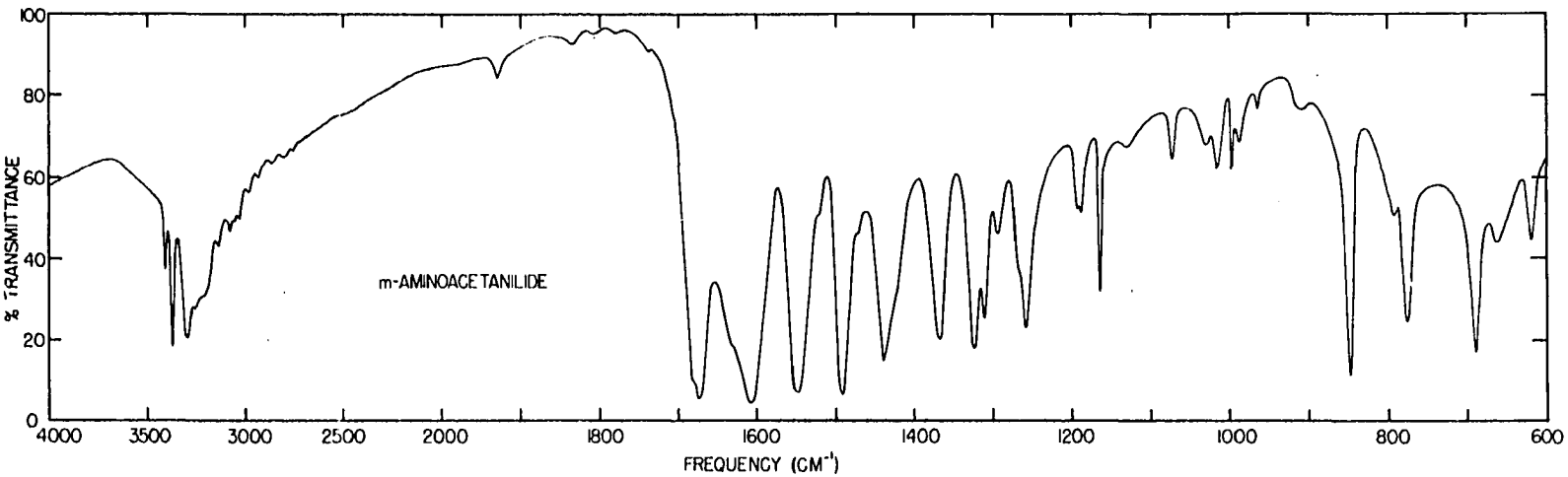

Figure 12. Potassium bromide disk spectrum of m-aminoacetanilide

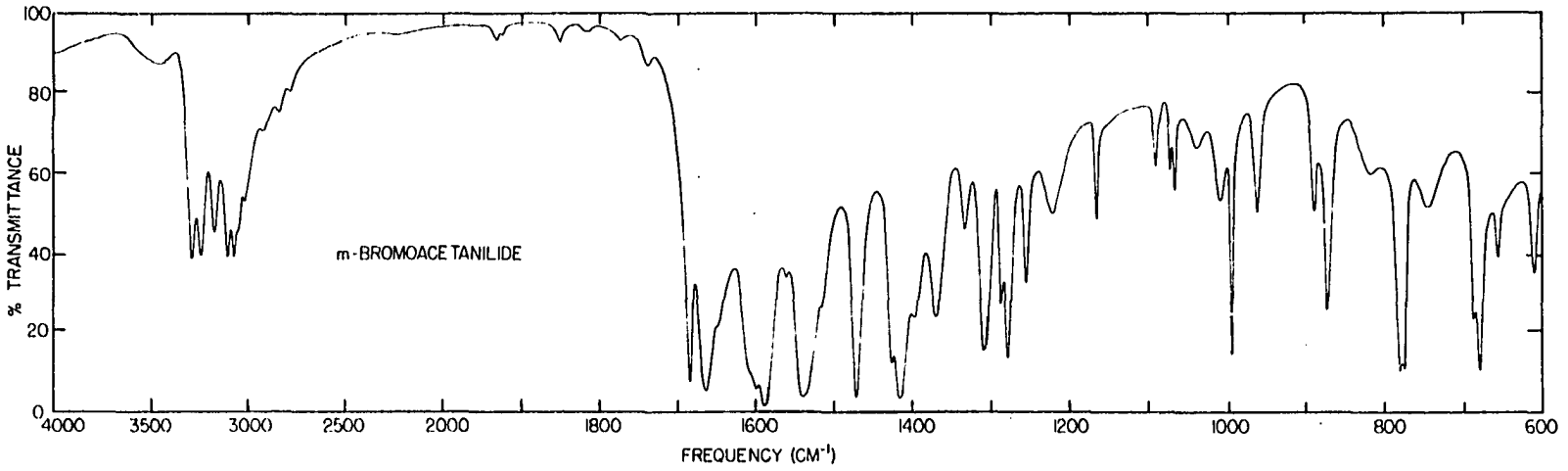

Figure 13. Potassium bromide disk spectrum of m-bromoacetanilide

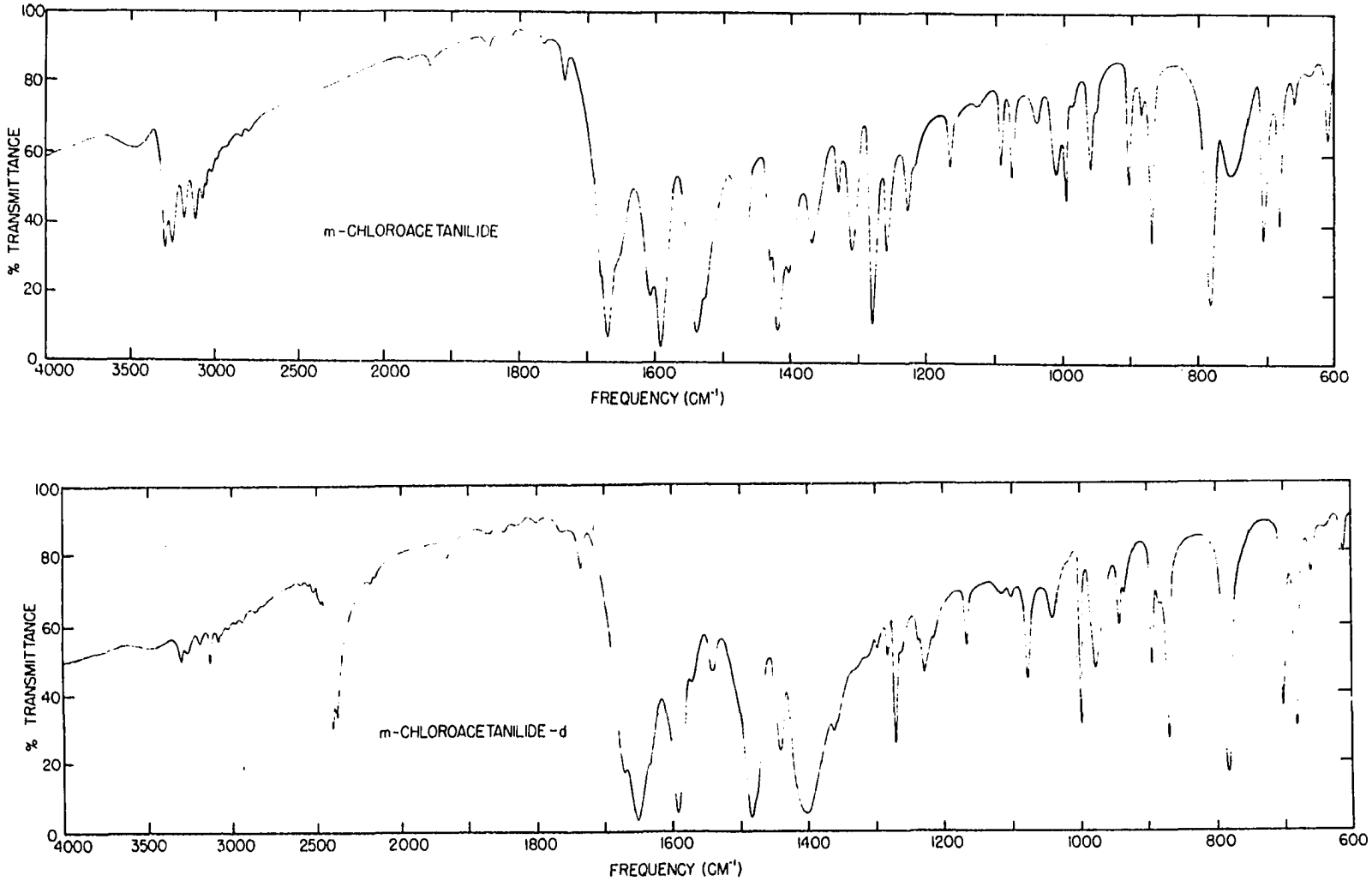

Figure 14. Potassium bromide disk spectra of m-chloroacetanilide and deuterated m-chloroacetanilide

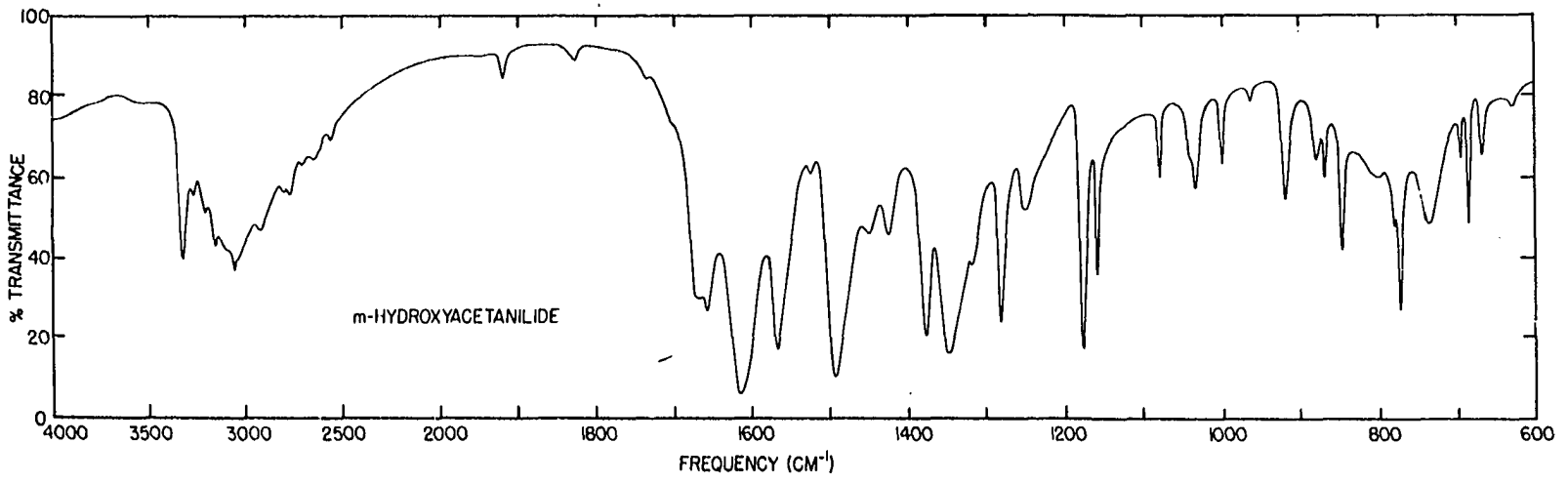

Figure 15. Potassium bromide disk spectrum of m-hydroxyacetanilide

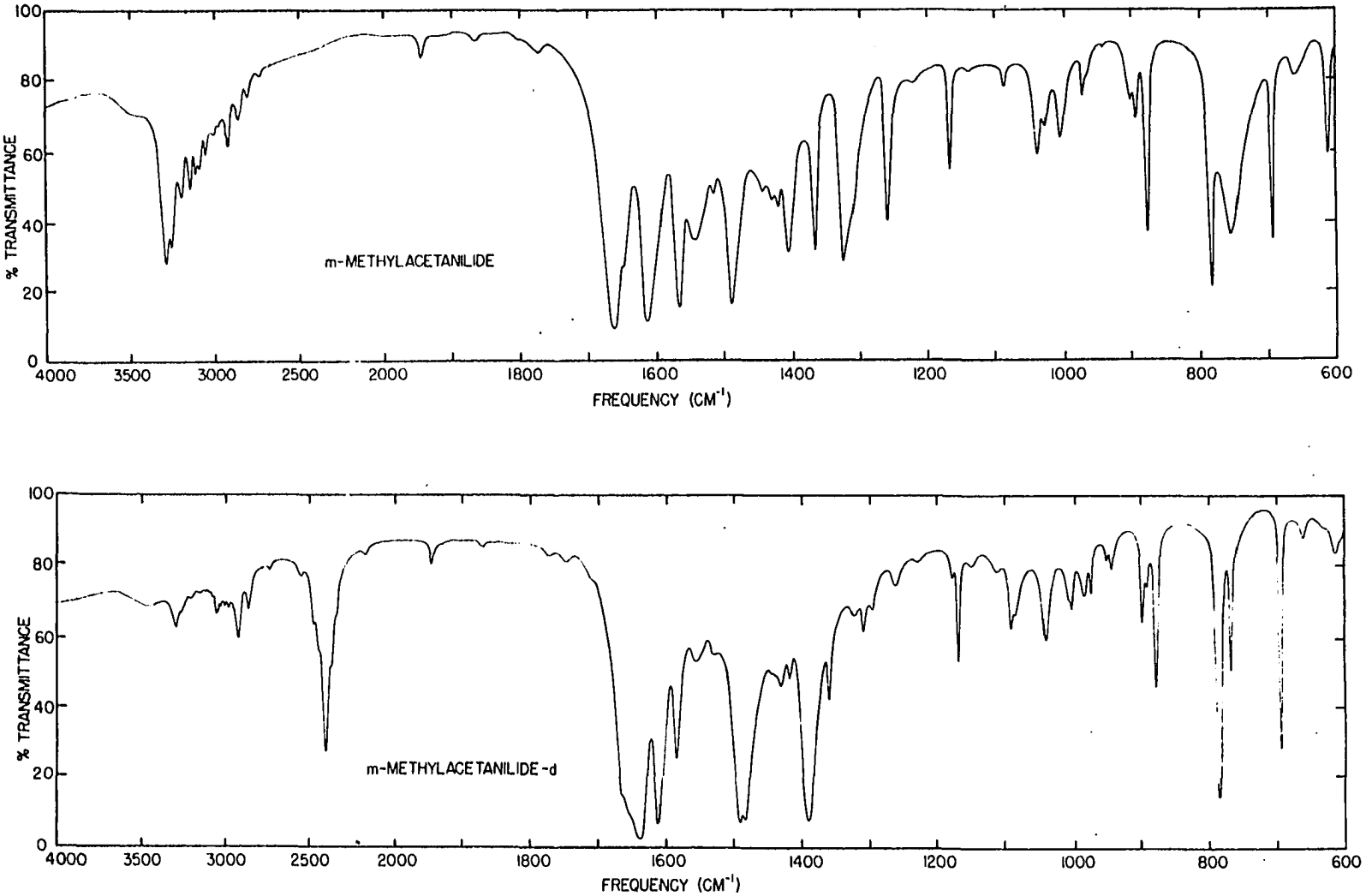

Figure 16. Potassium bromide disk spectra of m-methylacetanilide and deuterated m-methylacetanilide

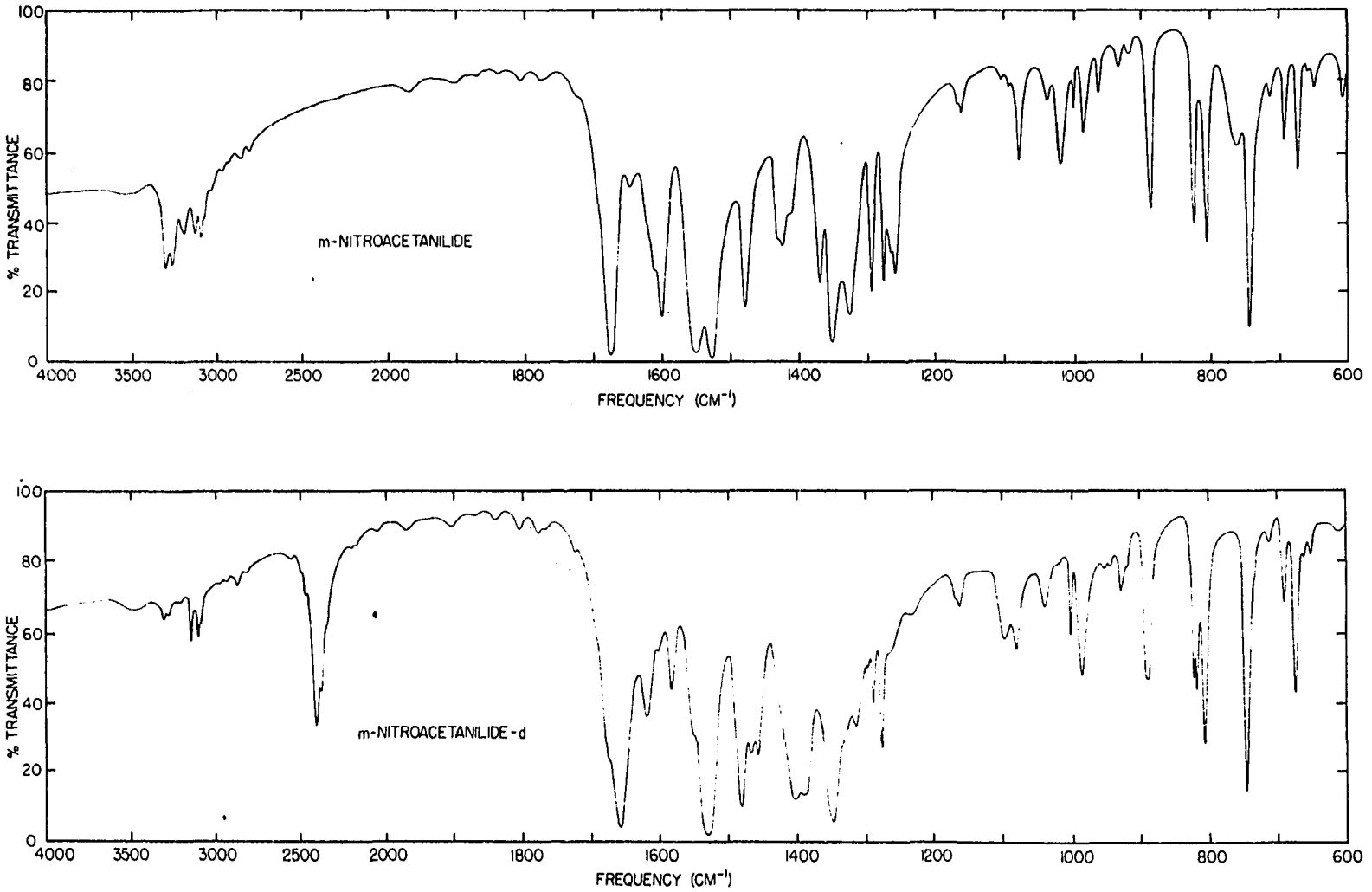

Figure 17. Potassium bromide disk spectra of m-nitroacetanilide and deuterated m-nitroacetanilide

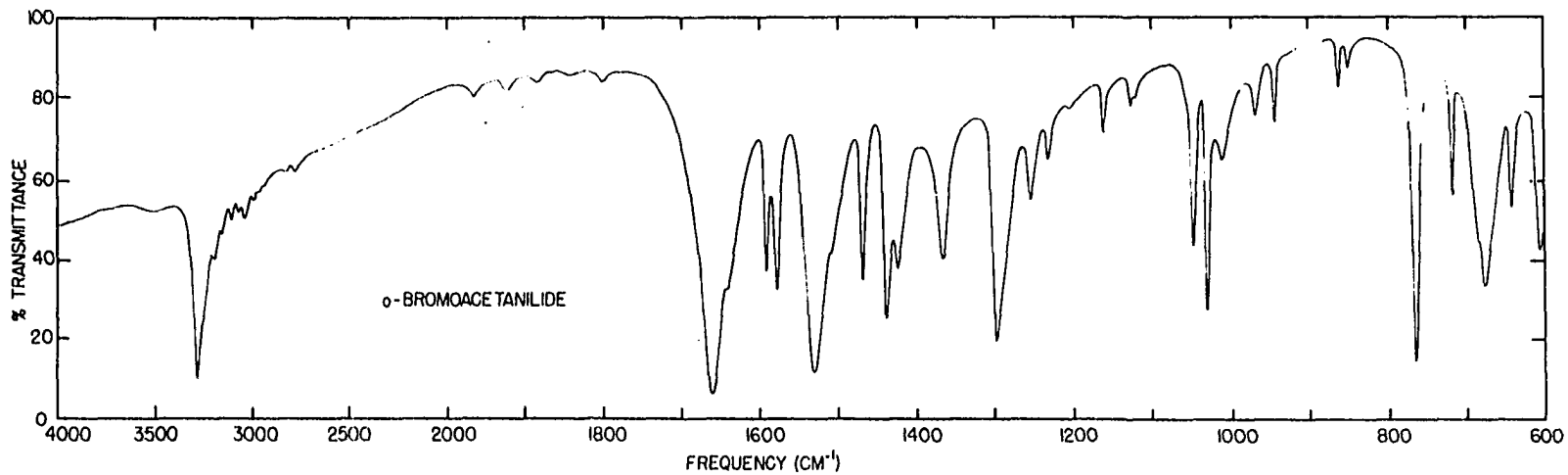

Figure 18. Potassium bromide disk spectrum of o-bromoacetanilide

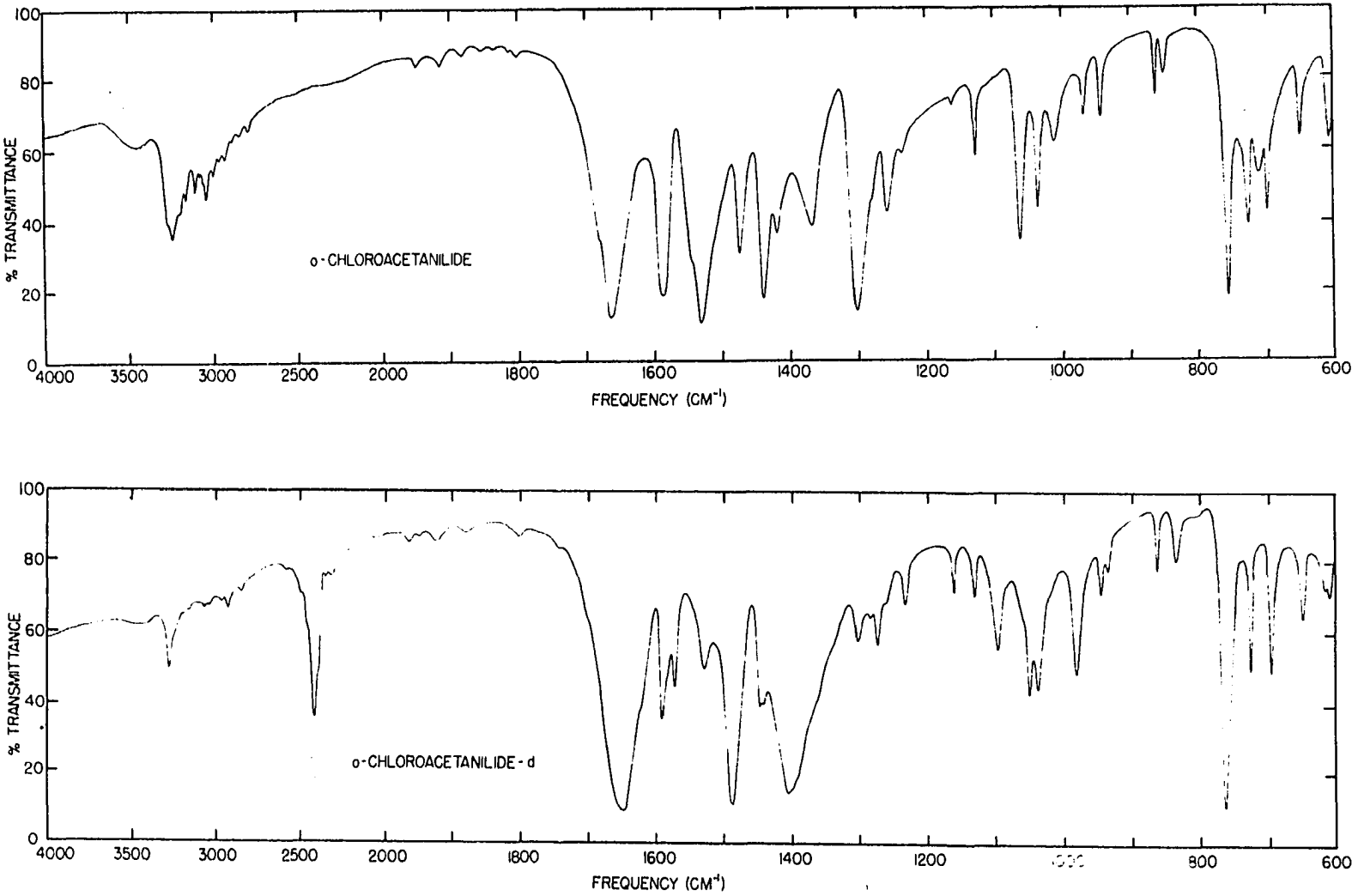

Figure 19. Potassium bromide disk spectra of o-chloroacetanilide and deuterated o-chloroacetanilide

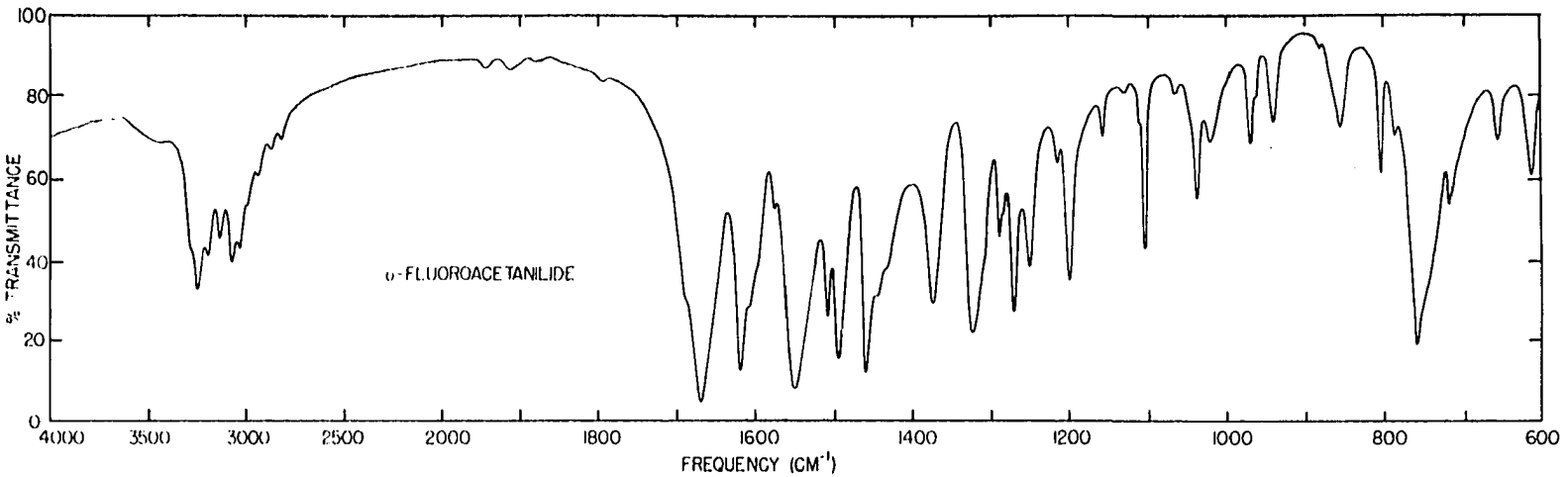

Figure 20. Potassium bromide disk spectrum of o-fluoroacetanilide

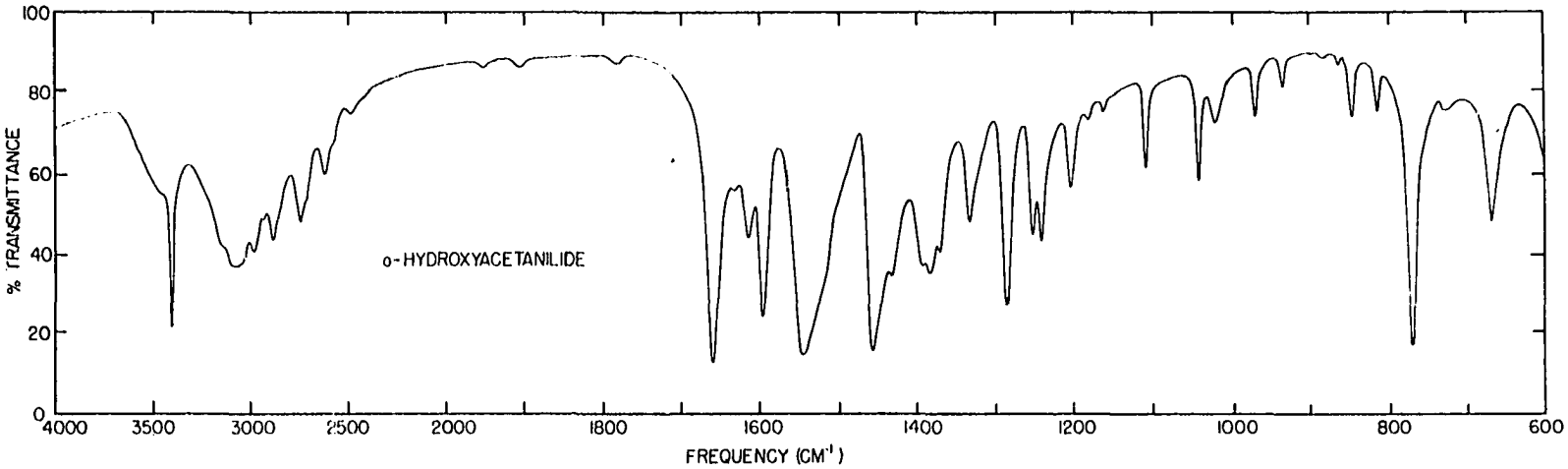

Figure 21. Potassium bromide disk spectrum of o-hydroxyacetanilide

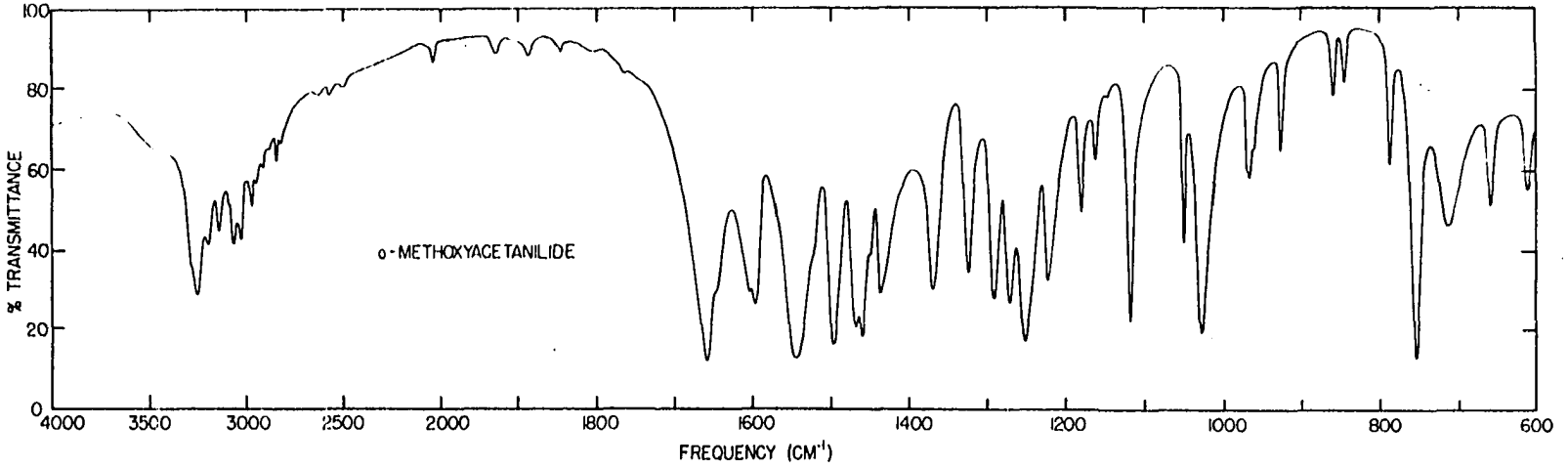

Figure 22. Potassium bromide disk spectrum of o-methoxyacetanilide

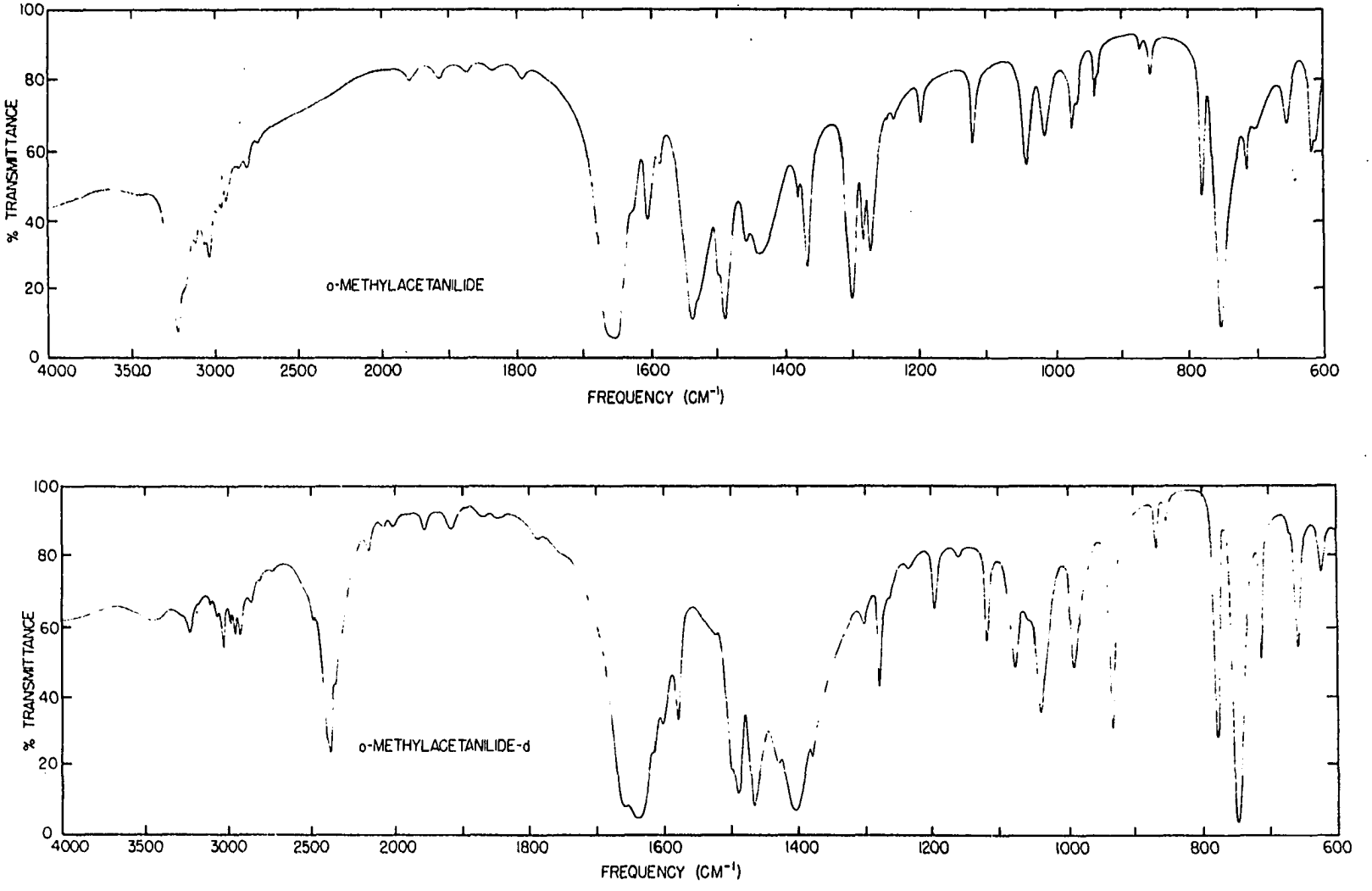

Figure 23. Potassium bromide disk spectra of o-methylacetanilide and deuterated o-methylacetanilide

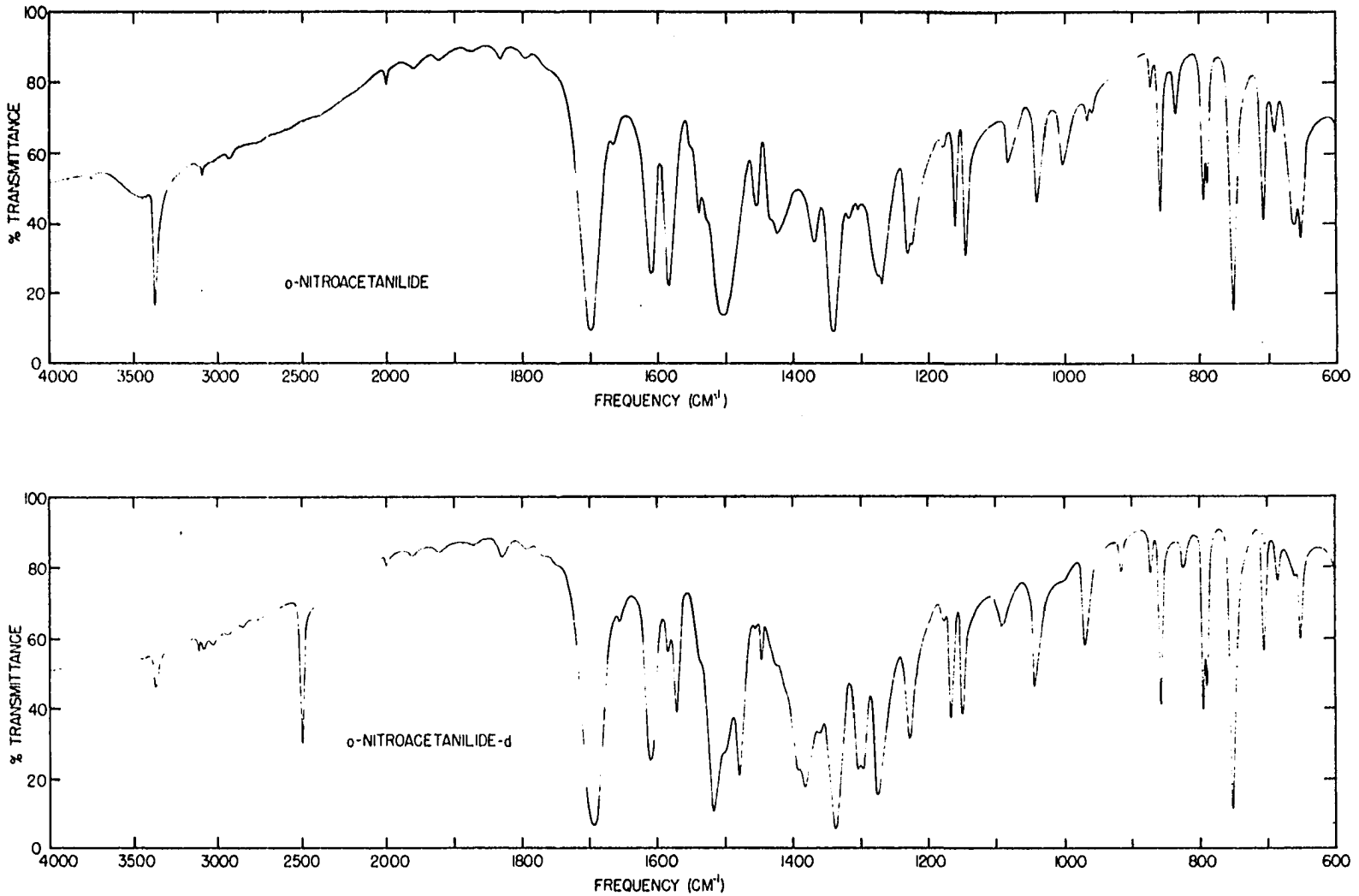

Figure 24. Potassium bromide disk spectra of o-nitroacetanilide and deuterated o-nitroacetanilide

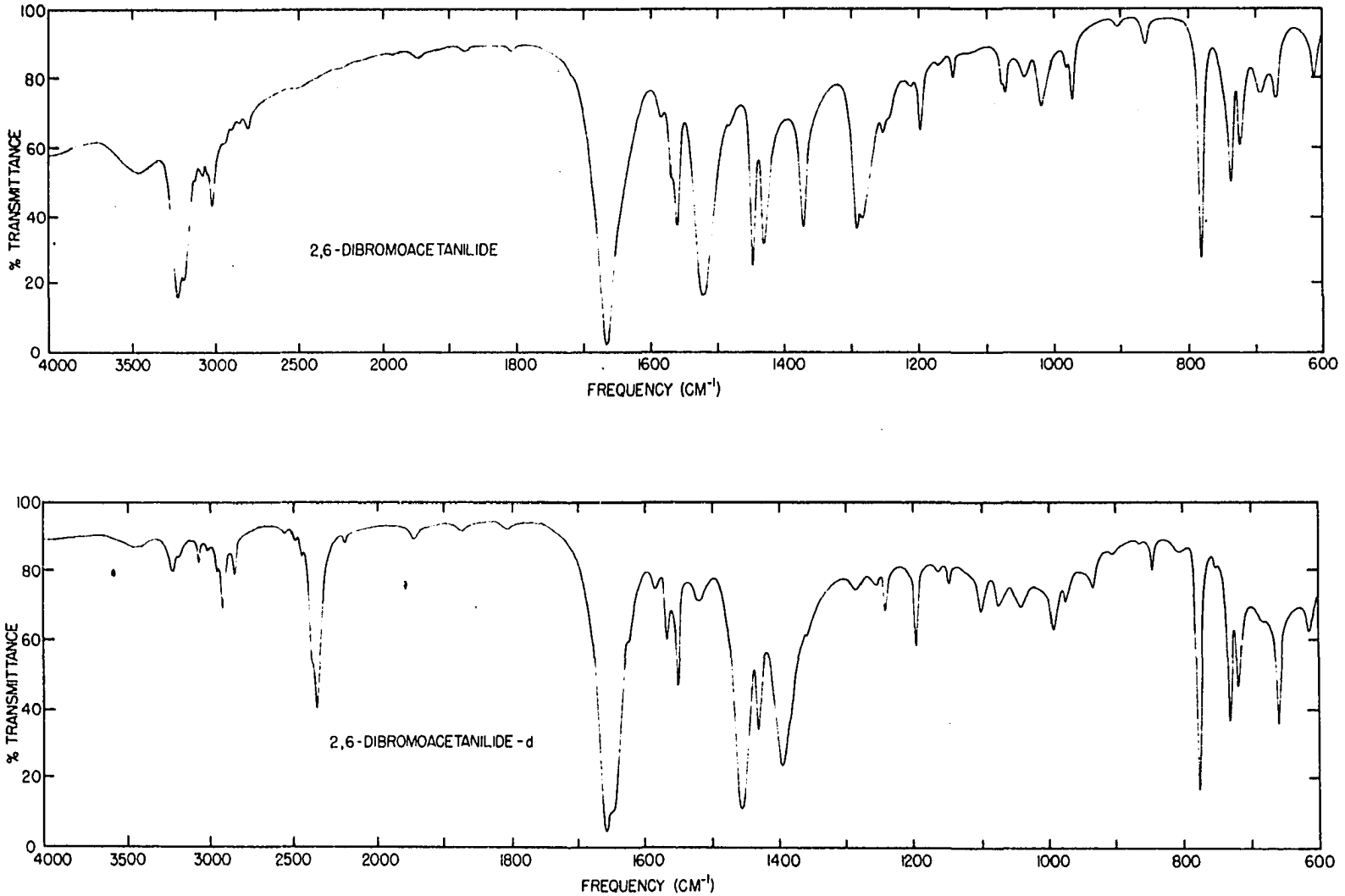

Figure 25. Potassium bromide disk spectra of 2,6-dibromoacetanilide and deuterated 2,6-dibromoacetanilide

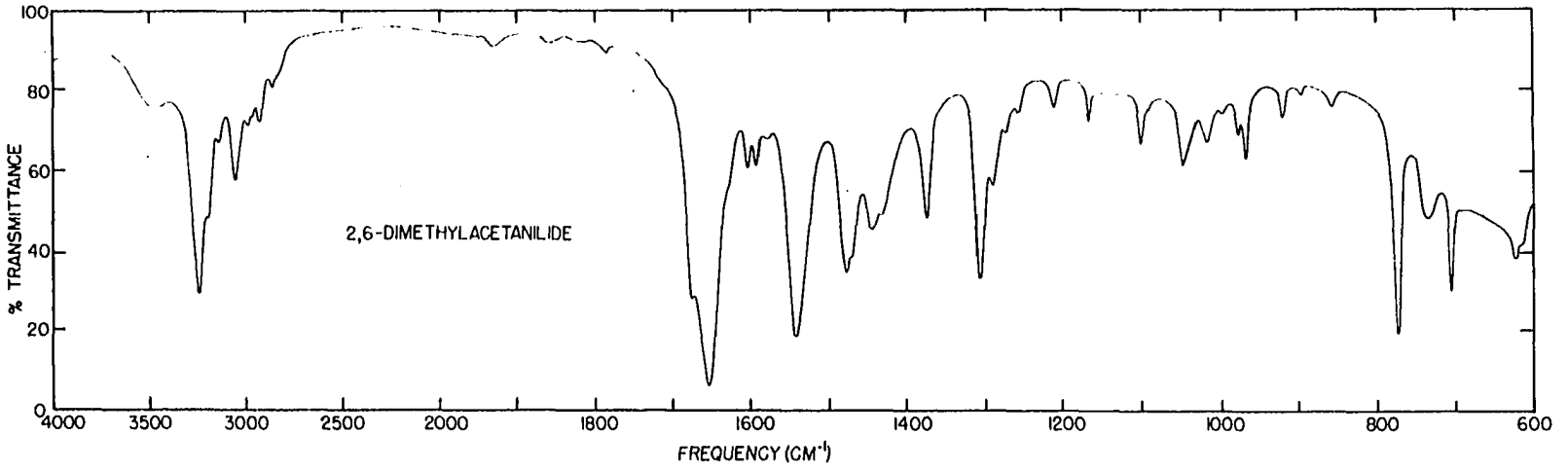

Figure 26. Potassium bromide disk spectrum of 2,6-dimethylacetanilide

THE NH STRETCHING REGION

The observed frequencies of the principal absorptions of N-monoaryl amides in the NH stretching region are tabulated in Table 2. A few typical spectra are shown in Figure 27.

Referring to the frequencies observed in the unbonded NH stretching region in solution, it is seen that two bands are often present in the 3400-3500 cm^{-1} region in carbon tetrachloride and at slightly lower frequencies in dibromomethane. The aminoacetanilides and o-methylacetanilide are exceptional and will be discussed more thoroughly below. These two bands have been assigned to the NH stretching vibrations of the cis and trans rotational isomers (62). Cyclic amides, which can exist only in the cis form, show only one band in the range 3440-3420 cm^{-1} while open-chained amides, such as benzanilide which has a trans configuration, show a single band at slightly higher frequencies. Hence, the trans form is considered to give rise to the higher frequency peak and it usually predominates in most open-chained secondary amides (62). Thompson and his co-workers (54, 62) have indicated that the relative intensities of these two peaks give a measure of the relative amounts of each isomer present. On this basis, most acetanilides exist in the trans structure to the extent of 95% or greater. Certain exceptions will be noted later.

Figure 27. Infrared spectra of typical N-monoaryl amides in the 2800-4000 cm^{-1} region

I_A Acetanilide in dibromomethane solution

I_B Acetanilide in a potassium bromide disk

II_A o-Chloroacetanilide in dibromomethane solution

II_B o-Chloroacetanilide on a potassium bromide disk

III_A p-Bromoacetanilide in dibromomethane solution

III_B p-Bromoacetanilide in a potassium bromide disk

IV_A m-Aminoacetanilide in dibromomethane solution

IV_B m-Aminoacetanilide in a potassium bromide disk

V_A 2,6-Dibromoacetanilide in dibromomethane solution

V_B 2,6-Dibromoacetanilide in a potassium bromide disk

VI_A o-Methylacetanilide in dibromomethane solution

VI_B o-Methylacetanilide in a potassium bromide disk

VII_A m-Chloroacetanilide in dibromomethane solution

VII_B m-Chloroacetanilide in a potassium bromide disk

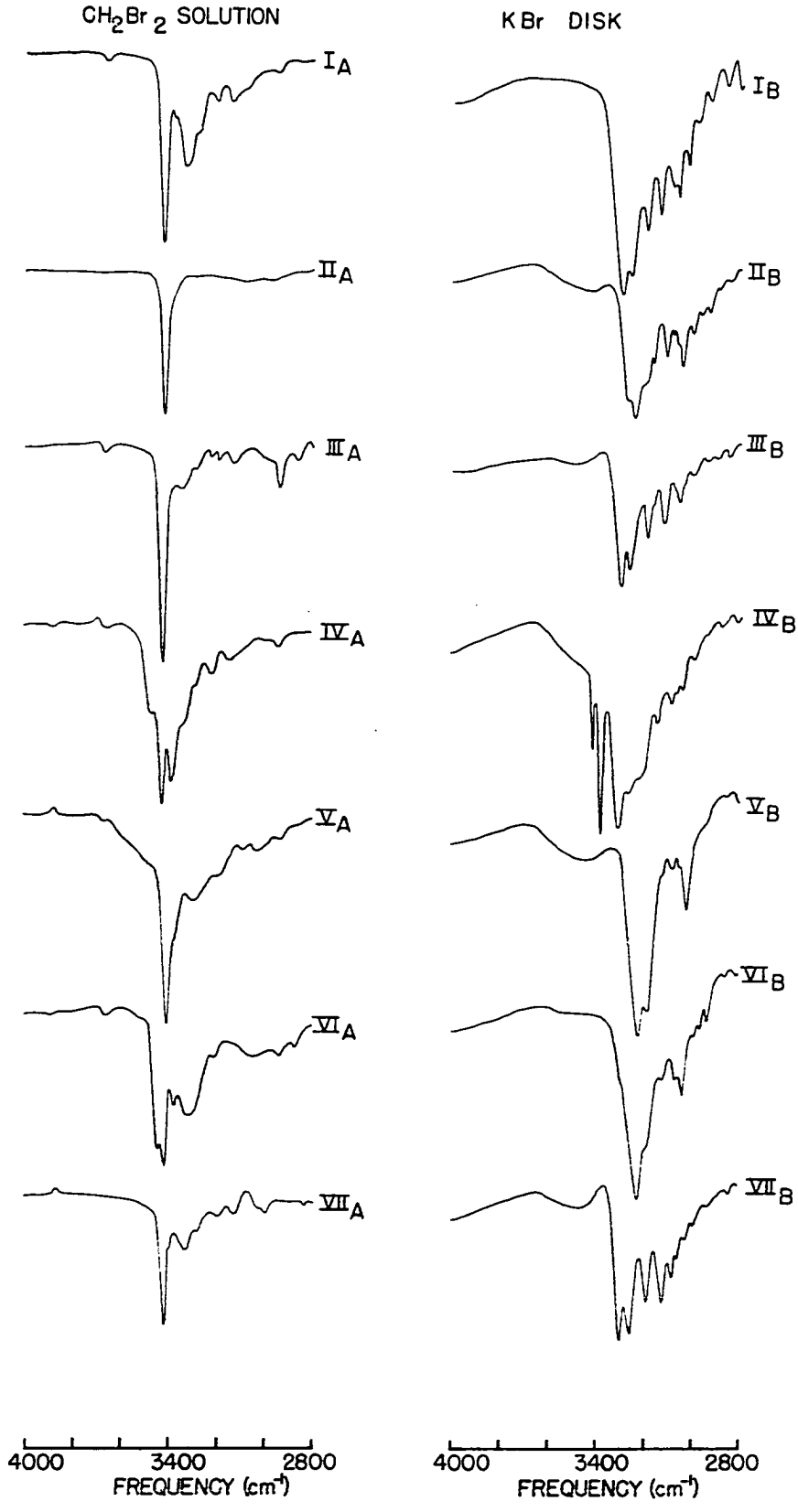
CH_2Br_2 SOLUTION
KBr DISK
I$_A$
II$_A$
III$_A$
IV$_A$
V$_A$
VI$_A$
VII$_A$
I$_B$
II$_B$
III$_B$
IV$_B$
V$_B$
VI$_B$
VII$_B$
4000
3400
2800
FREQUENCY (cm^{-1})
4000
3400
2800
FREQUENCY (cm^{-1})

Table 2. Observed frequencies for the principal absorption in the NH stretching region of N-monoaryl amides

	Compound	Dilute CCl_4 solution (cm^{-1})	CH_2Br_2 solution (cm^{-1})			KBr disk (cm^{-1})	
			Unbonded region	Bonded region[a]		Main absorption	Shoulder
1	Acetanilide	3447 3400	3421	3324	3286	3295	3261
2	Benzanilide	3449	3425	3352	-	3344	3303
3	Hexananilide	3444	3421	3326	-	3307	3268
4	p-Aminoacetanilide[b,c]		3470 3424 3375			3372 3290	3249
5	p-Bromoacetanilide	3447	3419	3335	3280	3294	3260
6	p-Chloroacetanilide	3447	3421 3395	-	-	3304	3262
7	p-Hydroxyacetanilide[b,c]		3424			3330 3295	3256
8	p-Iodoacetanilide	3446	3420 3380	3344	3280	3307	3260

[a]Lower frequency absorption is a poorly-defined shoulder on the higher frequency band.

[b]Spectrum not obtained in CCl_4 because of insolubility of the compound.

[c]Absence of absorption in dibromomethane is due to low solubility of compound.

Table 2. (Continued)

	Compound	Dilute CCl_4 solution (cm^{-1})	CH_2Br_2 solution (cm^{-1})			KBr disk (cm^{-1})	
			Unbonded region	Bonded region[a]		Main absorption	Shoulder
9	p-Methoxyacetanilide	3450	3422	3324	3276	3246	3277
10	p-Methylacetanilide	3448	3423 3376	3324	3264	3291	3257
11	p-Nitroacetanilide[b]		3413	3346	3315	3277	3303
12	m-Aminoacetanilide	3448	3465 3422 3380	3337	3285	3414 3380 3304	3263
13	m-Bromoacetanilide	3442 3400	3414	3328	3290	3293	3246
14	m-Chloroacetanilide	3444 3393	3419 3383	3330	3280	3299	3254
15	m-Hydroxyacetanilide[b,c]		3421			3328	3269
16	m-Methylacetanilide	3447 3401	3421 3370	3332	3284	3291	3258
17	m-Nitroacetanilide	3443	3417 3372	3344	3301	3305	3265
18	o-Bromoacetanilide	3417	3408 3373	-	-	3280	3257
19	o-Chloroacetanilide	3430 3399	3417	-	-	3242	3271

Table 2. (Continued)

	Compound	Dilute CCl_4 solution (cm^{-1})	CH_2Br_2 solution (cm^{-1})			KBr disk (cm^{-1})	
			Unbonded region	Bonded region[a]		Main absorption	Shoulder
20	o-Fluoroacetanilide	3450 3396	3424 3378	3321	-	3249	3285
21	o-Hydroxyacetanilide[b,c]		3425			3403	--
22	o-Methoxyacetanilide	3439 3387	3419	-	-	3251	3282
23	o-Methylacetanilide	3461 3439 3389	3435 3418 3371	3312	-	3225	3253
24	o-Nitroacetanilide	3371	3374	-	-	3372	--
25	2,6-Dibromoacetanilide	3431 3393	3402 3368	3289	-	3223	--
26	2,6-Dimethylacetanilide	3436[d] 3391[d]	3416 3371	3310	-	3237	--

[d]These data obtained from a saturated solution in 5.0 cm quartz cells.

In dilute solutions of o-methylacetanilide, there are three well-defined absorptions in the unbonded NH stretching region. The lowest frequency band at 3389 cm^{-1} undoubtedly arises from the ν(NH) of the molecules in the cis form. The other two bands, however, must arise from trans species. As mentioned previously, there are two possible isomeric structures for ortho-substituted acetanilides. If o-methylacetanilide exists in the form of structure A on page 19, the methyl group would have a repulsive influence on the amide hydrogen atom resulting in a shorter and stronger NH bond. Thus, the 3461 cm^{-1} absorption in carbon tetrachloride probably arises from the NH stretching mode of molecules which exist in the form of structure A. However, the presence of the absorption at 3434 cm^{-1} in this same solvent may indicate the presence of some molecules in the form of structure B. In this structure, steric hindrance at C_6 will cause the amide group to be rotated well out of the plane of the phenyl ring. Since the hydrogen atom will now be less influenced by the other atoms in the molecule, a lower NH stretching frequency should be observed. It should be possible to get some qualitative measure of this lowering from 2,6-dimethylacetanilide. The plane of the amide group in such a molecule is probably almost perpendicular to that of the phenyl ring since there is steric hindrance at C_6 and field repulsion at C_2. Thus, the NH stretching frequency in this

compound should also be low. Because of the very low solubility of 2,6-dimethylacetanilide, it was necessary to use a saturated solution in 5.0 cm quartz cells in order to obtain a spectrum of this region. Only one trans peak was observed at 3436 cm^{-1} which is very close to the 3439 cm^{-1} absorption of o-methylacetanilide. Therefore, these peaks are assigned to structural forms in which the amide group is nearly perpendicular to the phenyl ring.

It is worthwhile to note that the cis peaks at 3370-3390 cm^{-1} in o-methyl-, 2,6-dimethyl- and 2,6-dibromoacetanilide are more intense than in the other anilides. On the basis of the relative intensities of the cis and trans peaks, 2,6-dimethylacetanilide exists to the extent of about 55% in the trans form and 45% in the cis form. The ratio of trans-to-cis in o-methyl- and 2,6-dibromoacetanilide is about two-to-one and three-to-one respectively. Thus, it appears that the cis form exists to a greater extent in amides which exhibit a non-planar structure.

In dibromomethane solution, shown in Figure 27, the trans peak of o-methylacetanilide is again split but the intensities of the two peaks are inverted from those observed in carbon tetrachloride. Thus, the non-planar structure is apparently preferred in the more polar solvent. The solvent molecules can probably interact more readily with the amide group in such structures.

Ortho-methoxyacetanilide and the ortho-halogen acetanilides do not exhibit a splitting of the trans peak in the dilute solution spectra. However, except for o-fluoroacetanilide, the absorptions lie at frequencies lower than those of acetanilide and most of the meta- and para-substituted derivatives. These electronegative substituents probably stabilize the molecules in the form of structure A on page 19 by their attractive influence on the amide hydrogen atom. The attraction lengthens the NH bond and thus gives rise to the lower frequency values. It might be expected that o-fluoroacetanilide would exhibit the lowest ν(NH) since the fluorine atom has the highest electronegativity. However, fluorine is also the smallest of the halogen atoms and thus the size of the ortho substituent must be the predominating factor as evidenced by the stepwise decrease in the unbonded ν(NH) frequencies as the size of the halogen atom increases. In 2,6-dibromoacetanilide, the attraction at C_2 (see page 18) is overcome by the steric interference between the carbonyl oxygen and the bromine atom at C_6. Hence a non-planar structure is assumed as evidenced by the value of 3431 cm^{-1} for ν(NH) in carbon tetrachloride.

The aminoacetanilides exhibit three absorptions in dilute dibromomethane. The spectrum of the meta derivative is shown in Figure 27, IV_A. The shoulders near 3470 cm^{-1} in both the para and the meta derivatives and the absorptions

near 3380 cm^{-1} are probably due to the asymmetric and symmetric stretching modes, respectively, of the NH_2 group. The corresponding modes in aniline are at 3481 cm^{-1} and 3395 cm^{-1} in dilute carbon tetrachloride solution (9). The absorptions near 3420 cm^{-1} undoubtedly arise from the ν(NH) of the amide group in the transconfiguration since its position is very near that observed for most of the acetanilides.

The single absorption present in the solution spectra of o-nitroacetanilide near 3370 cm^{-1} is at a frequency which is too low for an ν(NH) arising from unassociated molecules and too high to be ascribed to strong intermolecularly associated species. This may indicate the presence of either weak intermolecular association or of nonlinear hydrogen bonds. The constancy of the frequency of the absorption in going from solution to solid state spectra indicates that the hydrogen atom may be involved in strong intramolecular bonding. Indeed, previous cryoscopic (13, 14) and infrared (19) data have led to the conclusion that the amide hydrogen is intramolecularly hydrogen bonded to the nitro group to form the chelate structure,

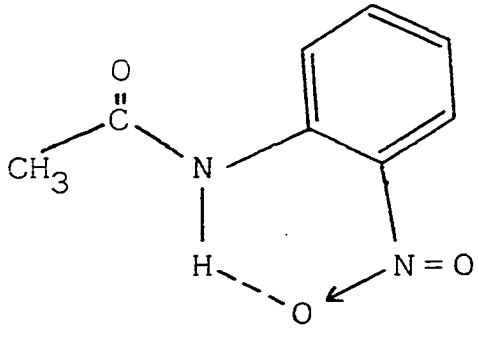

Such a hypothesis is further supported by the unusually high stretching frequency of the carbonyl group (see Table 3) in the solid state which indicates that the oxygen atom is essentially unassociated.

In concentrated solutions (bonded region column in Table 2), a broad absorption is usually present in the spectra of the anilides studied at 3290-3350 cm^{-1} in addition to the sharp peaks at 3400-3500 cm^{-1}. This absorption is not listed for carbon tetrachloride since only a few compounds were sufficiently soluble to exhibit this absorption. On dilution, this broad band gradually shifts to higher frequencies and weakens in intensity while the 3400-3500 cm^{-1} bands gain in intensity. All secondary amides exhibit similar behavior (7) and it is generally agreed that the absorption arises from the NH stretching mode of an associated trans species (10, 17, 26, 67). The present data is in agreement with this assignment. However, there is often a shoulder present on this absorption at 3260-3300 cm^{-1} which also weakens on dilution. Such a maximum could arise from the ν(NH) of other types of associated species but it is not possible to ascertain the exact nature of these species from the present data.

In the solid state spectra, typical examples of which are shown in Figure 27, the principal absorption lies in the range 3220-3330 cm^{-1}. Benzanilide, o-hydroxy- and o-nitroacetanilide exhibit higher frequencies and the amino-

acetanilides exhibit additional absorptions due to the NH_2 group. These compounds will be discussed separately below. In addition, there is generally a shoulder on this principal absorption but it is on the low frequency side of the absorption in some of the compounds and on the high frequency side in others. Abbott and Elliott (1) observed the principal NH stretching absorption in crystalline acetanilide at 3295 cm^{-1} with a shoulder at 3261 cm^{-1}. They assigned the 3295 cm^{-1} band to ν(NH) of associated trans species and presented evidence that the 3261 cm^{-1} absorption arises from coupling between adjacent molecules in the crystal lattice. Such an explanation may account for the splitting observed in this study and the variations in the position of the shoulder are probably due to crystal effects.

All the absorptions listed in Table 2 behave as expected on isotopic substitution. Nitrogen-15 substitution produces shifts of 5-10 cm^{-1} in both the solid state and solution spectra which are of the order expected for NH stretching vibrations. Deuteration of the amide group produced isotopic shifts of 1.33-1.37 in these absorptions, including the shoulder on the main absorption in the solid state. This observation lends further support to the hypothesis of Abbott and Elliott (1) regarding the origin of this shoulder. In solution, the ND stretching bands are substantially weaker than the corresponding NH absorptions. In the solid state,

however, there is no apparent loss of intensity and indeed the intensity of the main ν(ND) absorption may be slightly greater than the ν(NH). Also in the solid state spectra of the deuterated anilides, there are several very weak peaks in the 2000-2600 cm^{-1} region which are not present in the normal spectra. No detailed study of these peaks was made but they may arise from structural isomers or from overtone and combination bands of lower frequency absorptions.

Most of the meta- and para-substituted acetanilides exhibit solid state absorption spectra which are very similar to the spectrum of acetanilide except for the hydroxy and amino compounds. The presence of a fairly sharp absorption near 3330 cm^{-1} in the hydroxyacetanilides may indicate that there is some association via C=O---H-O bonds. Such association would decrease the availability of the carbonyl oxygen for participation in hydrogen bonding with the amide hydrogen atom permitting a higher ν(NH) frequency. In p-hydroxyacetanilide, however, there must also be some association via C=O---H-N bonds as evidenced by the 3295 cm^{-1} peak. Meta-aminoacetanilide, shown in Figure 27, IV_B, exhibits two sharp absorptions at 3414 cm^{-1} and 3380 cm^{-1}. The separation of these two bands is not large enough for them to arise from the asymmetric and symmetric NH_2 stretching modes. The 3380 cm^{-1} band is assigned to $\nu_{as}(NH_2)$ and the corresponding symmetric mode is probably obscured by the amide NH absorptions

near 3300 cm^{-1}. The origin of the 3414 cm^{-1} band is unknown but a similar extraneous band was observed in m-aminobenzamide (20). In p-aminoacetanilide, the 3372 cm^{-1} band is assigned to $\nu_{as}(NH_2)$ and the 3290 cm^{-1} and 3249 cm^{-1} peaks are considered to arise from the amide group. The symmetric NH_2 stretching band is again probably obscured.

The solid state spectrum of benzanilide is much less complex in the NH stretching region than most of the other anilides. This may be due to the fact that steric considerations prevent the amide linkage from assuming the cis configuration if a planar structure is to be maintained. The observed frequencies are also considerably higher than the corresponding NH stretching bands in acetanilide. The electrical effect of the additional phenyl group should be small and it is more likely that the bulky phenyl groups sterically prevent strong association from occurring in the solid state.

The solid state NH stretching frequency of o-hydroxyacetanilide is exceptionally high and is in the range expected for an NH stretching band arising from an unassociated molecule. This would indicate that the carbonyl group is not bonded to the amide hydrogen but rather is probably bonded to the hydroxyl group. Peltier et al. (57) have proposed that there is intramolecular hydrogen bonding present in this compound on the basis of the unusually low

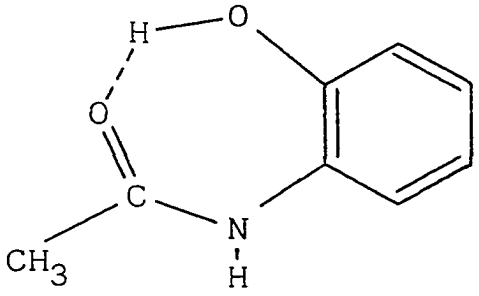

carbonyl frequency. The present data is in agreement with such a structure.

The solid state frequencies of the NH stretching bands of o-methyl-, 2,6-dimethyl- and 2,6-dibromoacetanilide are unusually low. As mentioned previously, these compounds probably exist in non-planar structures to a great extent in dilute solution. In such arrangements, the atoms of the amide linkage are less influenced by the atoms in the remainder of the molecule which normally tend to protect the amide group somewhat from large intermolecular effects. Hence, the very low solid state NH stretching frequencies indicate that these three compounds probably exist in non-planar structures in the solid state as well as in dilute solution.

The ortho-halogen acetanilides and o-methoxyacetanilide also exhibit relatively low NH stretching frequencies in the solid state but not as low as the three compounds mentioned above. However, this is expected since the solution frequencies are also low.

There is a weak absorption present in all the solid state spectra and most concentrated dibromomethane solution spectra at 3170-3220 cm^{-1}. Cyclic amides, which assume the cis configuration, exhibit their principal ν(NH) in the associated state at 3160-3200 cm^{-1} (16, 53). Hence, the 3170-3220 cm^{-1} peak in anilides could arise from the ν(NH) of associated species involving only cis molecules. The absence of the absorption in benzanilide, o-nitro- and o-hydroxyacetanilide, which exist only in the trans form, lends support to this assignment. However, it is also possible that the absorption arises from an overtone or combination mode of lower frequency absorptions. Cannon (12) has observed a band in nylon at 3200 cm^{-1} which he assigns to the combination mode of the amide I band (near 1650 cm^{-1}) and the amide II band (near 1550 cm^{-1}). The sum of the observed frequencies of the solid state amide I and II frequencies is plotted against the observed frequency of the 3170-3220 cm^{-1} band in Figure 28. Virtually all the points fall below the line of unit slope and thus if the observed absorption is the combination mode, it has been lowered by resonance with ν(NH) by varying amounts.

A peak at 3100-3160 cm^{-1} in the solid state and concentrated solution spectra of the anilides studied is unassigned. The band definitely arises from some NH mode since it is sensitive to ^{15}N and deuterium substitution. There are no

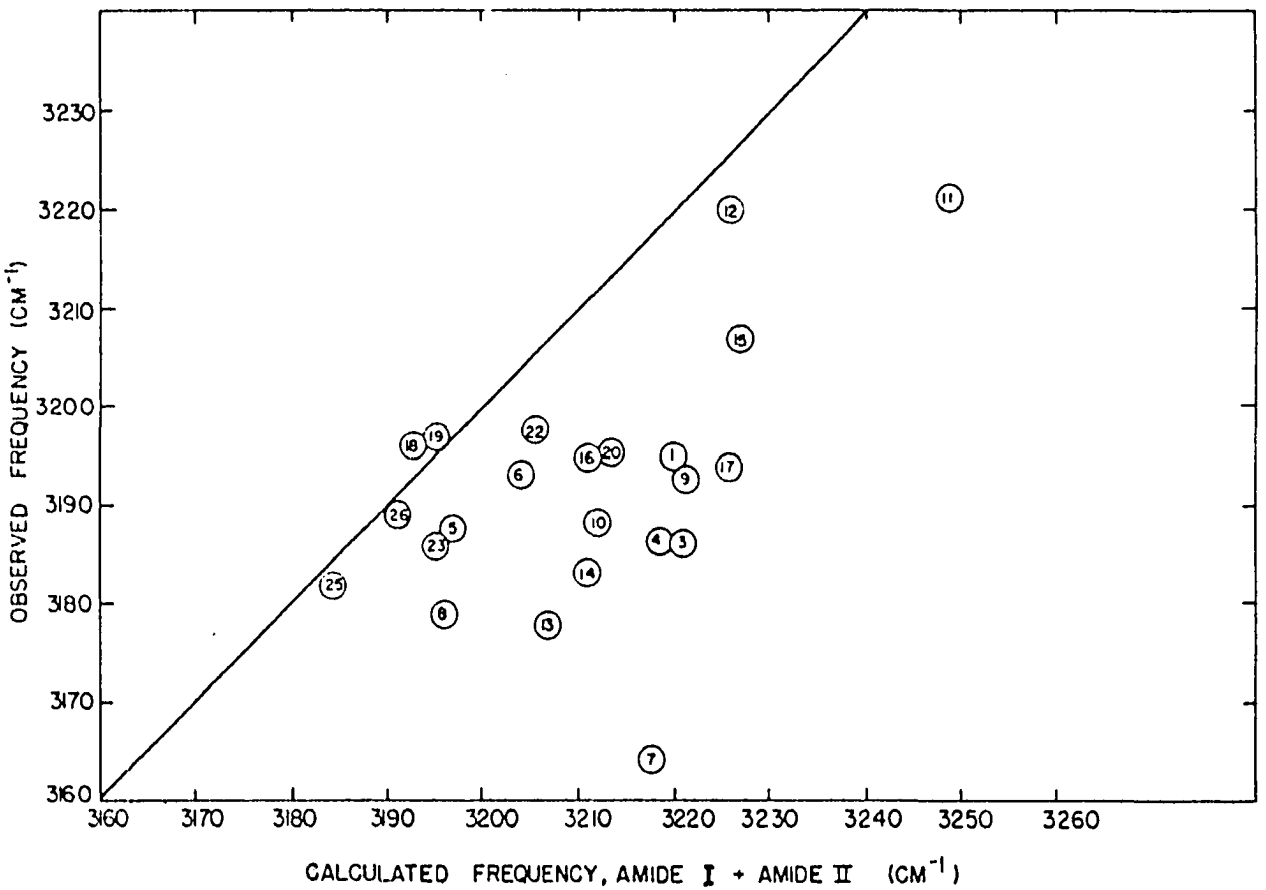

Figure 28. Plot of the observed frequencies of the 3200 cm^{-1} subsidiary peak of N-monoaryl amides in their potassium bromide disk spectra vs the sum of the frequencies of the amide I and amide II bands in the corresponding spectra (numbers within the circles refer to the compounds listed in Table 2)

possible overtone or combination modes to which this peak may be assigned and its frequency value is lower than that generally ascribed to cis isomers. It could arise from molecular coupling between NH stretching modes of the cis and trans molecules in the crystal lattice. This, however, does not explain the presence of the band in concentrated solutions.

Acetanilide, hexananilide, o-chloro- and p-nitroacetanilide exhibit peaks in the solid state spectra at 3081, 3095, 3044 and 3095 cm^{-1}, respectively, which shift by 9-13 cm^{-1} on ^{15}N substitution and disappear on deuteration. Most secondary amides exhibit an absorption at 3100-3060 cm^{-1} in the solid state and many assignments have been suggested for its origin (3, 4, 5, 10, 16, 37, 42, 53). The hypothesis of Miyazawa (50), however, is in best agreement with the above large ^{15}N shifts. He proposes that the peak arises from Fermi resonance between ν(NH) and the first overtone of the amide II band (a strong absorption near 1550 cm^{-1}) in trans amides. This overtone band is probably present in many of the other compounds studied but it is not possible to distinguish it with certainty from the aromatic CH stretching bands without the aid of ^{15}N data. In the deuterated anilides, it may be obscured by the methyl group absorptions at 2800-2950 cm^{-1}.

THE AMIDE I BAND

Outside of the NH stretching region, there are three bands normally used for the identification of amides. These are termed the amide I, II, and III bands. The amide I band generally lies in the range 1600-1700 cm^{-1}, the amide II band at 1500-1600 cm^{-1} and the amide III band at 1200-1350 cm^{-1}. All three of these bands are present in both primary and open-chained secondary amides, though the amide II and III bands generally lie at lower frequencies in secondary amides. Tertiary amides and cyclic lactams containing less than nine carbon atoms apparently do not exhibit an amide II band. These three bands will be discussed in detail since they are characteristic of amides and their origins are in some dispute.

The amide I band is usually assigned to the carbonyl stretching vibration, $\nu(C=O)$. Its presence in disubstituted amides where enolization is impossible and its lower frequency on association led early workers to accept this assignment (61, 69). The band could arise from the $\nu(C=N)$ of the enol form but there are numerous convincing arguments against such an assignment. The shift on ^{15}N substitution is small (5, 28), the shift on ^{18}O substitution is large (58), and the frequency shift on electrophilic substitution at the nitrogen is opposite in direction to that expected for a $\nu(C=N)$

(61, 69).

Certain workers have argued that the band is not a pure carbonyl absorption but rather that other motions are also involved. Foremost among these were Fraser and Price (21, 22) who proposed that the absorption arose from the asymmetric stretching mode of the O=C-N group, ν_{as}(O=C-N). Sandman (63) and Abbott and Elliott (1) measured transition moments of crystalline amides and found that the amide I vibration was distorted about 20° from the direction of the carbonyl bond. Abbott and Elliott also observed a 21 cm^{-1} lowering in the frequency of the amide I band in the crystalline state on deuteration of acetanilide but only a 7 cm^{-1} shift in very dilute solution. They attribute the 7 cm^{-1} shift to intramolecular causes and presume that the remaining 14 cm^{-1} arises from the difference in mass between a hydrogen bond and a deuterium bond. These observations (1, 63) are in support of the view of Fraser and Price (21, 22). However, Miyazawa *et al.* (52) performed a normal coordinate analysis on N-methylacetamide and diformylhydrazine and have concluded that the amide I band is essentially a pure ν(C=O) with negligible contribution from ν(C-N).

The frequencies of the amide I band in both the solid state and solution spectra of the anilides studied are listed in Table 3. The band intensities are all very strong except where otherwise noted.

Table 3. Frequency values of the amide I band in N-monoaryl amides

Compound	Frequency (cm^{-1})[a]		
	CCl_4 solution	CH_2Br_2 solution	KBr disk
Acetanilide	1706 1690(sh)	1693 1683(sh)	1664
Benzanilde	1689	1678	1656
Hexananilide	1703 1686(sh)	1690	1668
p-Aminoacetanilide[b]		1683	1667
p-Bromoacetanilide	1710	1696	1669
p-Chloroacetanilide	1712	1697	1665
p-Hydroxyacetanilide[b]		1687	1654
p-Iodoacetanilide	1710	1698	1670
p-Methoxyacetanilide	1700	1686	1659
p-Methylacetanilide	1702	1689	1662
p-Nitroacetanilide	1719[c]	1710	1682
m-Aminoacetanilide	1701	1689	1675
m-Bromoacetanilide	1713 1693(sh)	1700	1666

[a]The symbol sh indicates a shoulder which is present in the concentrated solution spectra but is absent in dilute solution.

[b]Spectrum not obtained in CCl_4 because of the insolubility of the compound.

[c]This value was obtained from a saturated solution using a 2.5 mm path length.

Table 3. (Continued)

Compound	Frequency (cm^{-1})[a]		
	CCl_4 solution	CH_2Br_2 solution	KBr disk
m-Chloroacetanilide	1712 1671	1698 1688(sh)	1671
m-Hydroxyacetanilide[b]		1693 1671(m)[d]	1658
m-Methylacetanilide	1705 1689(sh) 1677	1689	1664
m-Nitroacetanilide	1718	1706 1686(sh)	1675
o-Bromoacetanilide	1713	1699	1662
o-Chloroacetanilide	1712	1701	1664
o-Fluoroacetanilide	1712 1694(sh)	1696	1666
o-Hydroxyacetanilide[b]		1664	1660
o-Methoxyacetanilide	1701	1688	1659
o-Methylacetanilide	1705 1692(sh)	1691 1678(sh)	1657
o-Nitroacetanilide	1717	1708	1701
2,6-Dibromoacetanilide	1722 1707(sh)	1702	1664
2,6-Dimethylacetanilide[b]		1681	1651

[d]This absorption is of moderate intensity.

In very dilute solution, the amide I band is present as a single very strong absorption at 1680-1720 cm^{-1} in all the anilides studied except o- and m-hydroxyacetanilide. A number of investigators (23, 27, 55, 56, 57, 61, 70) have studied the amide I band of substituted acetanilides in dilute solution. It has been observed that the more strongly electron-attracting substituents cause the higher amide I frequencies and that a linear relationship exists between the amide I frequency in dilute solution and the Hammett σ value of the substituent (55, 56, 70). The present data is in substantial agreement with these previous investigations. The unusually low frequency of the amide I band in o-hydroxyacetanilide in solution has also been previously observed (57) and attributed to intramolecular hydrogen bonding between the carbonyl oxygen and the hydroxyl group. The evidence presented previously in the NH stretching region is in support of this hypothesis. Peltier et al. (57) also observed the additional absorption in m-hydroxyacetanilide and indicated that there may be chelation in this compound in the trans configuration. It seems more probable, however, that the 1671 cm^{-1} band arises from some associated species but it was not possible to prove this because of the unavailability of cells of sufficient path length to make dilution studies.

In concentrated solutions, several of the anilides exhibited a low frequency shoulder or asymmetry on the amide

I band which disappeared on dilution. Simultaneously, the broad absorptions in the bonded NH stretching region also weakened. This shoulder probably arises from the ν(C=O) of associated species. In concentrated carbon tetrachloride solutions of m-methyl- and m-chloroacetanilide, however, the absorptions at 1677 and 1671 cm^{-1}, respectively, were stronger than the bands above 1700 cm^{-1}. On gradual dilution, the 1670 cm^{-1} bands weakened and shifted to higher frequencies while the sharper bands above 1700 cm^{-1} gained in intensity. At high dilution, only the higher frequency bands were present. The lower frequency absorptions undoubtedly arise from the ν(C=O) of associated molecules and their extraordinary intensity probably accounts for the extremely high solubilities of these two compounds in carbon tetrachloride.

There is very little variation in the frequency of the amide I band in the solid state hence little structural information can be gained from this absorption. Ortho- and p-nitroacetanilide, however, do exhibit relatively high frequencies. The nitro group, by its mesomeric effect, causes a decrease in the polarity of the carbonyl bond and hence an increase in ν(C=O). This may account for the higher frequency in p-nitroacetanilide but can only in part account for the exceptionally high frequency in o-nitroacetanilide. If, however, the nitro group in the ortho position is intramolecularly bonded to the amide hydrogen, this hydrogen can bond

but very weakly intermolecularly to the carbonyl oxygen. Hence, ν(C=O) for o-nitroacetanilide in the solid state should lie in the region of an unassociated carbonyl stretching band and this indeed is observed.

The observed frequency shifts for the amide I band on isotopic substitution are listed in Table 4. The ^{15}N shifts are quite small indicating that there is very little nitrogen motion involved. The deuterium shift in solution is of the order observed by Abbott and Elliott (1). These authors ascribed this shift as being due to the contribution of ν(C-N) to the amide I vibration. The deuterium shifts in the solid state spectra are relatively large and vary considerably. As mentioned previously, the large shift in the amide I band on deuterating acetanilide has been ascribed (1) to the difference in mass between a hydrogen and a deuterium bond. However, the large variation in the shifts in the solid state suggests that other factors may be operative. The shift on deuteration in the solid state is plotted against the difference between the solid state and dilute carbon tetrachloride solution frequencies in Figure 29. The difference between the solid state and dilute solution frequencies, unless there is association even in dilute solution, should give some relative measure of the hydrogen bond strengths and hence the N----O distances in the solid state. That is, those compounds possessing the stronger intermolecular

Table 4. Observed frequency shifts for the amide I band on isotopic substitution of N-monoaryl amides

	Compound	Deuteration shift (cm^{-1})		^{15}N shift (cm^{-1})	
		KBr disk	CCl_4 solution	KBr disk	CCl_4 solution
1	Acetanilide	-24	-6	-1.6	<1
2	Benzanilide	-10	-6[a]	<1	<1
3	Hexananilide	-16	-6	-2.5	<1
4	p-Aminoacetanilide	-17	-7[a]	--	--
6	p-Chloroacetanilide	- 9	-4	--	--
9	p-Methoxyacetanilide	-27	-5	--	--
10	p-Methylacetanilide	-19	-5	--	--
11	p-Nitroacetanilide[b]	-19		-3.6	
14	m-Chloroacetanilide	-18	-7	--	--
16	m-Methylacetanilide	-24	-8	--	--
17	m-Nitroacetanilide	-17	-9[a]	--	--
19	o-Chloroacetanilide	-15	-6	-1.5	-1.7
23	o-Methylacetanilide	-16	-6	--	--
24	o-Nitroacetanilide	- 5	-7	-1.5	<1
25	2,6-Dibromoacetanilide	- 6	-1[a]	--	--

[a]These shifts were observed in dibromomethane since the solubilities in carbon tetrachloride were very low.

[b]Isotopic derivatives of p-nitroacetanilide were not run in solution.

Figure 29. Plot of the frequency shift of the amide I band on passing from the solid state to the dilute carbon tetrachloride solution spectra vs the frequency shift of the amide I band in the solid state on deuteration of N-monoaryl amides (numbers within the circles refer to the compounds listed in Table 4)

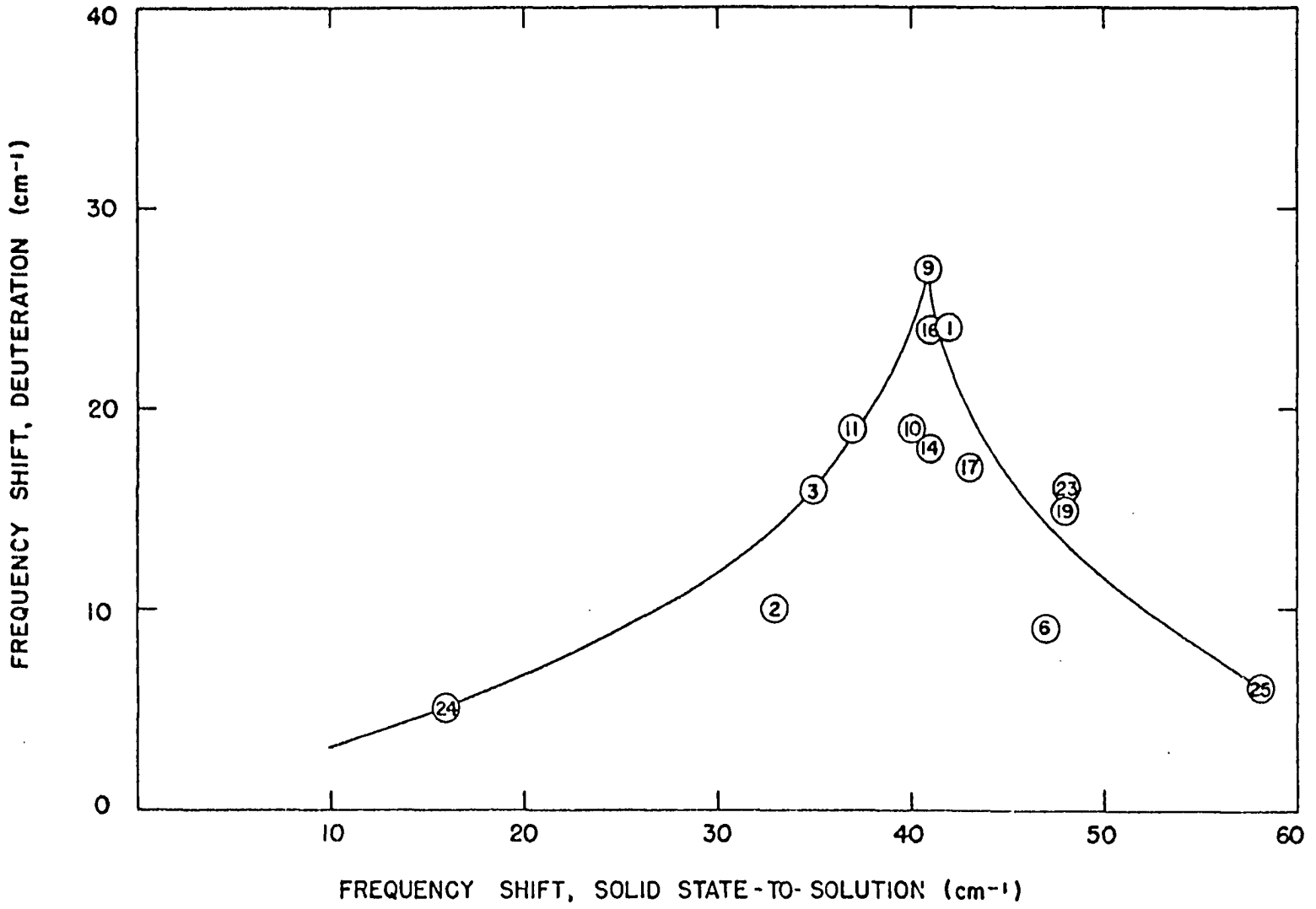
FREQUENCY SHIFT, DEUTERATION (cm⁻¹)
FREQUENCY SHIFT, SOLID STATE-TO-SOLUTION (cm⁻¹)
0
10
20
30
40
10
20
30
40
50
60
9
16
1
11
10
14
17
3
23
19
2
6
24
25

hydrogen bonds should exhibit the larger sensitivities to state of aggregation. Assuming that the N----O distances are the same for both hydrogen and deuterium bonds, larger deuterium shifts should be observed for strong hydrogen bonds than for weak bonds. Hence it might have been expected that the plot in Figure 29 would have resulted in a straight line with a positive slope rather than the contour shown. From the origin to the maximum, there is apparently an increasing mass effect with increasing hydrogen bond strength, as expected. Beyond the maximum, there is no reason to expect weak hydrogen bonds but yet the curve drops. It could be due to some coupling effect with δ(N-D) but such an effect should also be observed in the solution spectra. Hence, it must be due to some difference between the hydrogen and deuterium bonds. Gallagher (24) has performed a theoretical treatment on the deuterium isotope effect on the lattice parameters in hydrogen bonded crystals. This treatment predicts that weak hydrogen bonds may be strengthened by deuterium substitution and that strong hydrogen bonds are expanded. Specifically, for O-H---O bonds, he suggests that the expansion upon deuterium substitution reverses to a contraction for O----O distances greater than 2.77 Å. It is possible that similar changes in bond strengths occur in N-H---O bonds on deuteration but no data are available to substantiate this. Also, it is not known if changing hydrogen bond lengths affects the

infrared spectra appreciably, even in O-H---O bonds. But it is distinctly possible that the sharp drop in the curve in Figure 29 is due to the increased N----O distance of the stronger intermolecularly hydrogen bonded compounds on deuteration. If this does account for the observed phenomena, the reversal from expansion to contraction apparently occurs at an N----O distance of about 2.94 Å since this is the N----O distance in acetanilide (8), which lies near the maximum of the curve in Figure 29.

THE 1600-1200 CM^{-1} REGION

Open-chained secondary amides, polypeptides and proteins normally exhibit two strong absorptions in the 1200-1600 cm^{-1} region which are characteristic of the amide linkage (7). These are commonly referred to as the amide II and III bands. The amide II band generally falls in the range of 1510-1570 cm^{-1} while the amide III band is usually found near 1300 cm^{-1}. Similar absorptions are observed in primary amides at somewhat higher frequencies and their origins are generally ascribed to modes involving principally $\delta(NH_2)$ and $\nu(C-N)$, respectively. The nature of the vibrations in secondary amides, however, has been the subject of much controversy and numerous assignments have been suggested.

In early work (61, 69), the common view was that the amide II band arose from the NH in-plane deformation. This assignment was supported by the absence of the band in tertiary amides, its weakening on deuteration (15, 69), and its higher frequency in the solid state spectra as compared with solution spectra. However, the absence of the band in the Raman spectra of secondary amides and in the infrared spectra of cyclic lactams opposes this assignment.

Lenormant (43) has suggested that in the non-cyclic secondary amides a tautomeric equilibrium exists between a "ketonic" form,

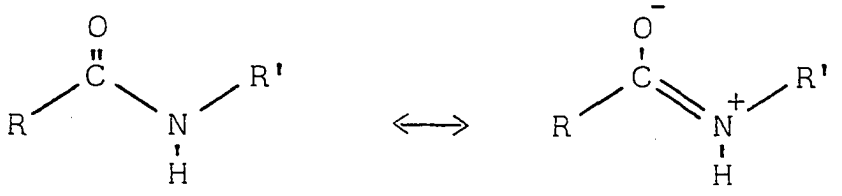

and a dimeric "pseudoionic" form,

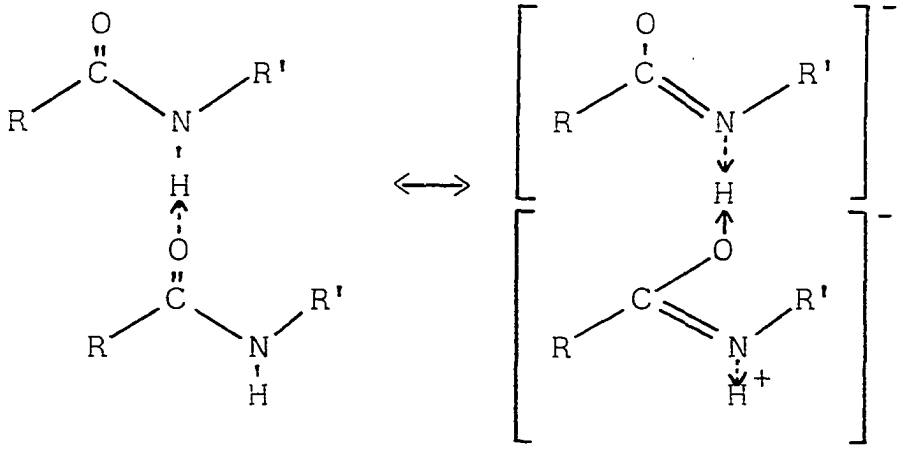

In the "ketonic" tautomer, the nonionic structure is presumed to predominate while in the "pseudoionic" tautomer both resonating structures make comparable contributions. Lenormant then assigns the amide I band to the ν(C=O) of the "ketonic" form and the amide II band to a Raman inactive vibration of the "pseudoionic" form. Letaw and Gropp (44) have proposed a similar assignment and explained the absence of the amide II band in tertiary amides to an accidental degeneracy of the ν(C=O) and ν(C-N). Gierer (26), however, observed that the amide II band persists in vapors where only unassociated molecules are present. He assigns the amide II

band to the asymmetric mode of the coupled deformation vibrations, δ(NH) and $\delta(CH_3)$-N* or $\delta(CH_2)$-N, in N-monoalkyl amides. The corresponding symmetric mode is assigned to the amide III band. According to Gierer, deuteration of N-methylacetamide essentially removes the coupling and the δ(ND) appears at 980 cm^{-1} and the $\delta(CH_3)$-N moves to 1490 cm^{-1}.

Fraser and Price (21, 22), as mentioned in the previous section, have indicated that coupling of ν(C-N) and ν(C=O) gives rise to an asymmetric and a symmetric O=C-N stretching mode. The asymmetric mode corresponds to the amide I band and the symmetric mode couples with δ(NH) to produce the amide II and III bands. Thus, the amide II band, according to Fraser and Price, is a mixed vibration consisting of an out-of-phase combination of ν(O=C-N) and δ(NH) in which the angular displacement of the hydrogen atom plays the greater part. The corresponding in-phase mode, which is primarily a C-N stretching motion, is assigned to the amide III band. A number of authors (5, 17, 18, 37) have agreed with these assignments and the work of Mecke and Mecke (48) on thioamides appears to support this view.

Recently the view of Fraser and Price has been severely criticized. Miyazawa et al. (51, 52) have shown, by calculations of vibrational energies, that the energy contribution

---

*This symbolism denotes a deformation mode of the methyl group attached to the nitrogen atom.

of the C=O bond in the amide II vibration is negligible compared to that of the C-N bond even though the absorption is not far removed from the amide I band. These calculations indicate that the amide II band consists of 60% δ(NH) and 40% ν(C-N) in N-methylacetamide. In the case of the amide III band, it was found (52) that $\nu(C\text{-}CH_3)$ makes a significant contribution and that this mode consists of 40% ν(C-N), 30% δ(NH) and 20% $\nu(C\text{-}CH_3)$. Pinchas et al. (58) report that the amide II and III bands of N-methylbenzamide are insensitive to ^{18}O substitution which further discredits the assignments of Fraser and Price.

On deuteration of N-methylacetamide the amide II and III bands at 1567 and 1299 cm^{-1}, respectively, disappear and new bands occur at 1475 and 960 cm^{-1} (5, 26, 51, 52). These absorptions are termed, respectively, the amide II' and III' bands. Fraser and Price ascribed the 1475 cm^{-1} band to an uncoupled ν(O=C-N) and the 960 cm^{-1} absorption to δ(ND). Miyazawa et al., however, have found that the contributions of $\nu(C\text{-}CH_3)$, $\nu(N\text{-}CH_3)$, δ(O=C-N) and δ(ND) are more important in the amide II' vibration than ν(C=O). Interaction of ν(C-N) with these motions is then sufficient to hold the frequency at a relatively high value. The calculations on the amide III' vibration (52) have shown that although δ(ND) makes a significant contribution, the contributions of $\nu(C\text{-}CH_3)$ and $\nu(N\text{-}CH_3)$ are equally important.

The nature of the amide II and III vibrations is even less certain in anilides. Mann and Thompson (46, 47) have studied acetanilide using polarized radiation and agree with the δ(NH) assignment for the amide II band. Abbott and Elliott (1) could come to no definite conclusions as to the nature of the amide II vibration but indicated that the view of Fraser and Price could not fully account for the observed changes in the spectra on deuteration. The strong absorption at 1325 cm^{-1} in crystalline acetanilide, which probably corresponds to the amide III band, weakened on deuteration and apparently shifted to 980 cm^{-1} (1). The transition moments of both the 1325 and 980 cm^{-1} absorptions were found to be about 80° to the direction of the NH bond and nearly in the plane of the amide group. These authors thus assigned the 1325 and 980 cm^{-1} bands to δ(NH) and δ(ND), respectively. Katritzky and Jones (39) assumed that the assignment of Miyazawa et al. for the amide II vibration is also correct for aromatic amides but assigned the absorptions near 1300 cm^{-1} to skeletal modes. Gray (28) agreed with the assignment of Abbott and Elliott (1) for the amide III vibration. However, he chose to assign the amide II band to a skeletal vibration of the C-C-N-C system in which the amplitude of the amide C-N bond is greatest.

The observed characteristic absorption frequencies of the amide group in the 1600-1200 cm^{-1} region of the

N-monoaryl amides studied are listed in Table 5. As indicated previously, the amide II band generally falls in the range 1510-1570 cm^{-1} while the amide III band occurs near 1300 cm^{-1}. Prominent absorptions arising from the phenyl ring occur near 1600, 1500 and 1450 cm^{-1} and will be discussed in a later section. An examination of the amide II band in the solid state spectra shown in Figures 1-26 reveals that a low frequency shoulder is present in some of the spectra. This shoulder is not listed in Table 5 but may arise from the amide II vibration of the molecules in the cis form or it may be due to molecular coupling of the type discussed in the section on the NH stretching region. A high frequency shoulder is frequently observed on the amide II band in the spectra of concentrated solutions. This shoulder is not listed in Table 5 but it disappears on dilution so it probably arises from the amide II band of associated species. Ortho-nitroacetanilide has been purposely omitted from Table 5 since the location of the amide II and III bands is uncertain. This compound will be discussed in more detail near the end of this section.

It will be noted from Table 5 that the absorptions listed generally lie at higher frequencies in the solid state spectra than in the dilute solution spectra. Such behavior is frequently indicative of the presence of bending vibrations. If the amide II absorption arose from a purely

Table 5. Observed frequencies of the characteristic amide group absorptions in the 1600-1200 cm^{-1} region of N-monoaryl amides

	Compound	Amide II (cm^{-1})		Amide III (cm^{-1})		ν(Ø-N)(H) (cm^{-1})	
		KBr disk	CH_2Br_2 soln.	KBr disk	CH_2Br_2 soln.	KBr disk	CH_2Br_2 soln.
1	Acetanilide	1556	1524	1323	1313	1264	1249
2	Benzanilide	1531	1525	1323	1316	1261	1253
3	Hexananilide	1553	1521	--[a]	--[a]	1259	1245
4	p-Aminoacetanilide	1552	1514[b]	1322	1314	1266	1230
5	p-Bromoacetanilide	1532	1511	1308	1304	1256	1245
6	p-Chloroacetanilide	1539	1510	1314	1304	1260	1245
7	p-Hydroxyacetanilide	1564	1507[b]	1328	--	1261	--
8	p-Iodoacetanilide	1534	1508	1315	1306	1258	1245
9	p-Methoxyacetanilide	1562	1512[b]	1321	1307	--[c]	--[c]
10	p-Methylacetanilide	1550	1517[b]	1323	1313	1264	1248
11	p-Nitroacetanilide	1567	1535	1304	1303	1269	--

[a]Absorption cannot be differentiated from other bands present.

[b]Amide II band is degenerate with phenyl absorption near 1515 cm^{-1}.

[c]Absorption obscured by strong band near 1250 cm^{-1} due to the methoxy group.

Table 5. (Continued)

Compound		Amide II (cm^{-1})		Amide III (cm^{-1})		ν(Ø-N)(H) (cm^{-1})	
		KBr disk	CH_2Br_2 soln.	KBr disk	CH_2BR_2 soln.	KBr disk	CH_2Br_2 soln.
12	m-Aminoacetanilide	1551	1531	1325	1323	1260	1248
13	m-Bromoacetanilide	1541	1516	1311	1300	1258	1246
14	m-Chloroacetanilide	1540	1517	1310	1299	1260	1248
15	m-Hydroxyacetanilide	1569	1530	1349	--	1283	1281
16	m-Methylacetanilide	1547	1530	1327	1307	1262	1245
17	m-Nitroacetanilide	1551	--[d]	1328	1320	1261	1248
18	o-Bromoacetanilide	1531	1518	1298	1299	1255	1241
19	o-Chloroacetanilide	1531	1520	1302	1303	1258	1244
20	o-Fluoroacetanilide	1547	1523	1320	1321	1268	1258
21	o-Hydroxyacetanilide	1545	1524	1333	1317	--[a]	--[a]
22	o-Methoxyacetanilide	1547	1528	1324	1334	--[c]	--[c]
23	o-Methylacetanilide	1538	1517	1301	1304	1274	1257
25	2,6-Dibromoacetanilide	1520	1481	1290	1237	1283	1265
26	2,6-Dimethylacetanilide	1540	1490	1305	1248	1289	1268

[d]Band obscured by strong absorption arising from the nitro group.

localized vibration, such as δ(NH), the size of the difference between the solid state and solution frequencies could give some qualitative measure of the degree of association in the solid state providing that there are no other crystal effects operative. Similar information could be obtained from the amide III band if it arose from a pure ν(C-N), though the effect of state would be small. However, these absorptions undoubtedly arise from mixed vibrations as evidenced by the isotopic substitution data presented below and by the lack of a direct relationship between the sensitivities of the amide II and III bands to changes of state. Indeed, it is probable that the amide II and III vibrations are tightly coupled but the degree of coupling may vary from compound to compound. Thus, it is not possible to separate the association, crystal and coupling effects from one another merely by considering the data in Table 5. However, by considering these data in conjunction with that obtained from isotopic substitution and from the other spectral regions, it is possible to obtain some qualitative measure of the contributions of these effects. It is also possible to determine more clearly the origins of the bands listed in Table 5.

The frequency shifts for the three principal amide group absorptions in the 1600-1200 cm^{-1} region on ^{15}N substitution are listed in Table 6. The isotopic ratio, ν_{14_N} / ν_{15_N}, for the amide II band varies from 1.005 to 1.008. Such ratios

are much larger than the 1.002 expected for a pure NH mode but much smaller than the 1.015 ratio expected for a C-N stretching vibration. The amide III and ν(Ø-N)(H)* bands exhibit ν_{14_N}/ν_{15_N} ratios in the range of 1.001-1.004. These data indicate that there is considerably more nitrogen motion in the amide II band than in either the amide III or ν(Ø-N)(H) bands.

On deuteration, the three absorptions listed in Table 5 disappear and new bands are present near 1400, 1270-1330 and 1080 cm^{-1} which are listed in Table 7. In addition, a strong absorption at 1390-1440 cm^{-1} disappears on deuteration and new bands are present near 1470 and 980 cm^{-1} in the deuterated anilides.

In several cases, it is very difficult to correlate the new bands in the deuterated compounds with the absorptions of the normal materials simply by comparing the shapes, intensities and solid state-to-solution sensitivity of the absorptions. This is illustrated for the amide II band by the spectra in Figures 30 and 31. Referring to the solid state spectra of acetanilide in Figure 30, the 1500, 1470 and 1400 cm^{-1} absorptions of the deuterated species could be correlated with the amide II, 1500 and 1435 cm^{-1} bands, respec-

---

*This symbolism, while not explicitly correct, will be used throughout this discussion to describe the 1260 cm^{-1} band in anilides. A more thorough description of the mode will be found later.

Table 6. Observed frequency shifts in the characteristic amide group absorptions in the 1600-1200 cm^{-1} region of N-monoaryl amides on nitrogen-15 substitution

Compound	Amide II (cm^{-1})		Amide III (cm^{-1})		ν(Ø-N)(H) (cm^{-1})	
	KBr disk	CH_2Br_2 soln.	KBr disk	CH_2Br_2 soln.	KBr disk	CH_2Br_2 soln.
Acetanilide	- 7.7	-10.7	-2.7	-3.2	-1.6	-3.5
Benzanilide	-10.6	- 8.9	-1.4	-2.0	<1	+2.1
Hexananilide	- 6.9	- 8.4	--[a]	-3.1	-2.1	-3.3
o-Chloroacetanilide	- 7.6	-11.4	-4.0	-5.7	-1.2	-2.0
p-Nitroacetanilide[b]	- 8.0		-2.2		-4.6	

[a]Position of amide III band in hexananilide is uncertain in the solid state.

[b]The spectrum of p-nitroacet-^{15}N-anilide was not obtained in solution due to its extremely low solubility.

Table 7. Observed frequencies of the characteristic amide group absorptions in the 1450-1000 cm^{-1} region of deuterated N-monoaryl amides

	Compound	Amide II' (cm^{-1}) (ν_{as}(C-N-C))		ν(Ø-N)(D) (cm^{-1}) (ν_s(C-N-C))		Amide III' (cm^{-1}) (δ(N-D))	
		KBr disk	CH_2Br_2 soln.	KBr disk	CH_2Br_2 soln.	KBr disk	CH_2Br_2 soln.
1	Acetanilide	1403	1400	1330	1323	1069	--
2	Benzanilide	1412	1401	1331	1325	--	--
3	Hexananilide	1425	1406	--	--	1027	--
4	p-Aminoacetanilide	1408	1407	1312	1311	1113	--
6	p-Chloroacetanilide	1383	1383	1301	--	1080	--
9	p-Methoxyacetanilide	1403	1396	--	--	1079	--
10	p-Methylacetanilide	1396	1389	1312	1312	1076	1065
11	p-Nitroacetanilide[a]	1400		1301		1079	
14	m-Chloroacetanilide	1401	1390	1298	--	1100	--
16	m-Methylacetanilide	1390	1401	1310	--	1085	--
17	m-Nitroacetanilide	1403	1391	1289	1293	1097	--
19	o-Chloroacetanilide	1404	1384	1273	1279	1094	1087
23	o-Methylacetanilide	1407	1388	--	--	1078	1065
25	2,6-Dibromoacetanilide	1397	1377	--	--	1100	--

[a]The spectrum of p-nitroacetanilide-d was not obtained in solution.

Figure 30. Infrared spectra of acetanilide and deuterated acetanilide in the 1800-1100 cm^{-1} region

A. Acetanilide in a KBr disk
B. Deuterated acetanilide in a KBr disk
C. Acetanilide in CH_2Br_2 solution
D. Deuterated acetanilide in CH_2Br_2 solution

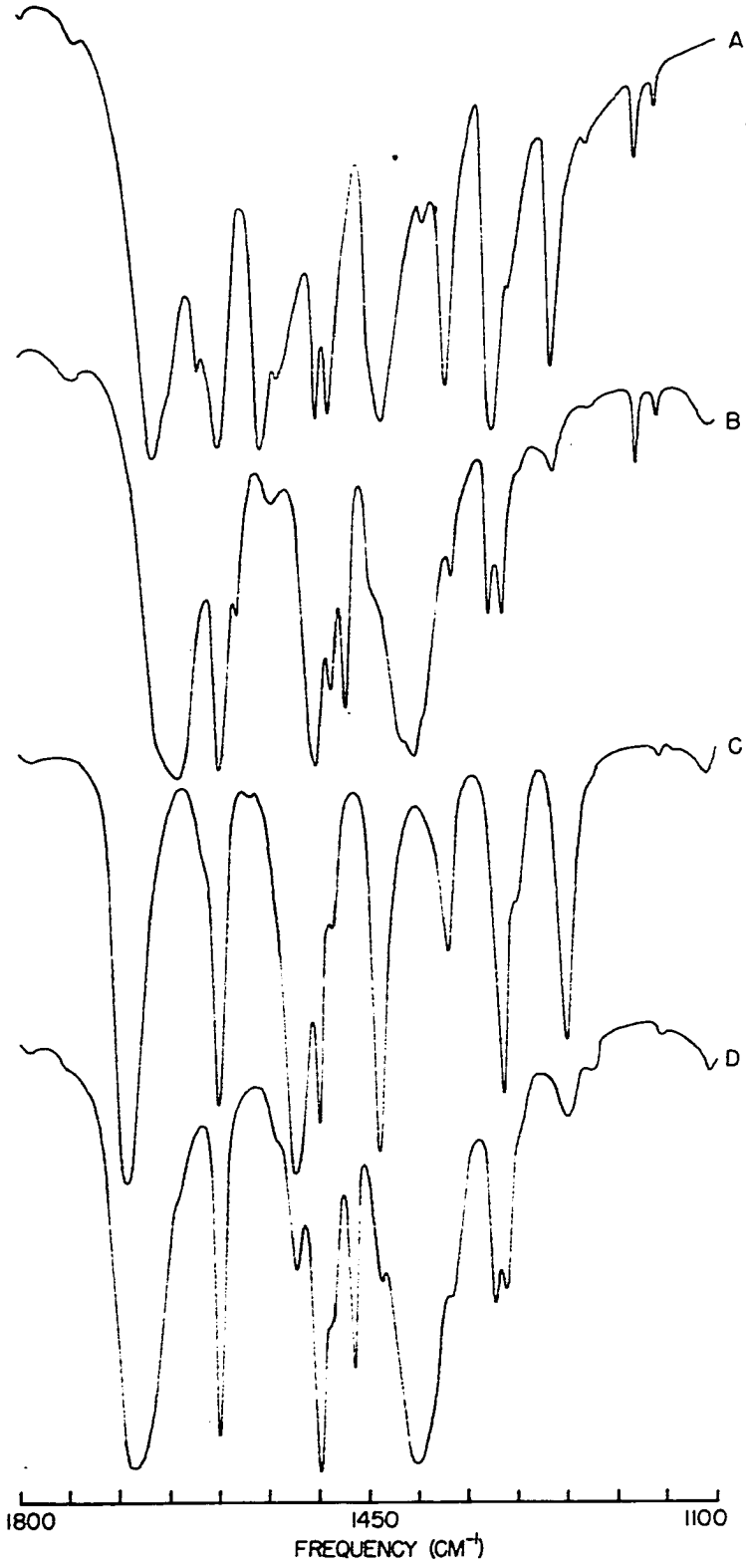
A
B
C
D
1800
1450
1100
FREQUENCY (CM⁻¹)

Figure 31. Infrared spectra of o-chloroacetanilide and deuterated o-chloroacetanilide in the 1800-1100 cm^{-1} region

A. o-Chloroacetanilide in a KBr disk
B. Deuterated o-chloroacetanilide in a KBr disk
C. o-Chloroacetanilide in CCl_4 solution
D. Deuterated o-chloroacetanilide in CCl_4 solution

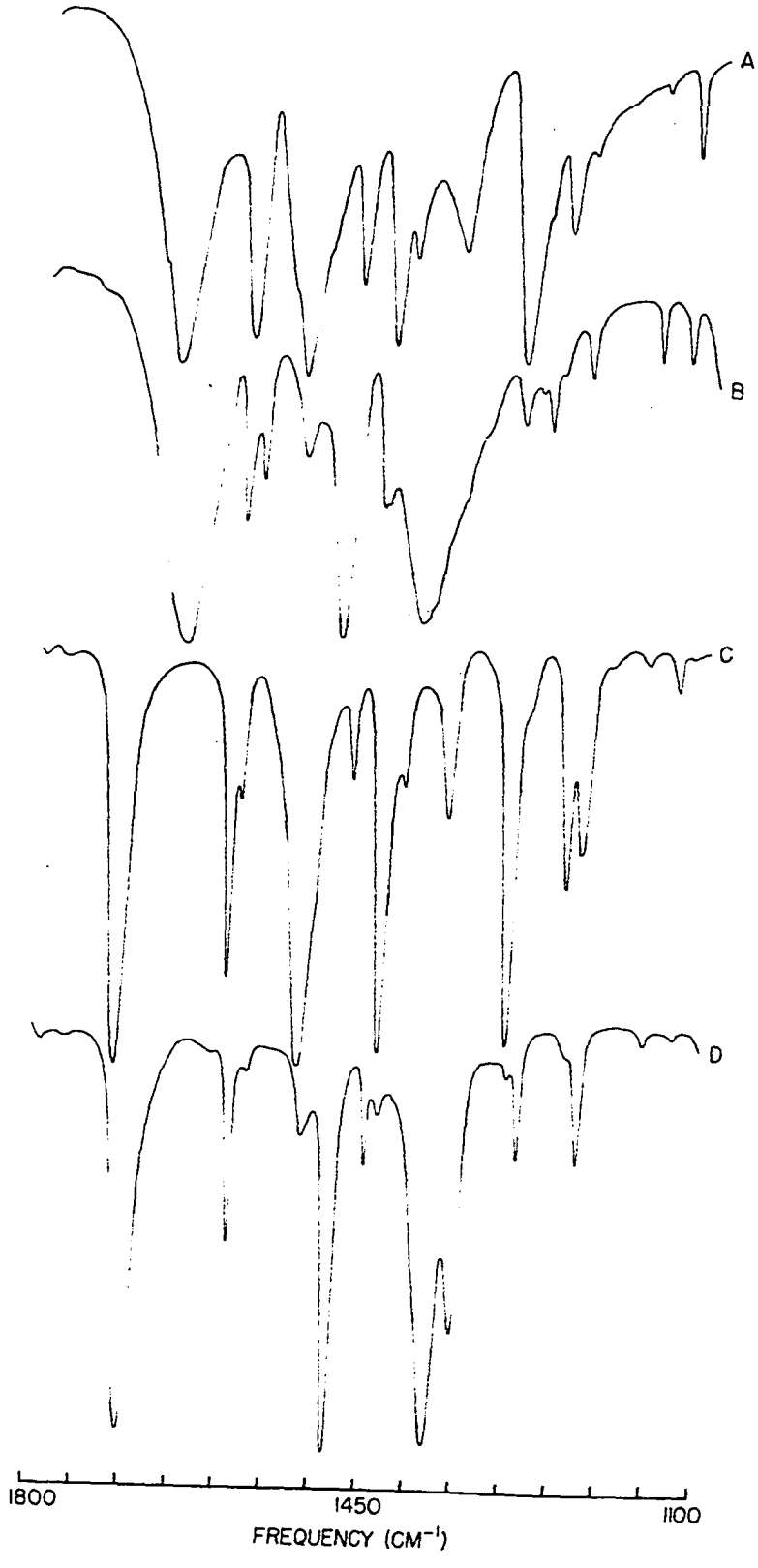
A
B
C
D
1800
1450
1100
FREQUENCY (CM⁻¹)

tively, of the normal compound. Similar conclusions could be made from the solution spectra in Figure 30. For o-chloroacetanilide in Figure 31, however, the amide II band has apparently shifted to 1400 cm^{-1} on deuteration while the 1430 cm^{-1} absorption has either shifted higher to 1487 cm^{-1} or lower and is obscured by the 1400 cm^{-1} band. The spectra in Figures 30 and 31 also indicate that the amide III and $\nu(\text{Ø-N})(\text{H})$ bands near 1300 and 1250 cm^{-1}, respectively, are strong absorptions. However, there are no new absorptions present below 1350 cm^{-1} in the spectra of the deuterated species which have an intensity that even approximates that of the original 1300 and 1250 cm^{-1} bands. There are new bands near 1080 and 980 cm^{-1} (not shown in Figures 30 and 31) but these are only of moderate-to-weak intensity. The new bands at 1330 and 1275 cm^{-1} in acetanilide-d and o-chloroacetanilide-d, respectively, are also much weaker than either the amide III or $\nu(\text{Ø-N})(\text{H})$ bands.

The use of ^{15}N substitution in acetanilide-d and o-chloroacetanilide-d aided in resolving these difficulties somewhat. The observed frequency shifts on ^{15}N substitution for the new absorptions in these two compounds are listed in Table 8. By comparing the data in Table 8 with the corresponding data in Table 6, it is evident that none of the absorptions in Table 8 exhibit shifts comparable to those of the amide II band. However, the magnitude of the ^{15}N shift

Table 8. Observed frequency shifts on nitrogen-15 substitution in acetanilide-d and o-chloroacetanilide-d for the possible absorptions characteristic of the -COND- group in the 950-1500 cm^{-1} region

Approximate absorption frequency (cm^{-1})	^{15}N shift in acetanilide-d (cm^{-1})		^{15}N shift in o-chloroacetanilide-d (cm^{-1})	
	KBr disk	CH_2Br_2 soln.	KBr disk	CH_2Br_2 soln.
1500	< 1	< 1	--	--
1480	- 4.8	< 1	- 3.6	- 2.4
1400	-13.9	-19.6	-15.4	- 8.5
1340[a]	- 2.0	- 1.5	- 2.0	< 1
1080	- 1.0	--	- 2.5	- 1.6
980	< 1	< 1	- 2.4	- 3.9

[a]This absorption is close to 1270 cm^{-1} in o-chloroacetanilide-d.

of the 1400 cm^{-1} absorption makes it the logical choice for the deuterium analog of the amide II band and is thus assigned to the amide II' band. The 1500 and 1480 cm^{-1} absorption listed in Table 8 probably arise from vibrations localized mostly in the phenyl ring or are skeletal modes and will be discussed in a later section. It is not possible, on the basis of the data in Table 8, to make definite assignments for the deuterium analogs of the amide III and ν(Ø-N)(H) bands. Justification for the assignments in

Table 7 will be presented below.

From the above discussion, it is evident that the amide II, amide III and ν(Ø-N)(H) vibrations are mixed since they are all affected by deuteration of the amide group. The amide II vibration must involve considerable nitrogen motion since it shows a large shift on ^{15}N substitution. This shift, however, is at most one-half that expected for a pure ν(C-N) so the assignment of Miyazawa *et al.* (51, 52) of 60% δ(NH) and 40% ν(C-N) is reasonable. However, if ν(C-N) made the major contribution to the amide III band, a fairly large ^{15}N shift might have been expected for this absorption. The fact, though, that only a small shift is observed does not discredit the assignment of Miyazawa (51, 52) since the amide III band is probably coupled to the 1260 cm^{-1} band. Such a coupling would prevent the amide III band from exhibiting the expected large ^{15}N shift. The insensitivity of the ν(Ø-N)(H) absorption to ^{15}N substitution is not unexpected. As will be seen later, this vibration involves considerable motion of the atoms in the phenyl ring and the amplitude of nitrogen motion is relatively small.

The coupling of the vibrational modes involved in the amide II, amide III and ν(Ø-N)(H) bands is apparently significantly altered by deuteration. This is not unexpected since δ(ND) is generally observed below 1100 cm^{-1} and is not likely to couple strongly with absorptions above 1300 cm^{-1}. The

^{15}N shift observed in the amide II' band is nearly that expected for an absorption arising solely from a ν(C-N). Also, the position (7, 20) and phase sensitivity is more like that expected for such a vibration. However, the vibration which involves considerable stretching of the phenyl-nitrogen bond should still give rise to an absorption near 1300 cm^{-1}, even in the deuterated compounds. Such a vibration would be very likely to couple with the ν(C-N) of the amide group. This would result in a symmetric and an asymmetric stretching vibration of the C-N-C system. The asymmetric mode would probably lie at a higher frequency and it is possible that the amide II' band arises mostly from this vibration. The corresponding symmetric vibration may give rise to the absorption at 1270-1330 cm^{-1} listed in Table 7. This is supported by the graph shown in Figure 32. Here, the difference in the frequencies between the amide III and ν(Ø-N)(H) bands of the undeuterated anilides is plotted against the difference between the amide II' and 1270-1330 cm^{-1} bands of the deuterated compounds. The linear relationship which exists between these pairs of bands indicates that the amide II' and 1270-1330 cm^{-1} absorptions may be coupled in a manner analogous to that of the amide III and ν(Ø-N)(H) bands. Thus, it is possible that the 1400 and 1270-1330 cm^{-1} bands of deuterated anilides arise from vibrations involving principally ν_{as}(C-N-C) and ν_{s}(C-N-C),

Figure 32. Plot of the difference between the amide II and ν(Ø-N)(H) frequencies *vs* the difference between the amide II' and ν(Ø-N)(D) frequencies in the potassium bromide disk spectra of N-monoaryl amides (numbers within the circles refer to the compounds listed in Table 6)

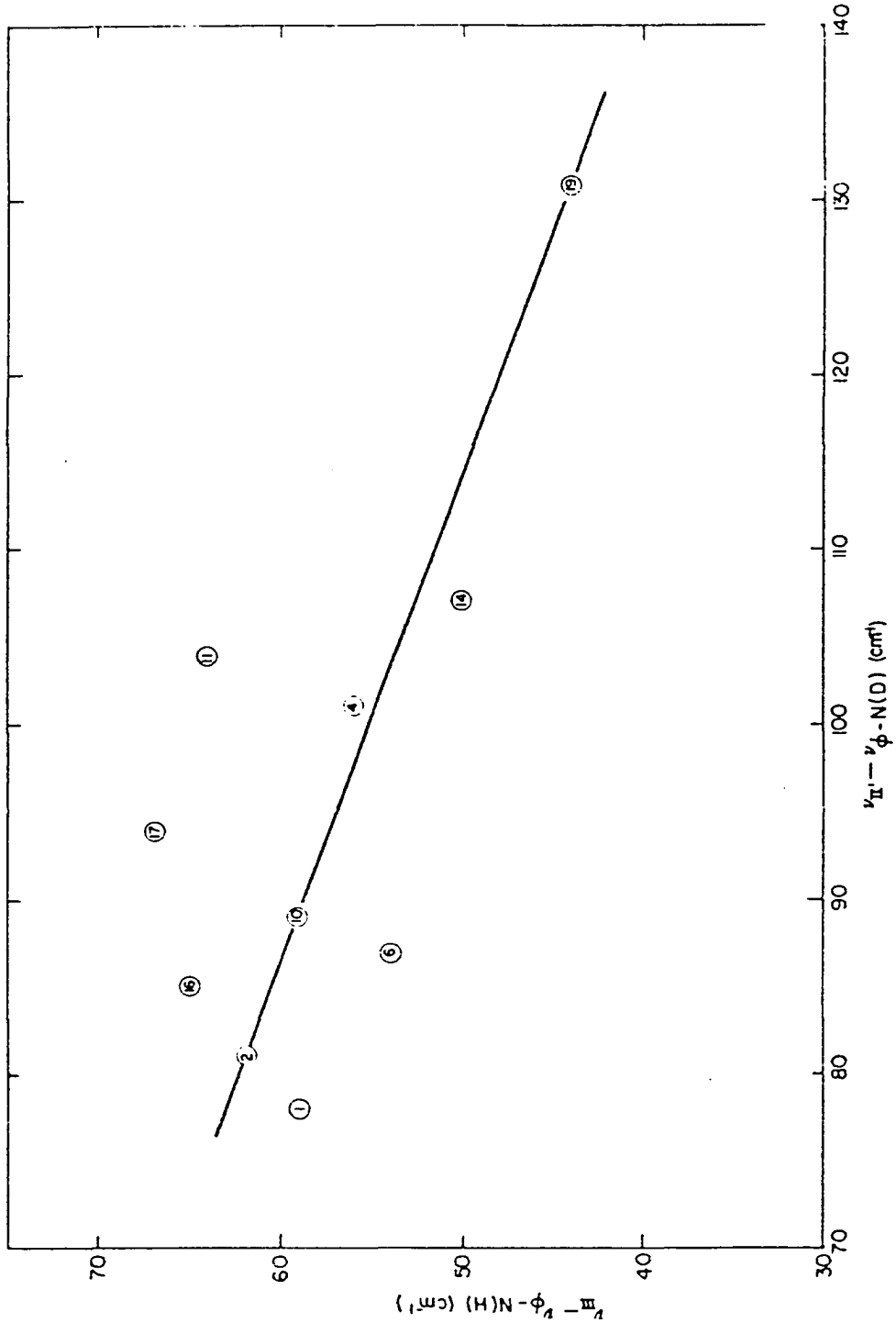
$\nu_{III} - \nu_{\phi\text{-}N(H)}$ (cm^{-1})
$\nu_{II'} - \nu_{\phi\text{-}N(D)}$ (cm^{-1})
70
60
50
40
30
140
130
120
110
100
90
80
70
1
2
3
4
5
6
7
8
9
10
11
12
13
14
15
16
17
18
19

respectively. Deviations from the graph in Figure 32 probably result from differences in the contribution of the phenyl ring to the 1270-1330 cm^{-1} band. The compounds containing the nitro group exhibit the largest deviations. This group, with its high electron-withdrawing power would be expected to exert the greatest influence on the phenyl-amide bond and thus have a large effect on absorptions involving these groups.

If the asymmetric and symmetric C-N-C stretching modes contribute to the amide II' and ν(Ø-N)(D) bands, they probably contribute to the amide III and ν(Ø-N)(H) vibrations of the normal compounds. Thus, the amide III vibration may consist principally of ν_{as}(C-N-C) coupled with δ(NH). The ν(Ø-N)(H) vibration may involve ν_s(C-N-C) and δ(NH) with considerable contribution from a vibration of the phenyl ring discussed later. Such complex vibrations may then account for the lack of ^{15}N sensitivity in these two absorptions.

As mentioned previously, Abbott and Elliott (1) have assigned the ND in-plane deformation to the absorption at 980 cm^{-1} in acetanilide-d. If the ν(C-N) and the δ(NH) of the secondary amide group strongly couple to yield the amide II and III bands, then the natural frequencies of these vibrations must be nearly equal. Since ν(C-N) is apparently near 1400 cm^{-1} in deuterated anilides, the natural frequencies

of ν(C-N) and δ(NH) in the normal compounds could not be below 1400 cm^{-1}. Since deuteration should result in an isotopic shift not to exceed 1.37 for an NH mode, δ(ND) could not be lower than 1020 cm^{-1}. If the natural frequencies of ν(C-N) and δ(NH) were degenerate and the splitting due to coupling was equal, then the average value of the amide II and III frequencies would be close to these natural frequencies. This average value is about 1425-1440 cm^{-1} for the anilides studied and thus δ(ND) should not lie lower than 1040-1050 cm^{-1}. Therefore, 980 cm^{-1} is too low to correspond to δ(ND) and the 1080 cm^{-1} absorption listed in Table 7 is assigned to this vibration and termed the amide III' band.

Further evidence for assigning the 1080 cm^{-1} band to the amide III' band comes from calculating the ratio $\nu_{II}\nu_{III}/\nu_{II'}\nu_{III'}$. Using the 1069 cm^{-1} absorption of acetanilide-d as the amide III' band, this product ratio is 1.37. If the 980 cm^{-1} frequency is used for $\nu_{III'}$, this ratio is 1.50. Miyazawa *et al.* (51) performed this calculation for N-methylacetamide and obtained a value of 1.37. Such a calculation assumes that δ(NH) is almost wholly divided up between the amide II and III bands and that other vibrations are not appreciably affected by deuteration. This is not strictly true, of course, but the 1.50 ratio is so far from the expected value that including the other vibrations which

are affected by deuteration would not be likely to bring the value down to near 1.37. Thus it seems unlikely that the 980 cm^{-1} band could be associated principally with δ(ND) as Abbott and Elliott (1) have concluded. From the spectra these authors have published, it is possible to correlate the 980 cm^{-1} band of crystalline acetanilide-d with the 1013 cm^{-1} band of acetanilide. Since they do not report their dichroism data on this 1013 cm^{-1} band nor on the 1069 cm^{-1} band of the deuterated species, it is not possible to interpret their spectra completely. More will be said about the 1013 cm^{-1} band in a later section.

To summarize, the amide II, amide III and 1260 cm^{-1} absorptions of N-monoaryl amides arise from mixed vibrations. The in-plane deformation of the NH group couples with the ν(C-N) of the amide group to yield the amide II and III bands. The amide III band then couples weakly with the phenyl-nitrogen stretching mode. The amide II vibration is probably very nearly that assigned by Miyazawa et al. (51, 52). The amide III band involves δ(NH), ν(C-N) and ν(Ø-N) and may best be described by ν_{as}(C-N-C) coupled with δ(NH). The 1260 cm^{-1} band arises principally from a substituent-sensitive phenyl mode but coupling with the amide III band causes ν_s(C-N-C) to make a considerable contribution. Upon deuteration, the coupling with δ(NH) is removed. The amide II' absorption arises from a vibration involving mostly

ν_{as}(C-N-C) whereas the ν(Ø-N)(D) band consists of ν_s(C-N-C) with considerable aromatic contribution. The δ(ND) vibration is positioned near 1080 cm^{-1} in deuterated anilides.

In the discussion thus far, the 1260 cm^{-1} band of N-monoaryl amides has been referred to as ν(Ø-N)(H). This is somewhat of a simplification. In monosubstituted benzenes, the stretching vibration of the Ø-X bond, where X is some substituent atom or group other than hydrogen, interacts with one of the ring breathing vibrations to yield a vibration termed the "q" mode (60). This mode is sensitive to the nature of X but is generally found in the 1030-1250 cm^{-1} region in monosubstituted benzenes (60, 71). Para-substituted benzenes exhibit two substituent-sensitive phenyl modes in the 1060-1300 cm^{-1} region (25, 36) each of which is specific for one of the substituents. For example, the spectra of para-substituted phenols (36) show a strong band near 1260 cm^{-1} which is assigned to ν(Ø-OH) and a second band in the 1069-1231 cm^{-1} region which varies considerably with the para substituent. This second band is assigned to a mode involving principally stretching of the Ø-X bond. Similar results are found (25) for other series of compounds such as anilines and bromobenzenes. On this basis then, substituted acetanilides should be expected to exhibit two absorptions in the 1050-1300 cm^{-1} region which arise from substituent-sensitive phenyl modes and one of these should be relatively

constant. In anilines, the $\nu(\text{Ø-NH}_2)$ is apparently near 1270 cm^{-1} (25). Thus, 1260 cm^{-1} is not an unreasonable position for $\nu(\text{Ø-N})(\text{H})$ in substituted acetanilides. More will be said about the other substituent-sensitive phenyl modes in a later section.

If there is strong coupling between the amide II and III bands in anilides, certain factors which affect the frequency of one of the absorptions should also be noted in the other. This is especially true of the changes due to the electrical effects of the substituent groups which alter the electron distribution within the amide group. Hence, there should be some relationship between the amide II and amide III frequencies of a given series of substituted acetanilides, for example, the para-substituted compounds. However, the inductive effects of substituents vary with position and the relationship for the ortho- and meta-substituted compounds would not be expected to be the same as that for the para derivatives. Thus, plots of ν_{II} vs ν_{III} should yield characteristic curves for each of the three types of substituted acetanilides. Those compounds which do not fall close to these curves must then be under the influence of other effects or possess a different degree of coupling than most of the anilides. These plots are shown in Figures 33, 34, and 35 for para-, meta- and ortho-substituted acetanilides, respectively.

For para-substituted acetanilides, the plots of ν_{II} vs ν_{III} are shown in Figure 33. In the solid state, most of the points fall close to a straight line and only p-nitro- and p-methoxyacetanilide deviate appreciably from this line. The nitro group, with its strong electron-withdrawing ability, has a large effect on the electronic structure of the ground state of the molecule. The double bond character of the amide C-N bond should be decreased and that of the phenyl-nitrogen bond increased but the partial positive charge on the nitrogen atom may not be appreciably altered. Thus, the vibrations of the C-N-C group may be appreciably different in p-nitroacetanilide than in the other acetanilide but δ(NH) may not be affected. Consequently, the effect of the nitro group may not change the amide II and III band frequencies to the same extent and a deviation from normal behavior should be observed. In addition, both the nitro and the methoxy group may interact intermolecularly in the solid state with the amide hydrogen. Indeed, these groups can probably effectively compete with the carbonyl group for bonding to the hydrogen atom. Since the amide I frequencies in these two compounds do not indicate a free carbonyl group, it is probable that the amide hydrogen interacts with both the carbonyl group and the nitro or methoxy group. On dissolution, this effect is destroyed and p-methoxyacetanilide obeys the linear relationship between the amide II and III bands in solution.

Figure 33. Plot of amide II frequency vs amide III frequency of para-substituted acetanilides (squares refer to dibromomethane spectra, circles refer to KBr disk spectra, and numbers refer to the compounds listed in Table 5)

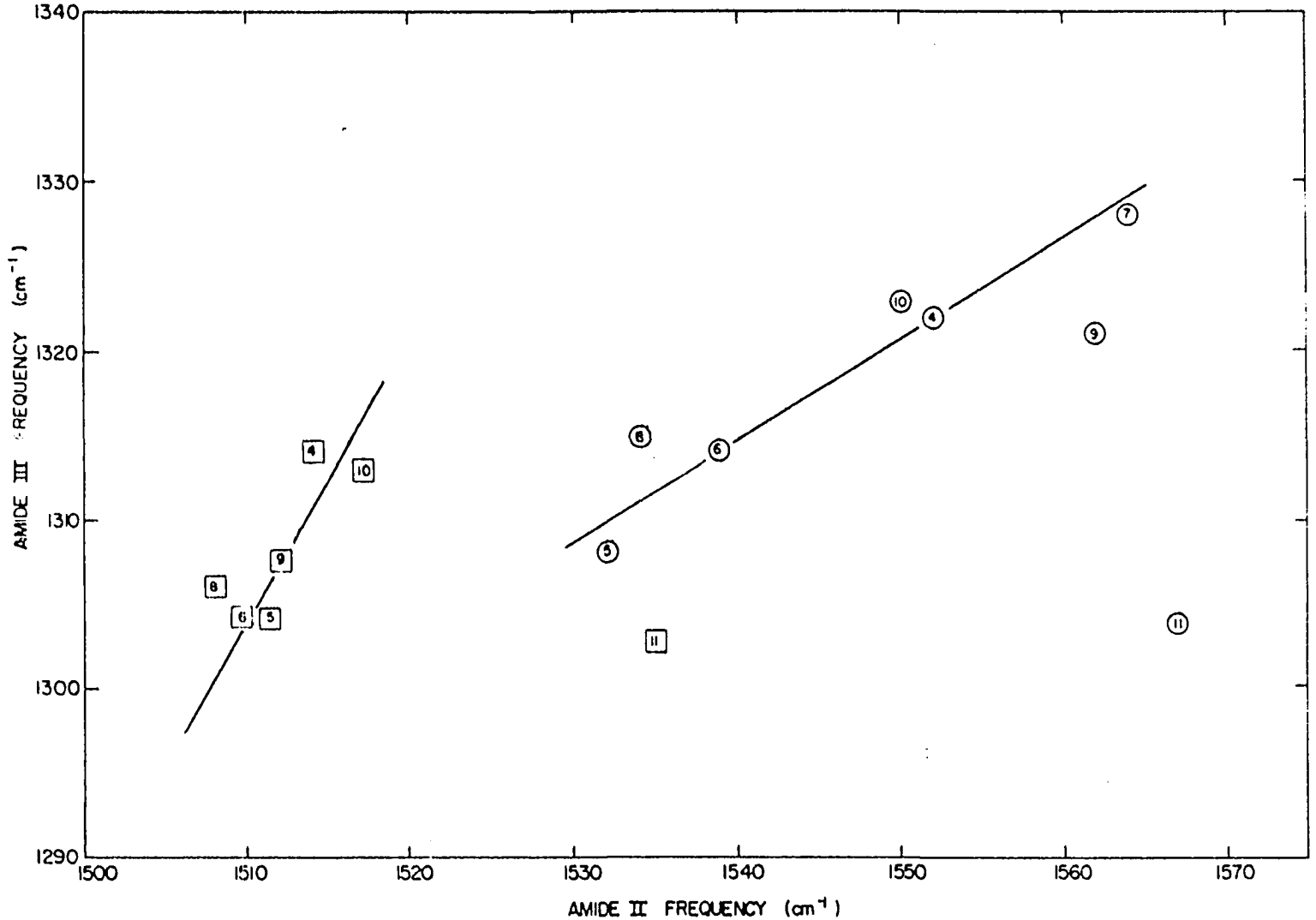
1340
1330
1320
1310
1300
1290
AMIDE III FREQUENCY (cm⁻¹)
1500
1510
1520
1530
1540
1550
1560
1570
AMIDE II FREQUENCY (cm⁻¹)
4
10
9
8
6
5
8
6
10
4
7
9
5
11
11

Para-nitroacetanilide still deviates appreciably, however, which indicates that the electronic effect discussed above is still predominant. In addition, it is possible that the amide II band in solution is held to a high value by interaction with the $\nu_{as}(NO_2)$ absorption at 1508 cm^{-1}.

For the meta-substituted acetanilides, the plots of ν_{II} vs ν_{III} in Figure 34 yield straight lines whose slopes are close to unity. Substituents in the meta position cannot mesomerically interact with the amide nitrogen atom so the variations in the amide II and III frequencies are due almost entirely to the inductive effect of the substituent. On comparing Figures 33 and 34, it is evident that the slope of ν_{II} vs ν_{III} for the solid state of the para derivatives is considerably less than that for the meta-substituted compounds. Thus, the mesomeric effects of the para substituents apparently affect the intermolecular interaction in the solid state of these compounds.

Only m-methylacetanilide deviates appreciably from the straight line in Figure 34. These deviations are perhaps associated in some way with the unusual solubility behavior of this compound. Other than this explanation, no others can be offered which will account for the deviations observed.

The amide II frequency is plotted against the amide III frequency of the ortho-substituted acetanilides in Figure 35. For the frequencies observed in dibromomethane solution, the

Figure 34. Plot of amide II frequency vs amide III frequency of meta-substituted acetanilides (squares refer to dibromomethane spectra, circles refer to KBr disk spectra, and numbers refer to the compounds listed in Table 5)

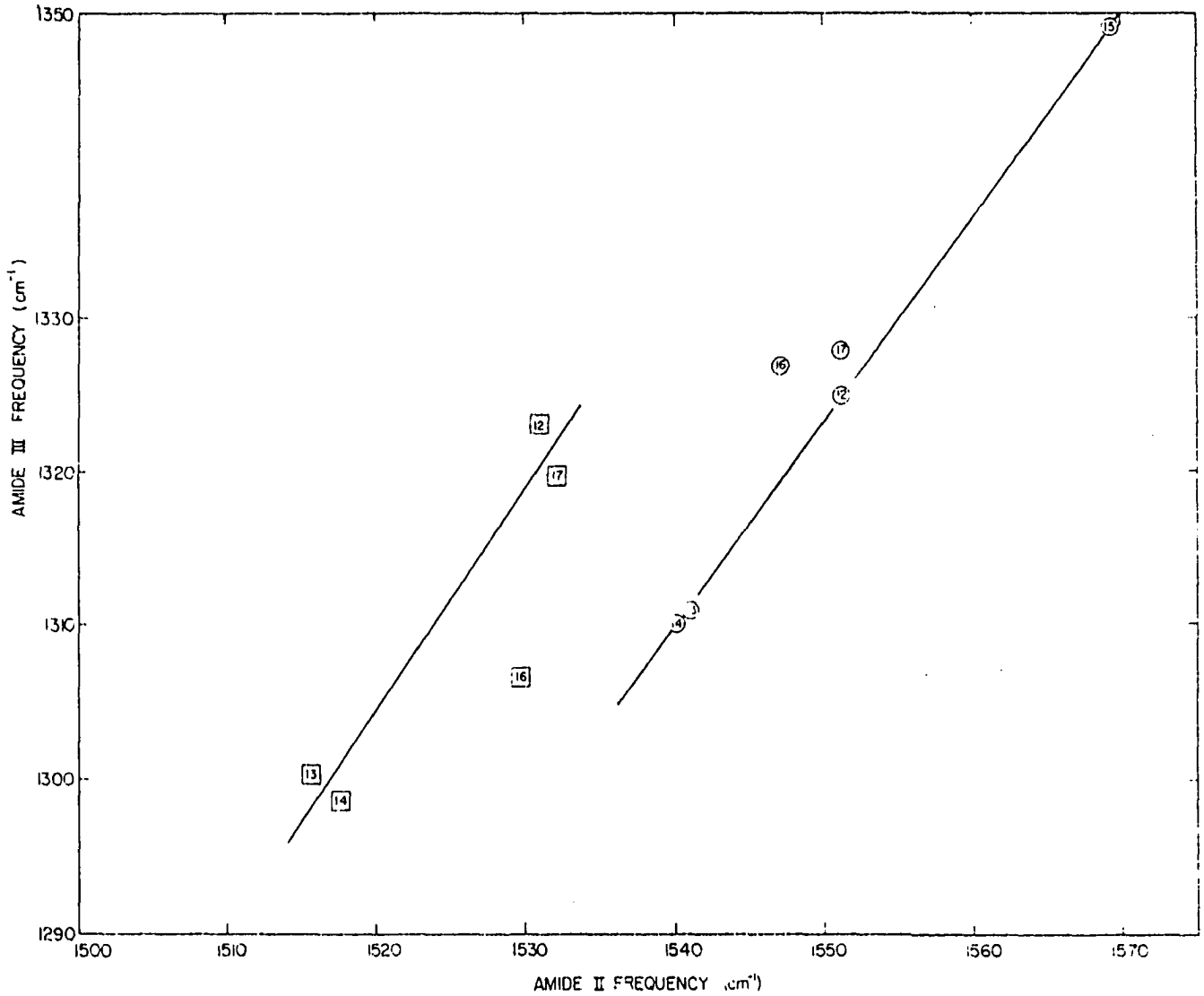
1350
1330
1320
1310
1300
1290
AMIDE III FREQUENCY (cm⁻¹)
1500
1510
1520
1530
1540
1550
1560
1570
AMIDE II FREQUENCY (cm⁻¹)
12
17
16
13
14
15
17
12
13

plot yields a straight line and all the points fall fairly close to this line. The slope of the line, though, is much larger than that observed for the other two groups of compounds. If there is considerable intramolecular interaction between the amide hydrogen and the ortho substituent, this effect will be most strongly observed in the vibrations involving δ(NH). Such interactions may change the natural frequency of δ(NH) and thus alter the coupling between δ(NH) and ν(C-N). The relative contributions of these modes to the amide II and III vibrations in ortho-substituted acetanilides may then be significantly different from the other substituted acetanilides. Since the nitrogen atom is in conjugation with the aromatic nucleus, the inductive and mesomeric effects of substituents on the phenyl ring would be more pronounced in the ν(C-N) and ν(C=O) frequencies than in absorptions arising from the NH bond. Since the amide III band shows a much larger variation in frequency than the amide II band in ortho-substituted acetanilides, it may be concluded that the contribution of ν(C-N) to the amide III band is significantly greater in these compounds than in the other groups of substituted acetanilides. In further support of this is the larger ^{15}N shift of the amide III band in o-chloroacetanilide (see Table 6) than in the other anilides.

For the solid state plot of ν_{II} vs ν_{III} of ortho-substituted acetanilides, several compounds exhibit con-

Figure 35. Plot of amide II frequency vs amide III frequency of ortho-substituted acetanilides (squares refer to dibromomethane spectra, circles refer to KBr disk spectra, and numbers refer to compounds listed in Table 5)

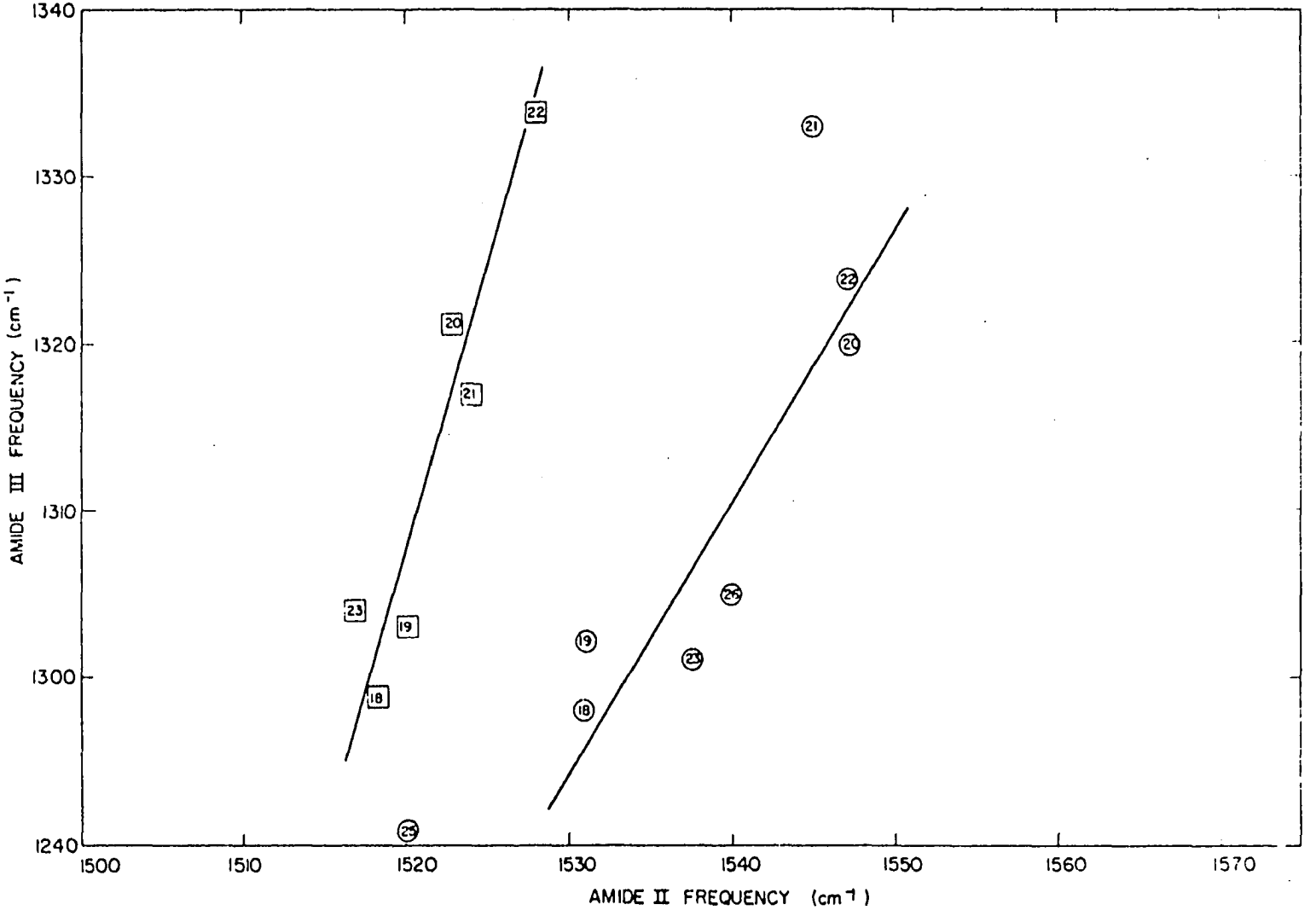
1340
1330
1320
1310
1300
1240
AMIDE III FREQUENCY (cm⁻¹)
1500
1510
1520
1530
1540
1550
1560
1570
AMIDE II FREQUENCY (cm⁻¹)
22
20
21
23
19
18
24
21
22
20
26
19
23
18

siderable deviation from the expected linear relationship. Ortho-bromoacetanilide, in which there is probably considerable attraction between the bromine atom and the amide hydrogen, lies above the line while o-methylacetanilide, where repulsion between the methyl and hydrogen exists, lies below the line. The diortho-substituted acetanilides lie on the same side of the line as the corresponding monosubstituted acetanilides which indicates that steric and field effects probably cause these deviations. Orthohydroxyacetanilide exhibits the largest deviation in Figure 35 and this is probably due to the existence of intramolecular association between the hydroxyl group and the carbonyl oxygen. Such bonding causes an increase in the double bond character of the C-N bond and thus an increase in the natural frequency of ν(C-N). This may account for the relatively high amide III frequency. Also, this intramolecular association prevents the carbonyl group from bonding strongly with the amide hydrogen. This weaker bonding would cause a lower δ(NH) frequency in the solid state and thus may account for the low amide II band frequency.

The solution frequencies of the amide II and III bands of the diortho-substituted acetanilides are too low to place on Figure 35. Even if the scales were extended, the two points would fall well off the line drawn in Figure 35. The unusually low frequencies of these absorptions for these two

compounds undoubtedly result from their non-planar structure but the exact reason for these phenomena is uncertain. In the non-planar structure, the amide hydrogen atom can probably interact with the π-electron cloud of the phenyl ring, especially during the in-plane deformation of the NH group. Since this interaction would be one of attraction, the amide II and III frequencies should be similar to those of the ortho-halogen acetanilides. This is observed in the solid state. However, the non-planar structure causes the amide hydrogen atom to be more prone to intermolecular association and thus the absorptions arising from the amide group should show large frequency shifts on passing from the solution spectra to the solid state spectra. This, too is observed but the frequencies in the solid state spectra should be higher than normal since the bonding is stronger. There may be some difference in the relative contributions of δ(NH) and ν(C-N) since the sensitivity to state is greater for the amide III band than for the amide II which is just the reverse of what is normally observed. However, this does not account for the unusually low frequencies either. All these effects are probably present and some combination of them may account for the observed phenomena.

Ortho-nitroacetanilide has been omitted from the discussion thus far because its spectral characteristics in this region are substantially different from the other

acetanilides. The spectra of o-nitroacetanilide and o-nitroacetanilide-d in the solid state and in solution are shown in Figure 36 for the 1100-1800 cm^{-1} region and the frequency values are reported in Table 9 for the 1200-1600 cm^{-1} region. There are no strong absorptions which exhibit consistently large ^{15}N shifts and disappear on deuteration which could correspond to the amide II band. Likewise, no prominent absorptions below 1400 cm^{-1} disappear on deuteration as the amide III and ν(Ø-N)(H) bands normally do. Thus, it is probable that there are no amide II and III bands, as such, in o-nitroacetanilide. Most of the absorptions listed in Table 9 show some sensitivity to isotopic substitution with both ^{15}N and deuterium. This behavior would seem to indicate that most of the absorptions in this region are rather strongly coupled. Such a situation is not unreasonable since coupling can occur through the intramolecular hydrogen bond as well as through the other covalent bonds of the molecule. It is highly unlikely, for example, that the nitro group could vibrate without some motion of the NH bond. The chelate ring may in fact yield a set of characteristic absorptions in the same manner as a phenyl ring. Thus, the nitro stretching modes, the δ(NH) and ν(C-N) of the amide group and the ν(C-C) modes of the phenyl ring all have their natural frequencies in this spectral region and it is highly possible that these vibrations couple to yield a set of

absorption bands characteristic of the

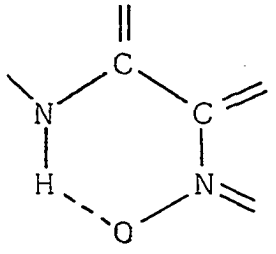

ring. Thus, none of the proposed vibrations in Table 9 make the total contribution to the mode giving rise to a given absorption band. In the undeuterated compound, most of the vibrations are probably strongly coupled to δ(NH) but δ(NH) probably does not make the major contribution to any of the vibrations. In the deuterated compound, however, the natural frequency of δ(ND) is too low to couple strongly with some of the higher frequency modes like $\nu_{as}(NO_2)$ and the phenyl ν(C-C) vibrations but may still couple strongly with the lower frequency modes such as $\nu_s(NO_2)$ and ν(Ø-N)(D). This coupling in the deuterated compound is sufficiently strong to hold δ(ND) to a high value but not strong enough to prevent it from exhibiting an absorption band to which it makes the major contribution.

Table 9. Observed frequencies and suggested assignments for the prominent absorptions of o-nitroacetanilide with frequency shifts produced by nitrogen-15 substitution and for o-nitroacetanilide-d in the 1200-1600 cm^{-1} region

KBr disk (cm^{-1})[a]			CCl_4 solution (cm^{-1})[a]			Suggested assignments
$\nu 14_{NH}$	$\Delta\nu 15\text{-}14$	$\nu 14_{ND}$	$\nu 14_{NH}$	$\Delta\nu 15\text{-}14$	$\nu 14_{ND}$	
1585(s)	-2.4	1574(m)	1588(vs)	-2.4	1575(w)	phenyl ν(C-C)
1541(w)	-6.8	1540(sh)	1532(mw)	+3.7	--	
1507(s)	-6.0	1519(s)	1501(vs)	-1.7	1522(vs)	$\nu_{as}(NO_2)$
--	--	1480(mw)	--	--	1485(ms)	phenyl ν(C-C)
1456(mw)	<1	--	1457(ms)	-1.7	--	phenyl ν(C-C) + $\delta_{as}(CH_3)$
--	--	1445(vw)	--	--	1447(vw)	$\delta_{as}(CH_3)$
1426(mw)	-2.3	--	1432(ms)	-5.4	--	ν(C-N)(H)
--	--	1382(m)	--	--	1375(vs)	ν(C-N)(D)
1371(mw)	<1	1361(vw)	1368(mw)	<1	1358(mw)	$\delta_s(CH_3)$
1344(ms)	-2.0	1339(ms)	1338(s)	-3.1	1336(vs)	$\nu_s(NO_2)$
1319(vw)	<1	--	1316(mw)	<1	--	phenyl ν(C-C)
--	--	1306(m)	--	--	1307(m)	δ(N-D)
1274(m)	-3.3	1277(m)	1278(ms)	-4.6	1275(vs)	ν(Ø-N)
1234(m)	-1.3	1229(mw)	1227(ms)	-3.0	1230(m)	

[a]Letters in parentheses indicate intensities relative to the amide I band.

Figure 36. Infrared spectra of o-nitroacetanilide and deuterated o-nitroacetanilide in the 1800-1100 cm^{-1} region

A. o-Nitroacetanilide in a KBr disk
B. Deuterated o-nitroacetanilide in a KBr disk
C. o-Nitroacetanilide in CCl_4 solution
D. Deuterated o-nitroacetanilide in CCl_4 solution

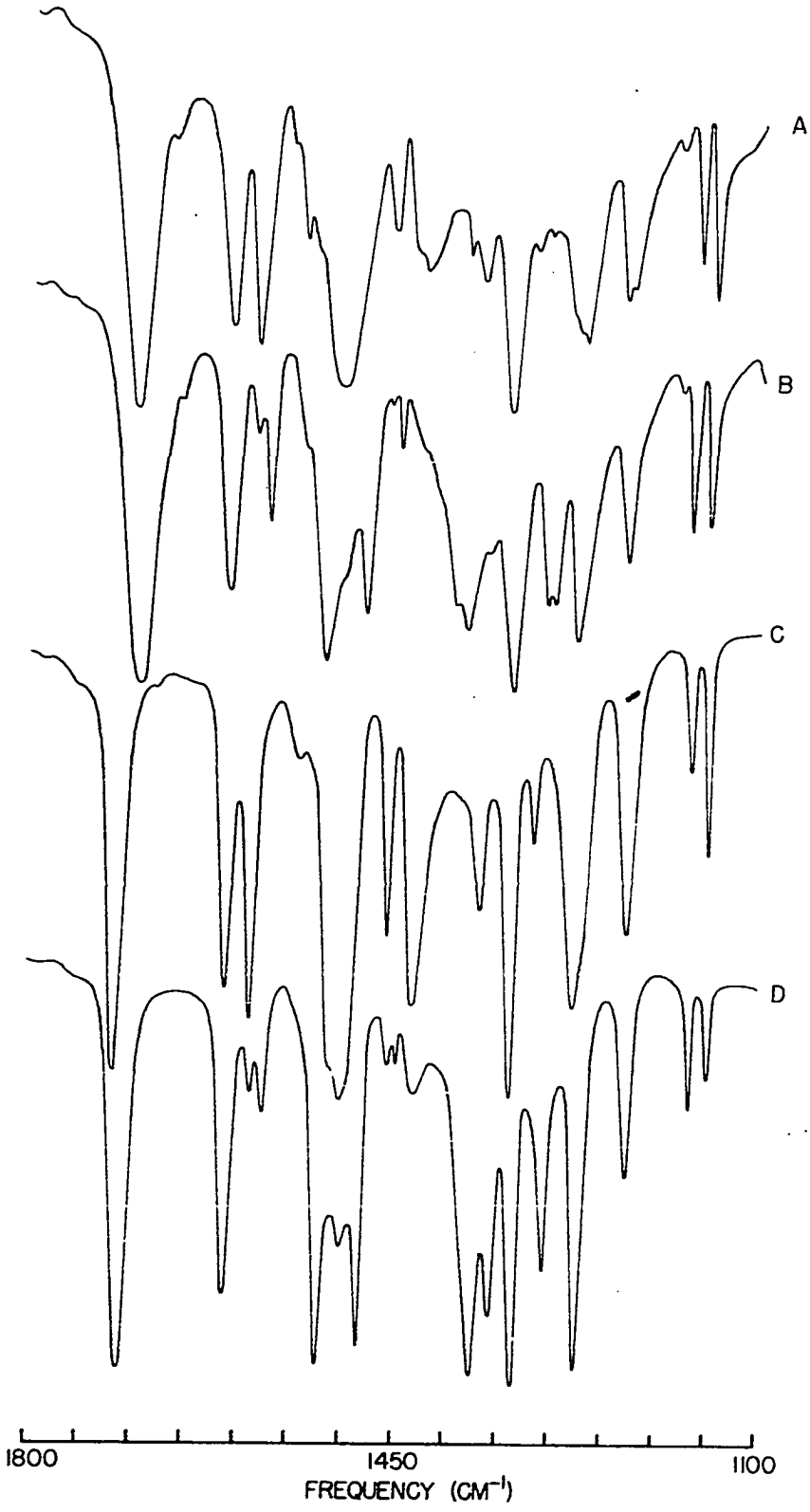
A
B
C
D
1800
1450
1100
FREQUENCY (CM⁻¹)

THE 1200-800 CM^{-1} REGION

Because of the absence of strong absorptions arising from the peptide linkage, this spectral region has received little previous attention. In simple aliphatic secondary amides, the absorptions in this region generally arise from vibrations localized in the alkyl groups, though some coupling with amide group vibrations has been observed (51). In the aromatic amides, there are several absorptions present which arise from the C-H in-plane deformations of the phenyl ring. However, three absorptions are present in most of the anilides studied which are sensitive to isotopic substitution. These absorptions may be characteristic of acetanilides and thus merit some consideration.

The observed frequencies of isotopic sensitive absorptions in this spectral region for anilides in potassium bromide disks are listed in Table 10. Not all of the compounds listed were isotopically substituted so the values in Table 10 were obtained by comparing the spectra of these compounds with those which were isotopically substituted.

The absorption at 1003-1032 cm^{-1} is generally of medium intensity, though it is sometimes partially obscured by other bands. It is a fairly broad band and lies 5-15 cm^{-1} lower in the solution spectra than in the solid state. The band is only slightly sensitive to ^{15}N substitution but it disappears

Table 10. Observed frequencies of isotopic sensitive absorptions in the 800-1200 cm^{-1} region of N-monoaryl amides in potassium bromide disks

Compound	Frequency (cm^{-1})[a]		
Acetanilide	1013(<1)	961(-11.1)	840(-8.3)
Benzanilide	--	885(-8.6)	836[b]
Hexananilide	1011(<1)	966(-8.7)	836(-9.5)
p-Aminoacetanilide	1007	961	867
p-Bromoacetanilide	1008	967	844
p-Chloroacetanilide	1016	969	845
p-Hydroxyacetanilide	1016	969	857
p-Iodoacetanilide	1015	967	840
p-Methoxyacetanilide	1018	970	835
p-Methylacetanilide	1014	965	852
p-Nitroacetanilide	1007(-2.4)	966(-12.8)	832(-4.4)
m-Aminoacetanilide	1017	966	-[c]
m-Bromoacetanilide	1010	963	-[c]
m-Chloroacetanilide	1012	962	-[c]
m-Hydroxyacetanilide	1032	962	-[c]
m-Methylacetanilide	1007	968	-[c]
m-Nitroacetanilide	1018	963	-[c]

[a]The values in parentheses indicate the shift on ^{15}N substitution.

[b]This absorption is very weak and was not present in the spectra of benzanilide-^{15}N.

[c]Absorption either is not present or is obscured by other bands.

Table 10. (Continued)

Compound	Frequency (cm^{-1})[a]		
o-Bromoacetanilide	1010	967	848
o-Chloroacetanilide	1011(-1.8)	967(-11.0)	849(-7.5)
o-Fluoroacetanilide	1018	968	853
o-Hydroxyacetanilide	1019	968	844
o-Methoxyacetanilide	1026	965	843
o-Methylacetanilide	1013	972	856
o-Nitroacetanilide	1003(<1)	967(<1)	836(-7.4)
2,6-Dibromoacetanilide	1015	970	861
2,6-Dimethylacetanilide	1014	973	853

on deuteration and apparently shifts to about 980 cm^{-1}. This 980 cm^{-1} band in acetanilide-d has been assigned by Abbott and Elliott (1) to δ(ND), but its intensity, shape, and sensitivity to state are comparable with the 1013 cm^{-1} band of the normal compound. N-alkyl acetamides (5, 17, 51) exhibit one or more bands in the 980-1050 cm^{-1} region which have been ascribed to the rocking vibration of the methyl group attached to the carbonyl carbon. Since the other absorptions in this region for acetanilides are easily assigned to aromatic modes, the 1003-1032 cm^{-1} band of acetanilides is assigned to $r(CH_3)$. The absence of the 1013 cm^{-1}

band in $CD_3CONHC_6H_5$ (1) and the presence of a new band near 875 cm^{-1} which exhibits dichroism similar to that of the 1013 cm^{-1} band further supports this assignment. The band is also absent in the spectrum of benzanilide where there is no alkyl group. However, the 30 cm^{-1} shift on deuteration indicates that $r(CH_3)$ is probably weakly coupled to vibrations of the amide group, either in the normal or in the deuterated compounds.

The second absorption listed in Table 10 generally lies in the range 960-975 cm^{-1} except for benzanilide. It is a sharp, moderately weak band and lies 2-17 cm^{-1} lower in the solution spectra than in the solid state. It shows a large downward shift on ^{15}N substitution in four of the five compounds and usually shifts 20-50 cm^{-1} lower on deuteration. Gray (28) has assigned the band to a skeletal mode of the C-C-N-C system in which there is considerable stretching of the phenyl-nitrogen bond. Such an assignment is in agreement with the present data except that the vibration is probably mixed with $\delta(ND)$ in the deuterated species thus causing the large shift on deuteration.

The third absorption listed in Table 10 falls in the range 830-885 cm^{-1} and is generally fairly weak in intensity. It is rarely observed in the solution spectra but exhibits a relatively large shift on ^{15}N substitution and shifts 4-24 cm^{-1} lower on deuteration. These data indicate that the

absorption arises from a vibration involving considerable nitrogen motion but only a small amount of hydrogen motion. Monosubstituted benzenes exhibit an absorption in the 650-800 cm^{-1} range which is sensitive to the nature of the ring substituent (60, 71). The vibration arises from an interaction of the C-X stretching mode with one of the planar ring deformations and is termed the "r" mode by Randle and Whiffen (60). Many para-disubstituted benzenes exhibit a similar absorption in the 700-860 cm^{-1} region (25). In the para-substituted phenols, Jakobsen (36) observed an absorption near 850 cm^{-1} which he assigned to a mode analogous to the "r" mode of Randle and Whiffen (60). However, there was also another absorption in these compounds at 600-800 cm^{-1}, which varied considerably with the nature of the para-substituent. Thus, substituted acetanilides might be expected to exhibit two substituent-sensitive phenyl modes in the 600-850 cm^{-1} region but one of these should be relatively constant. Therefore, the isotopically sensitive absorption at 830-885 cm^{-1} is assigned to the substituent-sensitive phenyl mode which involves considerable stretching of the phenyl-nitrogen bond. An attempt will be made to locate the second mode which involves considerable stretching of the phenyl-substituent bond in a later section. The absence of the 830-885 cm^{-1} band in the meta-substituted compounds makes this assignment questionable but the absorption may be obscured by other bands in these compounds.

CHARACTERISTIC AMIDE ABSORPTIONS BELOW 800 CM^{-1}

The lower frequency vibrations of the amide group consist mainly of skeletal bending motions, the one exception being the non-planar bending of the NH group. The phenyl group vibrations which involve bending of the ring and of the ring-substituent bonds also lie in the low frequency region. All of these motions involve low energies and thus are very susceptible to purturbations, especially as a result of coupling of modes. Thus, it is difficult to attribute the bands in this region to specific localized group vibrations, especially in N-monoaryl amides where the conjugative interaction between the phenyl ring and the -CONH- group is large. However, it is useful to attempt to identify the bands in this region which appear to be characteristic of N-monoaryl amides and to name them in accordance with the group mode which makes the major contribution to the vibration.

A moderately intense and broad absorption is present in the spectra of most proteins (6, 49) and secondary amides (7, 17, 18, 37, 41, 51) near 700 cm^{-1} which shifts to near 530 cm^{-1} on deuteration (18, 41, 51). This change by a factor of about 1.36 is almost exactly that expected for a pure NH out-of-plane deformation. It is generally agreed that this absorption arises from γ(NH), though Miyazawa *et al.* (51), who termed the absorption the amide V band,

indicated that other out-of-plane vibrations may also be involved.

The amide V band is easily identified in most N-monoaryl amides by its shape, intensity, and deuteration sensitivity. The proposed positions of the amide V and amide V' bands are listed in Table 11 along with the isotopic shift factors. These shifts are generally somewhat less than that theoretically expected for γ(NH) so there is undoubtedly some coupling with lower frequency modes involved. In certain compounds, the amide V band is apparently obscured by the strong phenyl mode near 750 cm^{-1}. This band does not weaken appreciably on deuteration but does become more narrow at the base of the band (see Figures 1, 3, 11).

Many secondary amides exhibit an absorption at 615-640 cm^{-1} which is generally ascribed to the in-plane deformation of the O=C-N group (18, 37). Miyazawa et al. (51) termed the absorption the amide IV band and assigned (52) it to 40% δ(O=C-N) and 30% ν(C-CH_3) in N-methylacetamide. This compound also exhibits an absorption of medium intensity near 600 cm^{-1}. Davies et al. (17) observed no sensitivity to deuteration in this band and assigned it to a torsional motion of the C-N bond. Miyazawa et al. (51) termed this absorption the amide VI band and assigned it to the out-of-plane deformation, γ(C=O). These latter authors, however, observed that the amide VI band disappeared on deuteration. They assumed that

Table 11. Observed frequencies of the amide V band and its deuterium analog in the potassium bromide disk spectra of N-monoaryl amides along with the ratio of corresponding frequencies

Compound	Amide V band (cm^{-1})	Amide V' band (cm^{-1})	Isotopic ratio V / V'
Acetanilide	-[a]	556	--
Benzanilide	651	483	1.35
Hexananilide	-[a]	563	--
p-Aminoacetanilide	730	554	1.32
p-Bromoacetanilide	742	--	--
p-Chloroacetanilide	751	561	1.34
p-Hydroxyacetanilide	714	--	--
p-Iodoacetanilide	732	--	--
p-Methoxyacetanilide	769	569	1.35
p-Methylacetanilide	755	556	1.36
p-Nitroacetanilide	-[a]	560	--
m-Aminoacetanilide	794	--	--
m-Bromoacetanilide	746	--	--
m-Chloroacetanilide	752	548	1.37
m-Hydroxyacetanilide	734	--	--
m-Methylacetanilide	755	574	1.32
m-Nitroacetanilide	761	571	1.33
o-Bromoacetanilide	676	--	--
o-Chloroacetanilide	710	502	1.41
o-Fluoroacetanilide	-[a]	--	--
o-Hydroxyacetanilide	-[a]	--	--
o-Methoxyacetanilide	711	--	--
o-Methylacetanilide	701	545	1.29
o-Nitroacetanilide	661	487	1.36
2,6-Dibromoacetanilide	689	508	1.36
2,6-Dimethylacetanilide	732	--	--

[a]Amide V band obscured by strong absorption near 750 cm^{-1}.

the amide VI' band was accidently degenerate with the amide IV' band in N-methylacetamide-d. Use of the product rule, then, indicated that γ(NH) also made some contribution to the amide VI band.

It should be noted that the order of numbering the amide group modes in this spectral region does not follow their relative frequency positions. The system employed here is that of Miyazawa *et al.* (51) and probably arises from the historical development of the identification of these absorptions.

The position of the amide IV and VI bands in N-monoaryl amides is somewhat less certain than the amide V band. Two absorptions, listed in Table 12-13, of moderate-to-weak intensity are present in the 575-675 cm^{-1} region of these compounds which exhibit some sensitivity to isotopic substitution. The absorption at 620-675 cm^{-1} shifts slightly lower on ^{15}N substitution but is insensitive to deuteration. These observations are consistent with those of other authors (17, 37, 51) for the amide IV vibration and the 620-675 cm^{-1} band is thus assigned to this mode. The fact, though, that this absorption apparently lies at a lower frequency in the para-substituted acetanilides than in the other anilides indicates that certain aromatic modes may make some contribution to this vibration.

The amide VI band is assigned to the absorption at

Table 12-13. Suggested frequencies for the amide IV and amide VI bands in the potassium bromide disk spectra of N-monoaryl amides

Compound	Amide IV band[a] (cm^{-1})	Amide VI band[a] (cm^{-1})
Acetanilide	664(-2.6)	608(-1.9)
Benzanilide	--	585(-4.5)
Hexananilide	675(<1)	575(-5.0)
p-Aminoacetanilide	627	604
p-Bromoacetanilide	629	607
p-Chloroacetanilide	--	610
p-Hydroxyacetanilide	628	606
p-Iodoacetanilide	628	606
p-Methoxyacetanilide	621	610
p-Methylacetanilide	622	608
p-Nitroacetanilide	621(<1)	603(-1.6)
m-Aminoacetanilide	668	591
m-Bromoacetanilide	659	611
m-Chloroacetanilide	658	610
m-Hydroxyacetanilide	666	593
m-Methylacetanilide	664	612
m-Nitroacetanilide	648	608
o-Bromoacetanilide	641	604
o-Chloroacetanilide	651(<1)	606(-2.5)
o-Fluoroacetanilide	656	611
o-Hydroxyacetanilide	667	598
o-Methoxyacetanilide	658	610
o-Methylacetanilide	657	617
o-Nitroacetanilide	652(-1.5)	596(-3.0)
2,6-Dibromoacetanilide	669	611
2,6-Dimethylacetanilide	--	620

[a]Frequency shifts produced by ^{15}N substitution given in parentheses.

575-620 cm^{-1}. It usually shows more sensitivity to ^{15}N substitution than the 620-675 cm^{-1} band but weakens or disappears on deuteration. There are no new absorptions at lower frequencies, except for the amide V' band, in the deuterated compounds to which this band may be correlated. Nor does the amide IV band gain appreciable intensity on deuteration as Miyazawa et al. (51) observed for N-methylacetamide. Thus, the amide VI band must lose considerable intensity on deuteration and either remain at the same position or shift and be obscured by other absorptions. However, since the absorption involving γ(C=O) would probably be somewhat sensitive to deuteration due to coupling with γ(NH), the amide VI vibration is assigned to the absorption at 575-620 cm^{-1} in N-monoaryl amides. The size of the ^{15}N shift, however, indicates that there is some nitrogen motion involved and perhaps γ(O=C-N) would be a more realistic description of the amide VI vibration instead of simply γ(C=O).

A line-chart representation of the spectra of the substituted acetanilides in the 800-300 cm^{-1} region is given in Figure 34. The characteristic amide absorptions are indicated by heavy lines. The order of these absorptions with decreasing frequency is amide V, amide IV and amide VI with the exception of p-chloroacetanilide and 2,6-dimethylacetanilide where no amide IV band was observed.

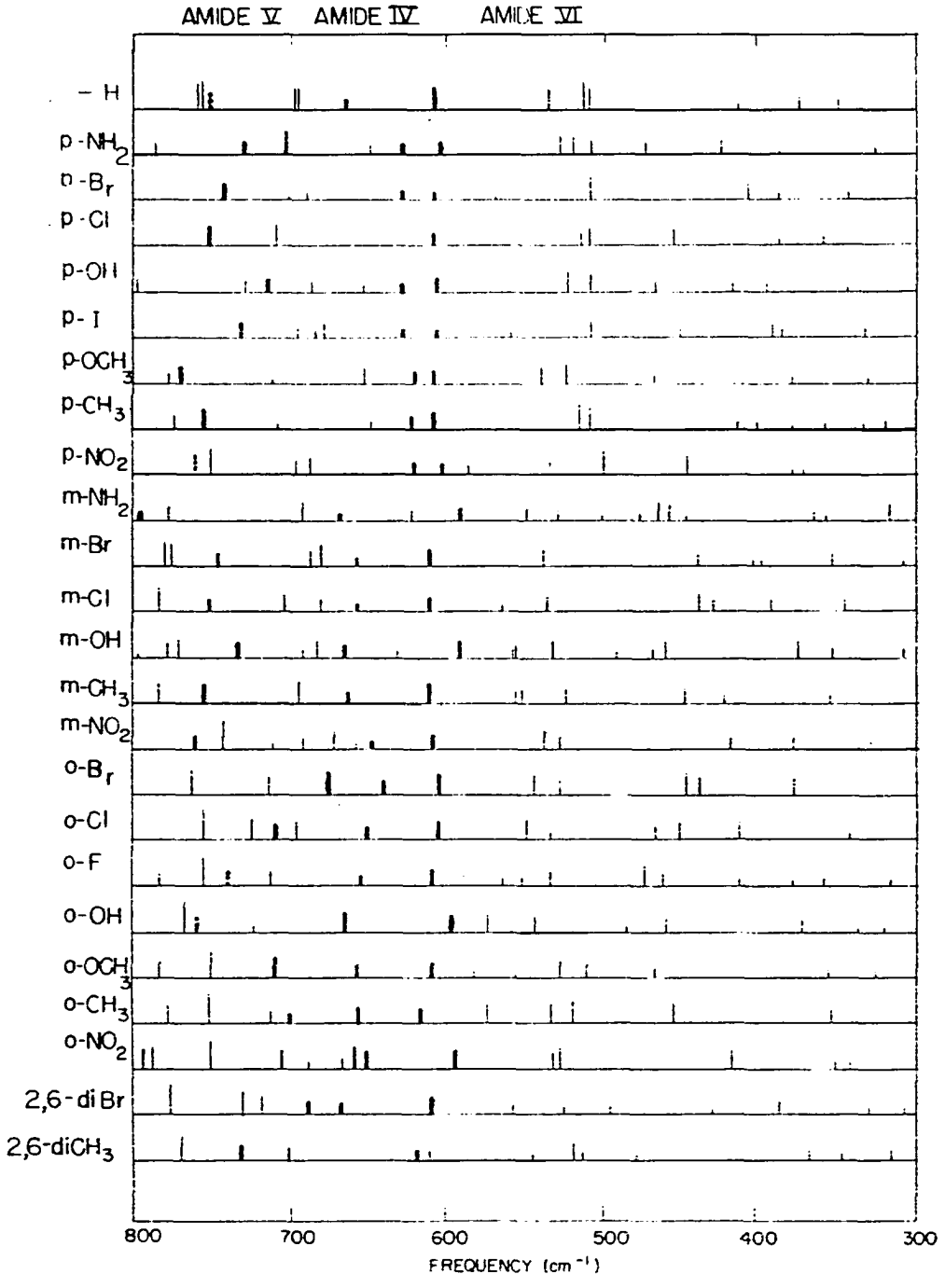

Figure 37. Line-chart representation of the infrared absorptions of substituted acetanilides in the 300-800 cm^{-1} region

ABSORPTIONS CHARACTERISTIC OF THE METHYL, PHENYL AND SUBSTITUENT GROUPS

Most of the absorptions present in the infrared spectra of N-monoaryl amides arise from portions of the molecule other than the -CONH- group. These absorptions are of limited value in correlation studies but a study of them may yield useful information concerning the overall structure of complex amide molecules. Therefore, the absorptions arising from vibrations localized principally in the methyl, phenyl and substituent groups of these compounds merit some consideration for the sake of completeness.

A methyl group should give rise to two C-H stretching, two C-H bending and a planar rocking vibration. In cases where rotational or stereoisomers are present, additional rocking vibrations are often observed. In alkanes, the asymmetric and symmetric stretching vibrations of the methyl group give rise to strong absorptions near 2962 and 2872 cm^{-1} respectively (7, 38). However, when the methyl group is adjacent to an oxygen atom or a carbonyl group, these stretching bands lose considerable intensity (7). The spectra of acetanilides consistently show a weak absorption at 2921-2947 cm^{-1}. Most of the spectra also exhibit a very weak peak at 2840-2869 cm^{-1}. Since these bands consistently appear in the acetanilides and are absent in benzanilide,

they are assigned to $\nu_{as}(CH_3)$ and $\nu_s(CH_3)$, respectively.

The asymmetric and symmetric deformation bands of the methyl group are found in the ranges 1430-1470 cm^{-1} and 1370-1380 cm^{-1}, respectively, when the methyl group is attached to a carbon atom (7, 38). When the methyl group is adjacent to a carbonyl group these absorptions are often found at the lower ends of the above quoted frequency ranges. In all acetanilides, an absorption is present at 1365-1378 cm^{-1} which is insensitive to state and ^{15}N substitution but weakens and shifts 0-15 cm^{-1} lower on deuteration of the amide group. The band is absent from the spectra of $CD_3CONHC_6H_5$ (1) and benzanilide. Aside from the deuteration sensitivity, all the evidence indicates that this absorption arises from $\delta_s(CH_3)$. It is highly probable, however, that the vibrations of the methyl group interact with those of the amide group since the C_8-C_7 (see page 18) bond distance in acetanilide is much shorter than the normal single bond distance (8). In complex molecules, such interactions may have a pronounced effect on the intensity of an absorption without appreciably altering its frequency. Deuteration of the amide group, then, may remove these interactions and permit the absorption to exhibit its normal intensity and frequency.

The location of the asymmetric methyl deformation mode is uncertain. Except for most of the para-substituted

acetanilides, all the anilides studied exhibit a strong and fairly broad absorption in the range 1426-1443 cm^{-1}. The absorption is at the same frequency in the corresponding solution spectra and disappears or weakens on deuteration. This behavior is similar to that of the 1370 cm^{-1} band. However, this strong absorption is also present in benzanilide and in $CD_3CONHC_6H_5$ (1). This, coupled with the absence of a strong absorption in the 1425-1450 cm^{-1} region of para-substituted acetanilides, is fairly strong evidence that the 1426-1444 cm^{-1} band does not arise principally from $\delta_{as}(CH_3)$. Abbott and Elliott (1) have suggested that this absorption might arise from a symmetric stretching vibration of the N-C=O group. However, since the absorption shows little ^{15}N sensitivity and is not present in the spectra of simple aliphatic amides (5, 17, 18, 51) or N-methylbenzamide (58), such an assignment seems unlikely. It is possible that aromatic or skeletal modes make the major contributions to the absorption and that the $\delta_{as}(CH_3)$ is simply obscured by this strong absorption.

A methyl rocking vibration has been identified at 1003-1032 cm^{-1} in a previous section and is tabulated for each anilide in Table 10. In several compounds, notably the para-substituted acetanilides, a weak, broad absorption is present near 1040 cm^{-1}. Miyazawa *et al.* (51) have indicated that there are two absorptions in N-methylacetamide which arise

from rocking vibrations of the carbonyl methyl group and one of these is at 1041 cm^{-1}. Thus it is possible that a second rocking mode occurs in acetanilides near 1040 cm^{-1} but that it is often obscured by aromatic absorptions. This may be further evidence of cis-trans isomerism in acetanilides.

The aromatic nucleus gives rise to the majority of the absorptions present in the infrared spectra of N-monoaryl amides. The absorptions arising from the phenyl ring are usually easily distinguished from the amide group bands as they are generally quite sharp. The observed frequency ranges for the phenyl absorptions which appear consistently in the spectra are listed in Table 14. The exact frequencies and intensities are given in the complete frequency tables in the Appendix. The notation used to describe the vibration type is that of Randle and Whiffen (60) and their assignments as well as those of other authors (25, 36, 71) aided in classifying the observed bands according to the kinds of motions involved.

Most of the aromatic absorptions are completely unaffected by deuteration of the amide group. However, the phenyl bands in the 1400-1650 cm^{-1} region consistently show some rather pronounced changes on deuteration. This is quite evident from the potassium bromide pellet spectra presented in the Experimental section. The two 1600 cm^{-1} bands often invert in intensity and shift lower by several wave numbers

Table 14. Proposed frequency ranges for absorptions characteristic of the phenyl group in N-monoaryl amides

Vibration[a] type	Type of substitution of the phenyl ring				
	Mono	Para	Meta	Ortho	2,6-Di
ν(C-C)	1610±10	1610±11	1609± 8	1604±13	1601
	1591±14	1594±11	1596± 5	1592±14	1587± 4
	1496± 4	1500±14	1485±11	1505±15	1475
	1450± 4	1449±11	1429±22	1450±10	1446
	1304± 3	1400±11	1297±15	1284±13	
		1301±11			
β(C-H)	1179± 1	1180± 8	1171± 6	1186± 6	1167± 1
	1163± 3	1170±10	1162± 3	1159± 4	1148
	1179± 3	1113±10	1081± 8	1129±22	1084±14
	1035± 7	1016±14	1035± 4	1035± 6	
ring	1000± 2		998± 2		
γ(C-H)	980± 3	943±18			
	913±15		904±15	934± 9	910± 8
	848± 1	844±23	864±13	865± 8	
	754± 3	787±36	789±18	760± 8	774± 4
Ø(C-C)	712±15	700±14	688± 8	707± 9	710± 9
	693± 2	650± 2[b]			
		511±12	530± 8	456±11	
	408± 5	428±38	451±13	360±18	378±10

[a] ν(C-C) denotes carbon-carbon stretching; β(C-H) denotes in-plane deformation; ring denotes in-plane C-C-C deformation or ring-breathing vibration; γ(C-H) denotes out-of-plane C-H deformation; Ø(C-C) denotes out-of-plane ring bending or torsional deformation of a C-C bond.

[b] This absorption may be more closely related to an in-plane than an out-of plane C-C deformation.

on deuteration or coalesce into one absorption. The band near 1500 cm^{-1} is often broader and stronger in the deuterated species than in the normal compounds but is usually at the same frequency. The absorptions in the 1390-1460 cm^{-1} region sometimes weaken on deuteration and occasionally shift to higher frequencies and gain intensity. There is no consistency whatsoever in any of these alterations so it is not possible to come to any conclusions as to the causes of these changes. It is probable that they are due to changes in the crystal structure of the solid state since many of these alterations on deuteration are not observed in the solution spectra.

A sharp absorption is present at 1451-1488 cm^{-1} in all the deuterated anilides which looks very much like a phenyl mode. The absorption is usually at the same frequency in solution as in the solid state except for the para-substituted acetanilides where it apparently lies at a lower frequency. Hadzi (30) observed a similar absorption in thiobenzanilide-d. He suggested that the absorption was not directly connected with the hydrogen-bonded thioamide group, but rather with a skeletal mode, interacting with the NH bending vibration or the ν(C-N) mode in the deuterated compound. Such a view is plausible for deuterated anilides since the absorption does exhibit some ^{15}N sensitivity.

Some suggested assignments for substituent-sensitive

phenyl modes in substituted acetanilides are listed in Table 15. These modes are vibrations of the phenyl ring which involve considerable stretching of the C-X bond, where X is the substituent other than the amide group. The designations, "q" and "r", were originally applied to monosubstituted benzenes (60) but the notations are used for the disubstituted compounds in Table 15 for simplicity. The assignments suggested for the "q" mode are relatively certain. However, in many cases it was difficult to distinguish the "r" mode from substituent-insensitive phenyl modes and hence it is probable that some of the assignments for this mode are in error. In cases where no frequency is listed in Table 15, other absorptions are present in the region where the substituent-sensitive mode was expected and probably obscured the "q" or "r" modes.

The absorptions which are characteristic of the nitro group are listed in Table 16. The vibrational modes of the nitro group are the NO_2 symmetrical stretching and deformation, the torsion about the C-N bond, the NO_2 asymmetrical stretching and in-plane rocking of the NO_2 group and the out-of-plane rocking. The NO_2 stretching modes have been previously assigned in nitroacetanilides (59) and nitrobenzene (29, 59, 71). They are easily identified by their strong intensity. There is considerable disagreement, however, over the positions of the remaining nitro group modes. Green et al. (29)

Table 15. Suggested frequencies for substituent-sensitive phenyl modes in substituted acetanilides in potassium bromide disks

Substituent	"q" mode (cm^{-1})	"r" mode (cm^{-1})
p-NH_2	--	846
p-Br	1070	700
p-Cl	1091	702[a]
p-OH	1244	809
p-I	1061	678
p-OCH_3	1246	769
p-CH_3	1210	773
p-NO_2	1113	688 or 849[b]
m-NH_2	1295	--
m-Br	1069	687
m-Cl	1091	705
m-OH	--	797
m-CH_3	1223	--
m-NO_2	1105	672 or 824[b]
o-Br	1046	--
o-Cl	1061	726
o-F	1102	801
o-OH	1242	812
o-OCH_3	1253	784
o-CH_3	1237	779
o-NO_2	1084	689 or 859[b]

[a]This peak observed in p-chloroacetanilide-d.

[b]See text.

Table 16. Observed frequencies of the characteristic nitro group absorptions in nitroacetanilides in potassium bromide disks

Vibrational mode	Frequency (cm^{-1})		
	p-NO_2	m-NO_2	o-NO_2
$\nu_{as}(NO_2)$	1504	1530	1507
$\nu_s(NO_2)$	1347	1352	1344
$\delta_s(NO_2)$ or "r"	849	824	859
"r" or $\delta_s(NO_2)$	688 or 698	672 or 692	689
Non-planar NO_2 rock	534	537	528
Planar NO_2 rock	444 or 378	417 or 377	418 or 351

assigned the strong absorptions in liquid nitrobenzene at 852 and 677 cm^{-1} to the substituent-sensitive phenyl vibration and the NO_2 symmetrical deformation, respectively. Wilcox et al. (71) inverted these two assignments. Nitrogen-15 substitution in nitrobenzene produced a large shift in the 852 and 704 cm^{-1} bands but not in the 677 cm^{-1} band.[1] The 704 cm^{-1} band has previously been assigned (29, 71) to a Ø(C-C) mode. The assignment of Green et al. (29) is preferred

[1]Kniseley, R. N., Iowa State University of Science and Technology, Ames, Iowa. Infrared spectra of nitrobenzene and nitrobenzene-^{15}N. Private communication (1962).

for the 824-859 cm^{-1} band in nitroacetanilides because of the greater sensitivity of its frequency to the position of the nitro group on the phenyl ring. The symmetric NO_2 deformation is very likely to be at 689 cm^{-1} in o-nitroacetanilide but its position is uncertain in the other two compounds.

Green et al. (29) and Wilcox et al. (71) also disagreed on the positions of the nitro rocking modes. Green et al. assigned the moderately intense band at 532 cm^{-1} in nitrobenzene to the non-planar rock and the weak 420 cm^{-1} band to the planar rock. Wilcox et al. inverted these assignments. The reasoning of Green seems more plausible and his assignments are accepted for nitroacetanilides. However, there are two absorptions listed in Table 16 for the planar NO_2 rocking mode and it is not certain which is the correct assignment.

The suggested assignments for some of the vibrations of the methoxy group in o- and p-methoxyacetanilide are listed in Table 17. The assignment of $\nu_{as}(CH_3)$ is uncertain since this mode could also give rise to an absorption appearing near 2965 cm^{-1} in these compounds. Henbest et al. (32), however, have identified an absorption at 2815-2832 cm^{-1} as being characteristic of the $-OCH_3$ group and assigned the band to $\nu_s(CH_3)$. Thus, the assignment indicated in Table 17 for $\nu_s(CH_3)$ is probably correct. The asymmetric methyl deformation mode has been assigned to a band at 1466 cm^{-1} in aniscle (71) and thus the assignment in Table 17 is reasonable.

Table 17. Observed frequencies of the absorptions characteristic of the methoxy group in methoxyacetanilides in potassium bromide disks

Vibrational mode	Frequency (cm^{-1})	
	$p\text{-}OCH_3$	$o\text{-}OCH_3$
$\nu_{as}(CH_3)$	2915	2908
$\nu_{s}(CH_3)$	2837	2837
$\delta_{as}(CH_3)$	1466	1467
$\nu(O\text{-}CH_3)$	1032	1026

Strong absorptions are present in anisoles at 1250 and 1040 cm^{-1} which arise principally from $\nu(\text{Ø-O})$ and $\nu(O\text{-}CH_3)$, respectively. The former absorption is listed in Table 15 as the "q" mode and the latter in Table 17.

The proposed assignments for the absorptions which arise principally from the O-H bond in hydroxyacetanilides are listed in Table 18. The OH stretching band is easily identified since it is a strong and very broad absorption. The frequency listed for $\nu(OH)$ in m-hydroxyacetanilide is only an approximate one since other absorptions present on the envelope of the band obscure the peak. The O-H in-plane deformation is believed to occur near 1200 cm^{-1} phenols (7, 36). The absorptions listed in Table 18 for $\delta(OH)$ are strong and fairly broad as might be expected for such a vibration in

Table 18. Proposed frequencies for the characteristic absorptions of the hydroxyl group in hydroxyacetanilides in potassium bromide disks

Vibration	Frequency (cm^{-1})		
	p-OH	m-OH	o-OH
ν(OH)	3164	3050	3086
δ(OH)	1228	1250	1204
γ(OH)	729	--[a]	724

[a]May be obscured by γ(NH) at 734 cm^{-1}.

the solid state. Alcohols generally exhibit very broad bands in the range 750-650 cm^{-1} which arise from out-of-plane bonded OH deformation modes (7). Jakobsen (36) indicated that this mode gives rise to a very broad, weak absorption near 664 cm^{-1} in the spectrum of solid phenol. The absorptions at 729 and 724 cm^{-1} in p- and o-hydroxyacetanilide are also very broad and very weak. The corresponding absorptions in m-hydroxyacetanilide is possibly obscured by the amide V band at 734 cm^{-1}.

Proposed assignments for three vibrations of the amino group in m- and p-aminoacetanilide are listed in Table 19. The NH_2 stretching modes were discussed in the section on the NH stretching region. The NH_2 scissor and rocking modes are readily identified by their broadness. For p-aminoacetanilide

Table 19. Suggested frequencies for characteristic vibrations of the amino group in aminoacetanilides in potassium bromide disks

Vibration	Frequency (cm^{-1})	
	p-NH_2	m-NH_2
$\nu_s(NH_2)$	3372	3380
NH_2 scissor	1602	1611
NH_2 rock	1131	1130

both bands disappeared on deuteration as expected. An attempt to locate the NH_2 wagging vibration was unsuccessful. There are several weak, broad absorptions in the 400-1000 cm^{-1} region which are affected by deuteration and it was not possible to differentiate the NH_2 wag from the other absorptions present.

SUGGESTIONS FOR FUTURE WORK

There are a number of paths which could be pursued in order to acquire a greater knowledge of the vibrations giving rise to the characteristic absorptions of the peptide linkage. Substitution of oxygen-18 into a compound such as acetanilide may aid in locating and ascertaining the nature of the vibrations giving rise to the amide IV and VI bands. Use of this isotope in acetanilide-d may also be of value in determining the origin of the 1465 cm^{-1} band in this compound.

A thorough study of an anilide, such as oxindole, which exists solely in the cis configuration may be extremely useful. Such a compound would not exhibit an amide II band but rather absorptions would be present which arise principally from δ(NH) and ν(C-N). The absence of strong coupling between these two modes would permit the determination of their natural frequencies and thus assignments suggested for the amide II, II', III and III' bands may be confirmed or discredited.

Valuable information concerning the infrared spectra of certain substituted acetanilides could be obtained by the use of polarized radiation. If the plane of the amide group in ortho disubstituted acetanilides is nearly perpendicular to that of the phenyl ring, the transition moments of ν(NH) and ν(C=O) may be nearly at right angles to those of the

planar phenyl modes. Dichroism studies on o-nitroacetanilide and its deuterium analog may also aid in correlating and assigning their absorptions in the 1300-1600 cm^{-1} region.

There is a great need for additional work in the spectral region below 650 cm^{-1}. Satisfactory assignment of the amide group vibrations and the substituent-sensitive phenyl modes requires a more thorough knowledge of the substituent-insensitive modes. A study of a number of simple disubstituted benzenes may yield this required information. Knowledge of the positions of substituent-sensitive absorptions may be very useful in ascertaining the nature and position of substituents in acetanilides and similar compounds.

The infrared spectra of certain ortho-substituted acetanilides indicate that there are non-bonded interactions, other than steric effects, between the substituent group and the amide hydrogen atom. Similar interactions may occur in other ortho-substituted aromatic compounds, such as anilines, phenols, and benzaldehydes. An infrared study of these compounds may lead to a greater understanding of non-bonding effects.

SUMMARY

The controversial amide I, II, and III bands of secondary amides have been studied in some detail. The amide I band is present near 1660 cm^{-1} in the solid state spectra and near 1700 cm^{-1} in dilute solution. The vibration giving rise to this absorption involves principally stretching of the carbonyl bond. The in-plane deformation of the NH group probably couples with the C-N stretching vibration of the amide group to yield the amide II and III bands at 1480-1570 and 1235-1350 cm^{-1}, respectively. The amide III vibration then couples weakly with the phenyl-nitrogen stretching mode near 1260 cm^{-1}. For the amide II vibration, δ(NH) probably makes a slightly greater contribution than ν(C-N). The amide III band involves δ(NH), ν(C-N) and ν(Ø-N) and may best be described by ν_{as}(C-N-C) coupled with δ(NH). The 1260 cm^{-1} band arises principally from a substituent-sensitive phenyl mode but ν_s(C-N-C) may make a considerable contribution. Upon deuteration, coupling with δ(NH) is removed and the amide II' band near 1400 cm^{-1} probably involves mostly ν_{as}(C-N-C). An absorption at 1270-1330 cm^{-1} is the deuterium analog of the 1260 cm^{-1} band and arises from ν_s(C-N-C) with considerable contribution from motions within the phenyl ring. The δ(ND) vibration is near 1080 cm^{-1} in deuterated anilides.

Other absorptions characteristic of the -CONH- group

have been identified. The so-called amide V band is a medium, broad absorption in the 650-800 cm^{-1} region and is assigned to the out-of-plane NH bending mode. The amide IV band at 620-670 cm^{-1} probably arises from a vibration involving principally δ(O=C-N). An absorption is generally present in anilides at 575-620 cm^{-1}. This absorption is termed the amide VI band and γ(O=C-N) probably makes the major contribution to the vibration.

A number of specific structural proposals have been made. The spectra of o-nitro- and o-hydroxyacetanilide indicate that intramolecular hydrogen bonding occurs in these compounds. There is considerable evidence that non-bonded interactions exist between the substituent and the amide hydrogen in certain ortho-substituted acetanilides. It is also postulated that the plane of the amide group of ortho-disubstituted acetanilides is nearly perpendicular to that of the phenyl ring.

Frequency ranges have been stated for most of the absorptions arising from the phenyl ring and methyl group in substituted acetanilides. Assignments have also been suggested for modes characteristic of the various substituent groups.

BIBLIOGRAPHY

1. Abbott, N. B. and Elliott, A. Proc. Roy. Soc. (London) A234, 247 (1956).

2. Arnall, F. and Lewis, T. J. Soc. Chem. Ind. 48, 159 (1929).

3. Astbury, W. T., Dalgliesh, C. E., Darmon, S. E. and Sutherland, G. B. B. M. Nature 162, 596 (1948).

4. Badger, R. M. and Rubalcava, H. Proc. Natl. Acad. Sci. U. S. 40, 12 (1954).

5. Beer, M., Kessler, H. B. and Sutherland, G. B. B. M. J. Chem. Phys. 29, 1097 (1958).

6. _____, Sutherland, G. B. B. M., Tanner, K. N. and Wood, D. L. Proc. Roy. Soc. (London) A249, 147 (1959).

7. Bellamy, L. J. "The infrared spectra of complex molecules." 2nd ed. New York, N. Y., John Wiley and Sons, Inc. 1956.

8. Brown, C. J. and Corbridge, D. E. C. Acta Cryst. 7, 711 (1954).

9. Buswell, A. M., Downing, J. R. and Rodebush, W. H. J. Am. Chem. Soc. 61, 3252 (1939).

10. _____, _____ and _____. J. Am. Chem. Soc. 62, 2759 (1940).

11. Cannon, C. G. Mikrochim. Acta 1955, 555 (1955).

12. _____. Spectrochim. Acta 16, 306 (1960).

13. Chaplin, H. O. and Hunter, L. J. Chem. Soc. 1938, 375 (1938).

14. _____ and _____. J. Chem. Soc. 1938, 1034 (1938).

15. Darmon, S. E. Discuss. Faraday Soc. 9, 325 (1950).

16. _____ and Sutherland, G. B. B. M. Nature 164, 440 (1949).

17. Davies, M., Evans, J. C. and Jones, R. L. Trans. Faraday Soc. 51, 761 (1955).

18. De Graaf, D. E. and Sutherland, G. B. B. M. J. Chem. Phys. 26, 716 (1957).

19. Dyall, L. K. and Hambly, A. N. Australia J. Chem. 11, 513 (1958).

20. Farquhar, E. L. "Infrared spectra of primary aromatic amides." Unpublished Ph. D. thesis. Ames, Iowa, Library, Iowa State University of Science and Technology. 1962.

21. Fraser, R. D. B. and Price, W. C. Nature 170, 490 (1952).

22. _____ and _____. Proc. Roy. Soc. (London) B141, 66 (1953).

23. Freedman, H. H. J. Am. Chem. Soc. 82, 2454 (1960).

24. Gallagher, K. J. "The isotope effect in relation to bond length in hydrogen bonds in crystals." In Hadzi, D., ed. "Hydrogen bonding." pp. 45-54. New York, N. Y., Pergamon Press. 1959.

25. Garrigou-Lagrange, C., Lebas, J. M. and Josien, M. L. Spectrochim. Acta 12, 305 (1958).

26. Gierer, A. Z. Naturforsch. 8b, 644 (1953).

27. _____. Z. Naturforsch. 8b, 654 (1953).

28. Gray, L. S. "Characteristic infrared absorption frequencies of nitrogen-containing bonds." Unpublished Ph. D. thesis. Ames, Iowa, Library, Iowa State University of Science and Technology. 1958.

29. Green, J. H. S., Kynaston, W. and Lindsey, A. S. Spectrochim. Acta 17, 486 (1961).

30. Hadzi, D. J. Chem. Soc. 1957, 847 (1957).

31. Hauser, C. R. and Renfrow, W. B., Jr. J. Am. Chem. Soc. 59, 121 (1937).

32. Henbest, H. B., Meakins, G. D., Nicholls, B. and Wagland, A. A. J. Chem. Soc. 1957, 1462 (1957).

33. Herz, E. and Wagner, J. Monatsh. 76, 32 (1946).

34. Ikuta, M. Am. Chem. J. 15, 39 (1893).

35. Jacobs, W. A. and Heidelberger, M. J. Am. Chem. Soc. 39, 1448 (1917).

36. Jakobsen, R. J. Wright Air Development Division, Technical Report 60-204. 1960.

37. Jones, R. L. J. Mol. Spectroscopy 2, 581 (1958).

38. Jones, R. N. and Sandorfy, C. "The application of infrared and raman spectrometry to the elucidation of molecular structure." In Weissberger, A., ed. "Technique of organic chemistry." Vol. 9 pp. 247-580. New York, N. Y., Interscience Publishers, Inc. 1956.

39. Katritzky, A. R. and Jones, R. A. J. Chem. Soc. 1959, 2067 (1959).

40. _____ and Lagowski, Mrs. J. M. J. Chem. Soc. 1958, 4155 (1958).

41. Kessler, H. K. and Sutherland, G. B. B. M. J. Chem. Phys. 21, 570 (1953).

42. Klemperer, W., Cronyn, M. W., Maki, A. H. and Pimentel, G. C. J. Am. Chem. Soc. 76, 5846 (1954).

43. Lenormant, H. Ann. Chim. 5, 459 (1950).

44. Letaw, H., Jr. and Gropp, A. B. J. Chem. Phys. 21, 162 (1953).

45. Lord, R. C. and Miller, F. A. Applied Spectroscopy 10, 115 (1956).

46. Mann, J. and Thompson, H. W. Proc. Roy. Soc. (London) A192, 489 (1948).

47. _____ and _____. Proc. Roy. Soc. (London) A211, 168 (1952).

48. Mecke, R. and Mecke, R. Chem. Ber. 89, 343 (1956).

49. Miyake, A. J. Polymer Sci. 44, 223 (1960).

50. Miyazawa, T. J. Mol. Spectroscopy 4, 168 (1960).

51. _____, Shimanouchi, T. and Mizushima, S. J. Chem. Phys. 24, 408 (1956).

52. _____, _____ and _____. J. Chem. Phys. 29, 611 (1958).

53. Mizushima, S., Shimanouchi, T., Nagakura, S., Kuratani, K., Tsuboi, M., Baba, H., and Fujioka, O. J. Am. Chem. Soc. 72, 3490 (1950).

54. Moccia, R. and Thompson, H. W. Spectrochim. Acta 10, 240 (1957).

55. O'Sullivan, D. G. and Sadler, P. W. J. Org. Chem. 21, 1179 (1956).

56. _____ and _____. J. Chem. Soc. 1957, 2839 (1957).

57. Peltier, D., Pichevin, A. and Bonnin, A. Bull. Soc. Chim. France 1961, 1691 (1961).

58. Pinchas, S., Samuel, D. and Weiss-Broday, M. J. Chem. Soc. 1961, 2666 (1961).

59. Randle, R. R. and Whiffen, D. H. J. Chem. Soc. 1952, 4153 (1952).

60. _____ and _____. "The characteristic vibration frequencies of substituted benzenes." In Sell, G., ed. "Molecular Spectroscopy." pp. 111-128. London, England, The Institute of Petroleum. 1955.

61. Richards, R. E. and Thompson, H. W. J. Chem. Soc. 1947, 1248 (1947).

62. Russel, R. A. and Thompson, H. W. Spectrochim. Acta 8, 138 (1956).

63. Sandman, I. Proc. Roy. Soc. (London) A232, 105 (1955).

64. Sheppard, N. "Infrared spectroscopy of hydrogen bonding-band widths and frequency shifts." In Hadzi, D., ed. "Hydrogen bonding." pp. 85-105. New York, N. Y., Pergamon Press. 1959.

65. Shriner, R. L. and Fuson, R. C. "The systematic identification of organic compounds." 3rd ed. New York, N. Y., John Wiley and Sons, Inc. 1948.

66. Smith, A. E. and Orton, K. J. P. J. Chem. Soc. 93, 1249 (1908).

67. Suzuki, I., Tsuboi, M., Shimoanouchi, T. and Mizushima, S. Spectrochim. Acta 16, 471 (1960).

68. Thatte, V. N. and Joglekar, M. S. Phil Mag. (7) 19, 1116 (1935).

69. Thompson, H. W., Brattain, R. R., Randell, H. M. and Rasmussen, R. S. "Infrared spectroscopic studies on the structure of penicillin." In Clarke, H. T., Johnson, J. R. and Robinson, R., eds. "The chemistry of penicillin." pp. 382-414. Princeton, N. J., Princeton University Press. 1949.

70. _____ and Jameson, D. A. Spectrochim. Acta 13, 236 (1958).

71. Wilcox, W. S., Stephenson, C. V. and Coburn, W. C., Jr. Wright Air Development Division, Technical Report 60-333. 1960.

ACKNOWLEDGMENTS

The author would like to express his gratitude to Dr. V. A. Fassel for the assistance provided throughout the course of this investigation and especially for his useful suggestions concerning the preparation of this manuscript.

A special thanks is extended to Mr. Richard N. Kniseley for his most helpful suggestions and cooperation given during this investigation.

The ^{15}N labeled ammonium sulfate was furnished by Drs. F. H. Spedding and J. Powell.

Finally, the author would like to extend a special thanks to his wife, Norma, without whose patience, understanding, and encouragement this investigation could not have been completed.

APPENDIX

In the following tables, the notations in parentheses indicate the intensities of the absorptions relative to that of the amide I band. The meanings of these notations are as follows:

vvs = very, very strong; stronger than amide I band
vs = very strong
s = strong
ms = medium to strong
m = medium
mw = medium to weak
w = weak
vw = very weak
vvw = very, very weak; less than 2% transmission above the base line
sh = shoulder
var = variable intensity; absorption usually disappears on dilution
* = residual absorption due to incomplete deuteration

Table 20. Observed absorption frequencies of acetanilide with frequency shifts produced by ^{15}N substitution

KBr disk		CH_2Br_2 solution		CCl_4 solution	
Frequency (cm^{-1})	Shift (cm^{-1})	Frequency (cm^{-1})	Shift (cm^{-1})	Frequency (cm^{-1})	Shift (cm^{-1})
		3421(m)	-9	3447(mw)	-9
				3400(vvw)	-9
		3353(sh)	-21		
3295(ms)	-10	3324(var)	-10		
3261(sh)	-5	3286(sh)	-2		
3195(mw)	-6	3197(vw)	-5		
3137(mw)	-6	3137(vw)	-13		
3081(sh)	-13				
3063(mw)	-3			3065(vw)	-3
3025(vw)	-5			3033(vw)	-7
2976(vw)	-6				
2932(vw)	-2	2932(vw)	-5	2932(vw)	<1
2860(vw)	-4			2851(vw)	+5
2805(vw)	-10				
1965(vw)	<1				
1950(vw)	<1				
1888(vvw)	<1				
1873(vw)	<1				
1852(vvw)	-2				
1805(vw)	<1				
1743(vw)	<1				
1664(vs)	-1.6	1693(vs)	-1.4	1706(vs)	<1
		1683(sh)	-3	1690(sh)	<1
1649(sh)	+2				
1620(sh)	-1.9	1618(sh)	-2		
1598(s)	<1	1601(s)	<1	1602(ms)	<1
1556(vs)	-7.7	1524(vs)	-10.7	1519(vs)	-9.6
1539(sh)	-8				
1501(m)	<1	1499(ms)	-1.5	1499(ms)	<1
1488(m)	<1	1486(sh)	-1.6	1480(vw)	<1
1446(sh)	<1				
1435(s)	-1.5	1438(vs)	-3.3	1437(s)	-3.6
1392(vw)	<1				
1369(ms)	<1	1368(ms)	<1	1366(mw)	<1
				1321(sh)	<1
1323(s)	-2.7	1313(s)	-3.2	1310(ms)	-2.4
1307(sh)	<1	1301(sh)	<1	1298(sh)	<1

Table 20. (Continued)

KBr disk		CH_2Br_2 solution		CCl_4 solution	
Frequency (cm^{-1})	Shift (cm^{-1})	Frequency (cm^{-1})	Shift (cm^{-1})	Frequency (cm^{-1})	Shift (cm^{-1})
1264(ms)	-1.6	1249(ms)	-3.5	1244(ms)	-2.4
1229(vw)	-3.7				
1180(mw)	<1			1179(vw)	<1
1160(w)	<1	1158(vw)	<1	1158(vw)	<1
1081(w)	<1	1080(w)	-1.3	1078(vw)	<1
1041(mw)	<1	1033(mw)	<1	1034(vw)	<1
1036(sh)	<1				
1013(mw)	<1	1005(mw)	-2.1		
999(mw)	<1	996(sh)	<1		
983(vw)	<1				
961(mw)	-11.1				
953(sh)	-				
907(m)	<1	902(mw)	-1.5	900(vw)	<1
849(w)	<1				
840(w)	-8.3				
759(sh)	<1				
755(vs)	<1	758(s)	<1		
697(sh)	<1				
694(s)	<1	694(s)	<1	692(m)	<1
668(sh)	+1.9				
664(mw)	-2.6				
608(s)	-1.9				
535(s)	-2.9				
512(vs)	<1				
508(sh)	<1				
413(vw)	<1				
372(w)	<1				
348(mw)	<1				

Table 21. Observed absorption frequencies of acetanilide-d with frequency shifts produced by ^{15}N substitution

KBr disk		CH_2Br_2 solution		CCl_4 solution	
(cm^{-1})	(cm^{-1})	(cm^{-1})	(cm^{-1})	(cm^{-1})	(cm^{-1})
		3421(*)	-	3447(*)	-
3295(*)	-				
3071(w)	<1			3067(vw)	-3
3059(sh)	<1			3038(vw)	<1
2969(vw)	-4				
2932(vw)	-3	2932(vw)	-2	2929(w)	+2
2856(vvw)	-			2857(vw)	+4
		2541(mw)	-9	2557(w)	-16
2537(vw)	-4				
2475(sh)	-9				
2424(ms)	-9	2430(w)	-10		
2389(sh)	-31				
1965(vvw)	<1				
1950(vw)	<1				
1887(vvw)	<1				
1847(vw)	-2				
1808(vw)	-1				
1745(vw)	-2				
1640(vs)	+1.8	1686(vs)	<1	1700(vs)	+3.2
				1683(sh)	<1
1599(s)	<1	1600(ms)	<1	1602(ms)	<1
1582(sh)	<1				
1547(*)	-	1523(*)	-	1519(*)	<1
1502(vs)	<1	1499(vs)	<1	1501(s)	-1.8
1488(m)	<1	1488(sh)	<1	1483(w)	-1.7
1473(ms)	-4.8	1465(m)	<1	1466(mw)	-2.8
1444(*)	-	1438(*)	-	1437(*)	-
1416(sh)	-4				
1403(sh)	-13.9	1400(vs)	-19.6	1393(vs)	-14.6
1394(sh)	-				
1366(sh)	<1				
1330(mw)	-2.0	1323(mw)	-1.5	1323(m)	-2.5
		1313(*)	-	1310(*)	-
1315(m)	<1				
1298(vw)	<1			1299(vw)	-2
1265(*)	-	1249(*)	-	1244(*)	-
1227(vw)	-1.0				

Table 21. (Continued)

KBr disk		CH_2Br_2 solution		CCl_4 solution	
Frequency (cm^{-1})	Shift (cm^{-1})	Frequency (cm^{-1})	Shift (cm^{-1})	Frequency (cm^{-1})	Shift (cm^{-1})
1182(w)	<1			1179(vw)	<1
1161(vw)	<1	1157(vw)	<1		
1106(w)	<1			1104(vw)	<1
1085(w)	<1	1084(w)	<1.5	1080(w)	-
1069(mw)	-1.0				
1041(mw)	-	1033(w)	-	1032(vw)	-
1035(sh)	<1				
999(mw)	<1				
980(mw)	<1	967(mw)	<1		
967(vw)	<1				
938(mw)	-8.5				
926(vw)	-6.1				
907(mw)	<1	902(mw)	<1	901(vw)	<1
886(vw)	<1				
848(w)	<1				
828(sh)	<1				
816(w)	-5.3				
760(sh)	<1				
755(vs)	<1	758(vs)	<1		
697(sh)	<1				
695(s)	<1	694(s)	<1	692(mw)	<1
662(w)	-2.2				
556(m)	-3.5				
533(m)	-1.5				
509(ms)	<1				
413(vw)	-2.0				
370(w)	-4.0				
348(mw)	<1				

Table 22. Observed absorption frequencies of benzanilide with frequency shifts produced by ^{15}N substitution

KBr disk		CH_2Br_2 solution		CCl_4 solution
Frequency (cm^{-1})	Shift (cm^{-1})	Frequency (cm^{-1})	Shift (cm^{-1})	(cm^{-1})
		3425(mw)	-6	3449(w)
3344(m)	-8	3352(var)	-	
3303(sh)	<1			
3054(w)	<1			3068(w)
3041(sh)	<1			3035(vw)
1960(vw)	<1			
1940(vw)	<1			
1901(vw)	<1			
1751(vw)	-2			
1722(vw)	<1			
1656(vs)	<1	1678(vs)	<1	1689(vs)
1626(sh)	-1.2			
1620(sh)	<1	1617(vw)	<1	
1600(s)	-1.8	1599(s)	<1	1602(m)
1578(m)	<1	1581(mw)	<1	
1531(vs)	-10.6	1525(vs)	-8.9	1525(vs)
1502(sh)	<1	1500(sh)	<1	1501(sh)
1492(sh)	-2.1	1492(sh)	-1.1	1492(sh)
1449(m)	-1.5	1448(ms)	<1	1449(m)
1439(s)	-4.5	1437(vs)	-3.0	1436(vs)
1393(vw)	<1	1391(vw)	-1	
1323(s)	-1.4	1316(s)	-2.0	1313(ms)
1301(sh)	<1			
1261(ms)	<1	1255(ms)	+2.1	1253(ms)
		1245(sh)	-	1244(sh)
1179(mw)	<1			
1166(mw)	<1			
1114(w)	-6.6	1110(w)	-8	1111(sh)
				1101(w)
1076(mw)	<1	1075(mw)	<1	1074(mw)
1028(mw)	-1.3	1029(mw)	<1	1029(w)
1002(mw)	<1	1002(vw)	<1	
977(w)	<1			
969(sh)	<1			
928(mw)	<1	927(vw)	<1	
910(mw)	-4.1	904(w)	<1	
885(mw)	-8.6	886(w)	-9.0	

Table 22. (Continued)

KBr disk		CH_2Br_2 solution		CCl_4 solution
Frequency (cm^{-1})	Shift (cm^{-1})	Frequency (cm^{-1})	Shift (cm^{-1})	(cm^{-1})
836(vw)	<1			
792(mw)	-2.0	792(vw)	<1	
751(vs)	-1.4	757(ms)	+3.0	
716(s)	<1	711(ms)	<1	711(mw)
691(s)	<1	694(ms)	<1	691(mw)
682(sh)	<1			
651(mw)	-1.5			
617(w)	<1			
585(mw)	-4.5			
511(m)	-1.5			
403(w)	<1			
370(vw)	-2.0			
310(w)	-2.5			

Table 23. Observed absorption frequencies of benzanilide-d

KBr disk (cm^{-1})	CH_2Br_2 solution (cm^{-1})	CCl_4 solution (cm^{-1})
	3424(*)	3451(*)
3346(*)		
3054(w)		3071(w)
3037(sh)		3041(sh)
2962(vw)	2960(vw)	2968(vw)
2927(vw)	2927(w)	2937(w)
2853(w)	2850(w)	2860(w)
	2548(w)	
2539(vw)	2535(sh)	
2482(m)		
2445(sh)		
2382(vw)		
1958(vw)		
1941(vw)		
1900(vw)		
1873(vvw)		
1818(vvw)		
1775(vvw)		
1746(vvw)		
1698(vw)		
1646(vs)	1672(vs)	1690(vs)
1620(sh)	1619(vw)	
1599(s)	1600(ms)	1603(m)
1579(s)	1580(mw)	
1530(*)	1524(*)	1525(*)
1502(s)	1500(s)	1503(ms)
1492(sh)	1491(sh)	1487(sh)
1464(ms)	1463(ms)	1465(mw)
1448(ms)	1448(m)	1449(mw)
1439(*)	1437(*)	1436(*)
1412(vs)	1401(vs)	1394(vs)
1331(sh)	1325(mw)	1324(w)
1318(mw)		
	1316(*)	1313(*)
1300(w)		
1260(*)	1255(*)	1255(*)
1244(vw)	1245(sh)	
1180(w)		
1166(w)		

Table 23. (Continued)

KBr disk (cm^{-1})	CH_2Br_2 solution (cm^{-1})	CCl_4 solution (cm^{-1})
1147(vw)		
1138(vw)		
1106(vw)		1109(sh)
		1101(w)
1077(mw)	1076(w)	1077(w)
1030(mw)	1029(w)	1030(w)
1001(w)	1001(vw)	
983(mw)	975(w)	
979(sh)		
928(mw)	925(vw)	
906(mw)	903(vw)	
876(mw)	877(w)	
845(vw)		
812(vw)		
790(mw)	791(w)	
750(vs)	756(s)	
711(vs)	710(s)	
691(vs)	693(ms)	
679(sh)	684(sh)	
617(vw)		
579(mw)		
483(ms)		
423(vw)		
402(w)		
378(vw)		
309(w)		

Table 24. Observed absorption frequencies of hexananilide with frequency shifts produced by ^{15}N substitution

KBr disk		CH_2Br_2 solution		CCl_4 solution	
Frequency (cm^{-1})	Shift (cm^{-1})	Frequency (cm^{-1})	Shift (cm^{-1})	Frequency (cm^{-1})	Shift (cm^{-1})
		3421(ms)	-7	3444(m)	-8
3307(ms)	-11	3326(var)	-13	3344(var)	-8
3268(sh)	-6				
3203(mw)	-7	3200(var)	-11	3203(var)	-
3146(mw)	-8	3134(var)	-		
3095(mw)	-13				
3062(vw)	<1			3066(w)	<1
3045(sh)	-3				
3026(sh)	-3			3032(w)	-2
2960(sh)	<1	2960(vs)	<1	2964(s)	<1
2935(ms)	<1	2932(vs)	<1	2935(s)	<1
2901(sh)	<1	2872(ms)	<1	2876(m)	<1
2865(m)	<1	2862(m)	<1	2863(m)	<1
2811(vw)	<1				
2737(vw)	<1				
2630(vw)	<1				
1955(vvw)	<1				
1939(vw)	<1				
1876(vvw)	-2				
1860(vw)	<1				
1796(vw)	-2				
1684(sh)	<1				
1668(vs)	-2.5	1690(vs)	<1	1703(vs)	<1
1644(sh)	<1				
1619(sh)	-1.6	1618(sh)	<1		
1605(vs)	-3.6	1599(vs)	+1.8	1604(ms)	<1
		1539(var)	-		
1553(vs)	-6.9	1521(vs)	-8.4	1520(s)	-11.2
1501(s)	<1	1499(mw)	<1	1500(sh)	<1
1483(mw)	<1	1489(sh)	<1	1483(w)	<1
1466(ms)	<1	1466(mw)	<1	1467(mw)	<1
1454(sh)	<1			1461(sh)	-2.0
1444(s)	-2.2	1438(vs)	-2.6	1437(vs)	-3.6
1413(ms)	<1	1420(sh)	<1	1420(sh)	<1
1383(sh)	-1.2	1390(sh)	-		
1376(ms)	<1	1378(mw)	<1	1380(w)	<1
1326(s)	-1.6	1324(sh)	<1	1323(sh)	<1

Table 24. (Continued)

KBr disk		CH_2Br_2 solution		CCl_4 solution	
Frequency (cm^{-1})	Shift (cm^{-1})	Frequency (cm^{-1})	Shift (cm^{-1})	Frequency (cm^{-1})	Shift (cm^{-1})
1305(ms)	-1.9	1310(ms)	-3.1	1307(ms)	-2.6
1300(sh)	-2	1300(sh)	-2	1298(sh)	-1
1259(ms)	-2.1	1245(m)	-3.3	1244(ms)	-4.3
1245(sh)	-2				
1239(sh)	-2.5				
1190(ms)	-2.2			1172(m)	-2.5
1166(vw)	<1				
1114(sh)	-1.7	1105(sh)	<1	1103(mw)	<1
1107(w)	<1	1093(mw)	<1	1092(mw)	<1
1079(vw)	<1	1080(w)	-1.1	1080(mw)	-1.3
1061(vw)	<1				
1052(vw)	<1				
1034(mw)	<1	1030(w)	<1	1031(vw)	<1
1011(vw)	<1				
998(vw)	<1	1000(vw)	<1		
977(vw)	<1	981(sh)	<1		
966(ms)	-8.7	963(w)	-		
960(sh)	-				
898(mw)	<1	901(mw)	<1	900(mw)	<1
847(sh)	<1	855(vw)	<1		
836(mw)	-9.5	832(w)	-		
811(vw)	-				
756(vs)	<1	758(vs)	<1		
727(m)	<1				
691(ms)	<1	695(s)	<1	692(ms)	<1
675(vw)	<1	675(vw)	<1		
597(vw)	<1				
575(vw)	-5.0				
508(m)	<1				
444(mw)	<1				
367(w)	<1				
306(vw)	<1				

Table 25. Observed absorption frequencies of hexananilide-d

KBr disk (cm^{-1})	CH_2Br_2 solution (cm^{-1})	CCl_4 solution (cm^{-1})
	3421(*)	3444(*)
3307(*)		
3269(*)		
3200(*)		
3143(*)		
3079(vw)		3083(sh)
		3070(sh)
3045(vw)		3038(mw)
3027(vw)		
2959(s)	2959(s)	2962(s)
2934(s)	2931(s)	2933(s)
2901(sh)	2871(ms)	2874(m)
2863(m)	2859(ms)	2862(m)
2735(vw)		
2613(vw)		
	2539(mw)	2553(mw)
2502(sh)		
		2479(w)
2461(sh)		
2435(sh)		
2412(ms)	2413(var)	2416(var)
2388(sh)		
1955(vvw)		
1948(vw)		
1874(vvw)		
1858(vw)		
1794(vw)		
1733(vw)		
1672(sh)		
1652(vs)	1687(vs)	1697(vs)
1623(vw)		
1602(s)	1600(s)	1603(s)
1584(sh)		
1554(*)	1521(*)	1520(*)
1501(vs)	1500(s)	1501(vs)
1479(sh)	1489(sh)	1484(w)
1470(s)	1464(s)	1465(s)
1454(vw)		
1445(*)	1438(*)	1437(*)
1425(vs)	1406(vs)	1397(vs)
1413(sh)		

Table 25. (Continued)

KBr disk (cm^{-1})	CH_2Br_2 solution (cm^{-1})	CCl_4 solution (cm^{-1})
1377(mw)	1362(mw)	1369(vw)
1359(mw)		1353(vw)
1341(vw)		1335(vw)
1325(m)	1321(w)	1320(mw)
	1308(*)	1307(*)
1305(m)		
1262(*)	1244(*)	1244(*)
1246(vw)		
1201(mw)		
1180(vw)		1178(w)
1160(vw)		
1114(sh)		
1106(w)	1107(w)	1106(w)
1079(w)	1080(mw)	1080(mw)
1062(sh)		
1055(vw)	1054(vw)	
1034(mw)	1030(w)	1031(vw)
1027(mw)		
1005(w)		1008(w)
996(sh)	999(vw)	998(vw)
979(vw)		977(w)
958(m)	927(vw)	
899(mw)	900(w)	900(w)
887(vw)		
846(w)	852(vw)	
822(vw)		
809(vw)		
756(s)	761(vs)	
728(mw)		
691(ms)	693(ms)	692(ms)
675(vw)	672(vw)	
592(vw)		
563(mw)		
505(m)		
444(w)		
411(vw)		
362(vw)		

Table 26. Observed absorption frequencies of p-aminoacetanilide

KBr disk (cm^{-1})	CH_2Br_2 solution (cm^{-1})
3372(s)	3470(sh)
	3424(m)
	3375(mw)
3290(m)	
3249(sh)	
3186(sh)	
3128(w)	
3064(mw)	
3023(sh)	
2975(vvw)	
2928(vvw)	
2864(vvw)	
2821(vvw)	
1880(vw)	
1667(vs)	1683(vs)
1616(sh)	1623(m)
1602(ms)	1597(mw)
1552(s)	
1514(vs)	1516(vvs)
1456(vw)	
1426(mw)	1423(m)
1371(ms)	1370(m)
	1336(vw)
1322(ms)	1314(mw)
	1278(mw)
1266(s)	1250(ms)
1228(vw)	
1176(w)	
1131(vw)	1129(w)
1090(vw)	1103(w)
1031(vw)	1037(vw)
1016(sh)	1016(vw)
1007(w)	1004(w)
961(w)	
949(vw)	
933(vw)	
867(mw)	

Table 26. (Continued)

KBr disk (cm^{-1})	CH_2Br_2 solution (cm^{-1})
846(sh)	
829(s)	833(m)
785(mw)	
730(mw)	
703(m)	
650(w)	
627(mw)	
604(mw)	
527(ms)	
519(sh)	
507(m)	
472(m)	
424(mw)	
387(vw)	
324(vw)	

Table 27. Observed absorption frequencies of p-aminoacetanilide-d_3

KBr disk (cm^{-1})	CH_2Br_2 solution (cm^{-1})
	3424(*)
3381(*)	3375(*)
3308(*)	
3043(vw)	
2965(vvw)	
2928(vw)	
2860(vvw)	
2813(vvw)	
2586(vw)	2729(vw)
2520(ms)	2672(vw)
	2546(w)
2401(ms)	2535(sh)
2362(ms)	
2161(vw)	
2055(vvw)	
2028(vvw)	
1883(vw)	
1650(vs)	1676(vs)
1642(vs)	
1617(mw)	1624(mw)
1579(vw)	
1552(*)	
1514(vs)	1516(vs)
	1470(sh)
1456(s)	1441(mw)
1440(sh)	
1408(s)	1407(ms)
1361(w)	
1312(mw)	1311(mw)
1249(m)	
1292(m)	
1271(*)	1271(*)
	1261(w)
1230(vw)	
1180(w)	
1157(w)	
1113(mw)	1119(w)
1080(w)	

Table 27. (Continued)

KBr disk (cm^{-1})	CH_2Br_2 solution (cm^{-1})
1032(w)	1035(vw)
1015(vw)	
976(mw)	969(w)
956(vw)	
945(w)	
931(vw)	
850(sh)	
830(s)	837(mw)
826(s)	
775(mw)	
716(mw)	
646(m)	
626(mw)	
554(w)	
508(ms)	
409(mw)	
350(mw)	
299(vw)	

Table 28. Observed absorption frequencies of p-bromoacetanilide

KBr disk (cm^{-1})	CH_2Br_2 solution (cm^{-1})	CCl_4 solution (cm^{-1})
	3419(ms)	3447(mw)
3294(m)	3335(var)	
3260(mw)	3280(vvw)	
3187(mw)	3195(vvw)	
3115(mw)	3117(vvw)	
3053(w)		
2992(vvw)		
2928(vvw)	2928(vw)	
2892(vw)	2894(vvw)	
2850(vw)	2850(vvw)	
2799(vw)		
1897(w)	1889(vw)	
1879(vw)	1872(vvw)	
1825(vw)		
1679(sh)		
1669(vs)	1696(vs)	1710(vs)
1645(sh)	1644(vvw)	
1600(s)		
1586(s)	1590(s)	1592(m)
1532(vs)	1511(vs)	1510(s)
1486(s)	1491(ms)	
1446(sh)	1437(w)	
1395(vs)	1396(s)	1394(s)
1369(m)	1369(m)	1369(w)
1355(sh)	1345(vvw)	
1326(vvw)		
1308(s)	1304(s)	1302(m)
1290(sh)	1289(m)	1287(mw)
1256(ms)	1245(ms)	
1177(w)		
1173(sh)		
1117(vw)	1115(w)	
1105(vw)	1104(vw)	
1070(m)	1073(m)	1075(mw)
1040(w)	1035(w)	
1008(ms)	1009(ms)	
	1001(sh)	
967(w)	956(vvw)	

Table 28. (Continued)

KBr disk (cm^{-1})	CH_2Br_2 solution (cm^{-1})	CCl_4 solution (cm^{-1})
960(sh)		
956(vw)		
943(w)		
844(w)		
832(ms)	832(m)	
820(ms)		
814(sh)		
742(m)		
700(vw)	702(sh)	
689(mw)	691(w)	
629(w)		
607(vw)		
568(vw)		
507(ms)		
406(m)		
387(w)		
341(vw)		
303(vvw)		

Table 29. Observed absorption frequencies of p-chloroacetanilide

KBr disk (cm^{-1})	CH_2Br_2 solution (cm^{-1})	CCl_4 solution (cm^{-1})
	3421(m)	3447(w)
	3395(vvw)	
3304(ms)		
3262(sh)		
3193(mw)		
3128(mw)		
3114(sh)		
3070(w)		
2998(vw)		
2933(vw)	2929(vw)	
2857(vw)	2850(vvw)	
2797(vw)		
1901(mw)	1890(vw)	
1846(vvw)		
1672(sh)		
1665(vs)	1697(vs)	1712(vs)
1647(sh)		
1607(vs)		
1594(vs)	1593(ms)	
1539(vs)	1510(vs)	1506(s)
1489(vs)	1492(ms)	1496(sh)
1447(w)	1438(vw)	
1393(s)	1395(m)	1395(mw)
1370(s)	1369(mw)	1365(mw)
1352(vvw)		
1314(vs)	1304(s)	1303(mw)
1292(m)	1289(mw)	1287(w)
1260(ms)	1245(m)	
1236(w)		
1180(w)	1178(vw)	
1161(ms)		
1118(w)	1115(vw)	
1103(w)		
1091(s)	1094(m)	1095(m)
1041(mw)	1035(vw)	
1016(sh)	1002(w)	
1010(ms)	1012(m)	

Table 29. (Continued)

KBr disk (cm^{-1})	CH_2Br_2 solution (cm^{-1})	CCl_4 solution (cm^{-1})
969(m)	956(vvw)	
946(vw)		
942(vvw)		
845(sh)		
839(vs)		
830(vs)	832(m)	
822(s)		
751(ms)		
709(s)	711(w)	
610(mw)		
513(sh)		
509(ms)		
454(ms)		
387(w)		
358(vw)		
299(vw)		

Table 30. Observed absorption frequencies of p-chloroacetanilide-d

KBr disk (cm^{-1})	CH_2Br_2 solution (cm^{-1})	CCl_4 solution (cm^{-1})
	3421(*)	
3304(*)		
3264(*)		
3120(*)		
2959(sh)		
2928(vw)	2929(w)	
2854(vw)	2850(vw)	
	2540(w)	2556(vw)
2537(vw)		
2410(s)		
2378(sh)		
1901(mw)	1888(vw)	
1675(sh)		
1656(vs)	1693(vs)	1709(vs)
1647(sh)		
1620(vvw)		
1610(*)		
1596(ms)	1594(m)	
1574(w)		
1541(*)	1510(*)	1506(*)
1492(vs)	1493(ms)	1494(m)
1451(vs)	1434(m)	1432(mw)
1441(sh)		
		1394(m)
1383(vs)	1383(s)	1379(m)
1363(sh)	1360(sh)	
1353(sh)		
1329(vw)		
1317(*)	1304(*)	1303(*)
1301(m)	1289(mw)	1287(mw)
1280(vvw)		
1261(*)	1246(*)	
1237(vw)		
1182(w)		1177(w)
1162(m)		
1118(w)	1115(w)	
1104(mw)		
1090(s)	1093(ms)	1094(m)

Table 30. (Continued)

KBr disk (cm^{-1})	CH_2Br_2 solution (cm^{-1})	CCl_4 solution (cm^{-1})
1080(sh)		
1041(mw)	1034(vw)	
	1003(*)	
1010(ms)	1012(m)	
984(ms)	968(w)	973(w)
948(mw)		
941(vvw)		
	917(vw)	
839(vs)		
833(sh)		
828(vs)	833(ms)	
821(s)		
706(s)	709(mw)	
702(ms)		
610(*)		
561(ms)		
510(sh)		
506(s)		
452(s)		
386(w)		
355(vw)		
300(vw)		

Table 31. Observed absorption frequencies of p-hydroxyacetanilide

KBr disk (cm^{-1})	CH_2Br_2 solution (cm^{-1})
	3424(mw)
3330(m)	
3295(sh)	
3256(sh)	
3164(ms)	
3128(sh)	
3114(sh)	
3070(sh)	
3037(sh)	
2930(vw)	
2883(vw)	
2794(vw)	
2712(vw)	
2665(vw)	
2616(vw)	
2586(sh)	
2487(vvw)	
2374(vvw)	
1901(vw)	
1876(vw)	
1852(vw)	
1830(vvw)	
1654(vs)	1687(vs)
1624(vvw)	
1610(ms)	1604(mw)
1564(s)	
1516(sh)	1523(sh)
1507(vs)	1512(vvs)
1442(s)	
1373(m)	1369(mw)
1328(m)	
1302(vvw)	
1281(vvw)	
1261(ms)	
1244(mw)	
1228(s)	
1173(mw)	
1122(vw)	

Table 31. (Continued)

KBr disk (cm^{-1})	CH_2Br_2 solution (cm^{-1})
1108(mw)	
1032(sh)	
1016(mw)	
1009(sh)	
969(mw)	
955(vvw)	
925(vvw)	
857(w)	
838(ms)	834(ms)
809(m)	
797(mw)	
729(sh)	
714(mw)	
686(mw)	685(vs)
652(vw)	
628(w)	
606(mw)	
522(ms)	
507(ms)	
465(w)	
415(vw)	
394(vw)	
342(w)	

Table 32. Observed absorption frequencies of p-iodoacetanilide

KBr disk (cm^{-1})	CH_2Br_2 solution (cm^{-1})	CCl_4 solution (cm^{-1})
	3420(ms)	3446(w)
3307(ms)	3344(var)	
3278(vvw)	3280(var)	
3260(w)		
3184(mw)	3175(var)	
3115(mw)	3105(w)	
3058(w)		
2990(vw)		
2925(vvw)	2928(vvw)	
2849(vw)		
2826(sh)		
2785(vw)		
1889(w)		
1872(vw)		
1814(vw)		
1775(vw)		
1684(sh)		
1670(vs)	1698(vs)	1710(vs)
1639(mw)	1634(vw)	
1602(vs)		
1584(m)	1585(s)	1586(ms)
1534(vs)	1508(vs)	1504(vs)
1486(s)	1487(sh)	
1438(mw)	1438(w)	
1390(s)	1392(s)	1390(s)
1370(ms)	1368(m)	1367(w)
1339(w)	1341(vvw)	
1315(s)	1306(s)	1305(m)
1295(mw)	1289(ms)	1285(mw)
1258(ms)	1245(ms)	
1240(vvw)		
1232(vvw)		
1211(vvw)		
1182(mw)		
1113(w)	1115(w)	
1061(mw)	1061(mw)	1065(w)
1035(w)	1036(vw)	
1015(mw)		
1002(m)	1004(m)	

Table 32. (Continued)

KBr disk (cm^{-1})	CH_2Br_2 solution (cm^{-1})	CCl_4 solution (cm^{-1})
967(mw)	955(vw)	
954(vw)		
840(mw)		
823(vs)		
816(sh)		
732(m)	701(vw)	
696(w)		
684(sh)		
678(mw)	686(w)	
628(vw)		
606(w)		
559(vw)		
507(m)		
450(vvw)		
390(mw)		
384(sh)		
330(vw)		
302(vvw)		

Table 33. Observed absorption frequencies of p-methoxyacetanilide

KBr disk (cm^{-1})	CH_2Br_2 solution (cm^{-1})	CCl_4 solution (cm^{-1})
	3425(m)	3450(mw)
	3324(var)	
3277(sh)	3276(sh)	
3246(m)		
3193(w)	3201(var)	
3133(mw)	3133(var)	
3071(mw)		
3008(mw)		
2964(w)	2960(mw)	
2938(w)	2936(mw)	
2915(vw)	2912(w)	
2837(mw)	2837(mw)	
2043(vw)		
2006(vvw)	2014(vvw)	
1946(vvw)	1943(vvw)	
1931(vvw)		
1911(vw)		
1887(w)	1870(w)	
1861(vw)		
1767(vvw)	1778(vvw)	
1659(vs)	1686(vs)	1700(vs)
1650(sh)		
1621(vw)	1615(sh)	
1605(s)	1597(mw)	
1562(ms)		
1513(vvs)	1512(vvs)	1515(vvs)
1466(m)	1465(mw)	1466(ms)
1459(mw)	1457(sh)	1459(sh)
1441(m)	1442(mw)	1442(w)
1411(m)	1409(mw)	1407(mw)
1369(ms)	1369(mw)	1367(mw)
1352(vvw)		
	1328(sh)	1324(vw)
1321(m)	1307(sh)	
1304(mw)	1302(mw)	1300(mw)
1286(m)		
1246(vs)	1248(vs)	1246(vs)
	1239(sh)	1233(sh)

Table 33. (Continued)

KBr disk (cm^{-1})	CH_2Br_2 solution (cm^{-1})	CCl_4 solution (cm^{-1})
1225(sh)		
1183(sh)		1182(mw)
1176(mw)		1173(vw)
1133(vvw)	1126(vvw)	
1113(mw)	1111(mw)	1111(w)
1042(sh)		
1032(s)	1036(ms)	1043(mw)
1018(sh)	1003(vw)	
1011(sh)	1013(vw)	
970(mw)	959(vw)	
960(vvw)		
956(vvw)		
932(w)	927(vw)	
856(m)	855(sh)	
840(ms)	829(ms)	
835(sh)		
820(m)		
814(sh)		
777(sh)		
769(m)	759(vs)	
7131(vw)		
652(mw)	655(w)	
621(mw)		
610(mw)		
539(ms)		
523(ms)		
467(mw)		
379(w)		
330(w)		

Table 34. Observed absorption frequencies of p-methoxyacetanilide-d

KBr disk (cm^{-1})	CH_2Br_2 solution (cm^{-1})	CCl_4 solution (cm^{-1})
	3425(*)	3450(*)
3246(*)		
3112(vvw)		
3065(vw)		
3006(mw)		
2964(mw)	2959(mw)	
2938(mw)	2935(mw)	
2914(w)	2913(vw)	
2837(mw)	2835(mw)	
2585(vvw)		
	2543(mw)	
2540(vw)		
2485(vvw)		
2443(sh)		
2402(sh)		
2374(s)		
2350(sh)		
2158(vw)		
2049(vw)		
2003(vw)	2007(vvw)	
1940(vvw)	1943(vvw)	
1913(vw)		
1889(w)		
1861(vw)	1868(vw)	
1770(vvw)	1748(vvw)	
1632(vs)	1683(vs)	1695(vs)
1651(sh)		
	1616(w)	
1581(m)	1596(w)	
1544(*)		
1514(vs)	1516(vs)	1514(vs)
1475(ms)		
1465(ms)	1464(mw)	1467(mw)
1456(ms)	1453(sh)	
1441(m)	1442(ms)	1444(mw)
1432(m)		
	1406(*)	1408(*)
1403(s)	1396(ms)	1389(ms)

Table 34. (Continued)

KBr disk (cm^{-1})	CH_2Br_2 solution (cm^{-1})	CCl_4 solution (cm^{-1})
	1386(sh)	
1364(w)	1369(w)	1364(mw)
1352(vvw)		
1310(m)	1299(ms)	1299(mw)
1299(ms)		
1251(s)	1246(vs)	1249(vs)
1224(sh)		1234(w)
1183(sh)		1183(mw)
1177(ms)		1175(mw)
1130(vw)	1125(vvw)	
1114(m)	1112(mw)	1112(w)
1079(mw)		
1041(sh)		
1030(s)	1036(ms)	1043(m)
1013(sh)		
987(ms)	968(mw)	972(m)
956(vw)		
946(mw)	920(vw)	
932(w)		
851(m)		
840(s)	831(ms)	
830(sh)		
819(s)		
812(sh)		
761(ms)	766(mw)	
714(vw)		
652(mw)	656(w)	
622(mw)		
569(m)		
539(ms)		
521(ms)		
465(mw)		
374(vw)		
330(w)		

Table 35. Observed absorption frequencies of p-methylacetanilide

KBr disk (cm^{-1})	CH_2Br_2 solution (cm^{-1})	CCl_4 solution (cm^{-1})
	3423(m)	3448(mw)
	3376(vvw)	
3291(ms)	3324(var)	
3257(sh)	3264(var)	
3188(mw)	3189(var)	
3126(mw)	3133(var)	
3068(mw)		
3049(sh)		
3037(sh)		
3002(vw)		
2969(vw)		
2947(w)		
2922(w)	2925(w)	
2869(vw)	2868(vw)	
2799(w)		
2732(vvw)		
1899(w)	1892(vw)	
1792(vw)		
		1718(sh)
1662(vs)	1689(vs)	1702(vs)
	1615(sh)	
1606(ms)	1594(m)	1593(w)
1550(s)		
1535(vw)		
1511(ms)	1517(vs)	1519(s)
1455(m)	1452(w)	
1443(sh)		
1402(ms)	1404(m)	1402(m)
1379(mw)		
1365(ms)	1368(mw)	1366(mw)
1323(s)	1313(s)	1313(ms)
1304(sh)	1298(mw)	1298(mw)
1264(m)	1248(m)	
1230(vw)		
1210(w)		
1182(w)		
1123(sh)	1120(w)	1122(w)
1114(w)	1110(w)	

Table 35. (Continued)

KBr disk (cm^{-1})	CH_2Br_2 solution (cm^{-1})	CCl_4 solution (cm^{-1})
1041(mw)	1037(w)	
1022(w)	1020(w)	
1014(mw)	1003(w)	
991(w)		
965(w)	958(vw)	
961(sh)		
957(sh)		
938(w)	936(vw)	
852(vw)	853(vw)	
821(vs)	820(m)	
773(sh)	772(vw)	
755(ms)		
708(vvw)	705(vvw)	
648(w)		
622(mw)		
608(m)		
514(s)		
507(sh)		
413(vw)		
400(w)		
378(vvw)		
356(w)		
332(vw)		
317(w)		

Table 36. Observed absorption frequencies of p-methylacetanilide-d

KBr disk (cm^{-1})	CH_2Br_2 solution (cm^{-1})	CCl_4 solution (cm^{-1})
	3423(*)	3448(*)
3291(*)		
3088(vvw)		
3046(vw)		
2999(vvw)		
2973(w)		
2947(mw)		
2924(w)	2925(vw)	
2867(w)	2866(vw)	
2733(vvw)		
2583(vvw)		
	2546(mw)	2556(vw)
2535(vw)		
2472(sh)	2490(vvw)	
2408(ms)	2445(var)	
2374(sh)		
2152(vw)		
1900(w)	1892(vw)	
1793(vw)		
		1718(m)
1658(*)		
1643(vs)	1681(vs)	1697(vs)
1618(ms)	1617(mw)	1619(w)
1575(w)	1593(vw)	
1559(*)		
1517(vs)	1516(vs)	1519(ms)
1470(vs)		
1455(mw)		
1444(sh)		
1428(m)	1433(ms)	1431(mw)
1396(vs)	1389(vs)	1384(s)
1360(mw)	1362(vw)	1360(mw)
1322(*)		
1312(ms)	1312(m)	1312(m)
1290(vvw)		
1265(*)	1249(*)	
1210(vw)		
1183(w)		

Table 36. (Continued)

KBr disk (cm^{-1})	CH_2Br_2 solution (cm^{-1})	CCl_4 solution (cm^{-1})
1121(sh)	1120(w)	1122(w)
1113(mw)	1110(vw)	
1076(mw)		
1041(m)	1037(w)	
1020(vw)	1019(vw)	
992(mw)	990(vw)	
980(mw)	966(w)	
960(vw)		
941(sh)		
938(mw)	933(vvw)	
845(w)	844(vvw)	
829(sh)	830(sh)	
820(vs)	822(mw)	
766(mw)	766(vw)	
707(vw)	705(vvw)	
649(vw)		
622(mw)		
556(m)		
512(s)		
506(sh)		
414(vvw)		
398(w)		
377(vvw)		
354(w)		
333(vw)		
317(w)		

Table 37. Observed absorption frequencies of p-nitroacetanilide with frequency shifts produced by ^{15}N substitution

KBr disk		CH_2Br_2 solution[a]
Frequency (cm^{-1})	^{15}N shift (cm^{-1})	(cm^{-1})
		3413(s)
		3346(vw)
3303(sh)	-5.3	3315(sh)
3277(ms)	-7.8	
3221(mw)	-6.7	
3161(w)	-7.6	
3130(vw)	<1	
3122(sh)	<1	
3095(mw)	-9.1	
3057(sh)	-7.8	
3025(sh)	-4	
2938(vw)	-1.7	
2891(vw)	-12	
2825(vw)	-	
1919(w)	<1	
1780(vw)	<1	
1682(vs)	-3.6	1710(vs)
1619(ms)	-3.9	1613(s)
1598(ms)	<1	1600(s)
1567(s)	-8.0	1535(vs)
1504(vs)	-2.7	1508(vs)
1495(sh)	<1	
1412.5(sh)	-2.0	
1404(m)	-1.9	
1399(sh)	-	
1375(m)	-1.6	
1347(s)	<1	
1333(ms)	<1	
1313(vvw)	-	
1304(s)	-2.2	1303(ms)
1269(s)	-4.6	
1188(sh)	<1	

[a]These data obtained from a saturated solution in 2.5 mm cells.

Table 37. (Continued)

KBr disk		CH_2Br_2 solution[a]
Frequency (cm^{-1})	^{15}N shift (cm^{-1})	(cm^{-1})
1180(mw)	<1	
1113(s)	<1	
1029(w)	<1	1036(w)
1007(m)	-2.4	1001(ms)
966(mw)	-12.8	953(vw)
955(vvw)	-	
866(ms)	-2.8	866(ms)
849(vs)	<1	
832(mw)	-4.4	
816(vw)	<1	
751(s)	<1	
698(m)	-3.4	
688(m)	<1	
621(mw)	<1	
603(mw)	-1.6	
586(mw)	-1.6	
534(mw)	<1	
499(ms)	<1	
444(ms)	<1	
378(w)	-1.4	
370(sh)	<1	

Table 38. Observed absorption frequencies of p-nitroacetanilide-d

KBr disk (cm^{-1})	CH_2Br_2 solution[a] (cm^{-1})
	3420(*)
3303(*)	
3277(*)	
3221(*)	
3133(sh)	
3114(w)	
3093(*)	
2929(vw)	
2888(vvw)	
2832(vw)	
	2537(vw)
2528(vw)	
2475(sh)	
2441(sh)	
2399(ms)	
2167(vvw)	
1920(w)	
1779(vw)	
1686(*)	
1663(vs)	1714(m)
1632(vw)	
1618(*)	
1603(sh)	1615(s)
1595(s)	1598(s)
1562(*)	1535(*)
1508(sh)	
1502(vs)	1508(vs)
1451(ms)	
1400(ms)	
1393(sh)	
1376(sh)	
1341(vs)	
	1303(*)
1301(mw)	

[a]These data obtained from a saturated solution in 2.5 mm cells.

Table 38. (Continued)

KBr disk (cm^{-1})	CH_2Br_2 solution (cm^{-1})
1269(*)	
1180(w)	
1113(ms)	
1079(vw)	
1028(w)	
1013(vw)	
978(m)	968(w)
955(vvw)	
941(vw)	
931(mw)	
863(ms)	
849(vs)	
827(vw)	
815(w)	
751(s)	
694(m)	
688(m)	
621(w)	
604(*)	
585(mw)	
560(mw)	
533(mw)	
496(ms)	
442(m)	
376(mw)	
368(sh)	

Table 39. Observed absorption frequencies of m-aminoacetanilide

KBr disk (cm^{-1})	CH_2Br_2 solution (cm^{-1})	CCl_4 solution (cm^{-1})
	3422(ms)	3448(mw)
3414(mw)		
3380(m)	3465(mw)	
	3380(sh)	
3304(ms)	3337(var)	
3263(sh)	3285(var)	
3220(sh)	3212(w)	
3143(vw)	3143(vw)	
3083(vw)		
3060(sh)		
3036(vw)		
2984(vw)		
2933(vw)	2935(vw)	
2864(vvw)		
2807(vw)		
2751(vvw)		
1931(w)		
1836(vw)		
1810(vvw)		
1781(vvw)		
1740(vw)		
1683(sh)		
1675(vs)	1689(vs)	1701(vs)
1632(sh)		
1611(vs)	1620(vs)	1622(ms)
	1610(sh)	
	1594(mw)	
	1550(var)	
1551(vs)	1531(vs)	
1523(vvw)		
1494(vs)	1494(s)	1495(ms)
1473(vvw)		
1441(s)	1452(s)	1450(ms)
	1437(sh)	
1370(ms)	1370(ms)	1367(m)
	1333(var)	
1325(s)	1323(ms)	1321(m)
1312(mw)	1310(mw)	

Table 39. (Continued)

KBr disk (cm^{-1})	CH_2Br_2 solution (cm^{-1})	CCl_4 solution (cm^{-1})
1295(mw)	1281(vw)	
1268(sh)		
1260(ms)	1248(ms)	
1194(sh)		
1190(mw)		
1165(ms)	1164(ms)	1164(m)
1130(vw)	1107(vw)	
1074(w)	1074(vw)	
1031(w)	1034(w)	
1017(mw)	1012(mw)	
998(mw)	995(w)	
990(w)		
966(w)	960(vw)	
	948(vw)	
910(w)	908(vw)	
851(s)	864(mw)	
	842(vw)	
794(w)		
777(m)	777(m)	
692(ms)	689(m)	
668(w)		
622(mw)		
591(mw)		
548(m)		
529(mw)		
499(vw)		
475(w)		
463(ms)		
456(sh)		
445(vw)		
363(w)		
355(w)		
315(m)		

Table 40. Observed absorption frequencies of m-bromoacetanilide

KBr disk (cm^{-1})	CH_2Br_2 solution (cm^{-1})	CCl_4 solution (cm^{-1})
	3418(m)	3442(m)
		3400(vvw)
3293(ms)	3328(var)	3328(mw)
3246(ms)	3290(var)	3269(sh)
3178(m)	3180(vw)	3183(vw)
3110(mw)	3115(vw)	3122(vw)
3077(mw)		3083(vw)
3058(sh)		
3019(vw)		
2923(vvw)		2933(vvw)
2843(vw)		
2797(vw)		
1933(vw)		
1926(sh)		
1852(vw)		
1816(vvw)		
1777(vvw)		
1741(vw)		
1686(ms)		
1666(vs)	1700(vs)	1713(vs)
		1693(sh)
1648(vvw)		
1601(sh)	1606(sh)	
1591(vvs)	1588(vvs)	1594(vs)
1563(vvw)		
1541(vs)	1516(vs)	1514(s)
1519(sh)		
1474(vs)	1480(vs)	1480(vs)
1428(sh)		
1418(vs)	1417(vs)	1415(s)
1399(sh)	1400(m)	1397(ms)
1373(m)	1371(m)	1369(m)
1335(mw)	1326(vvw)	
1311(ms)	1300(ms)	1299(ms)
1290(sh)		
1282(ms)	1273(ms)	1271(m)
1258(mw)	1246(ms)	1243(ms)
	1239(sh)	1234(ms)

Table 40. (Continued)

KBr disk (cm^{-1})	CH_2Br_2 solution (cm^{-1})	CCl_4 solution (cm^{-1})
1224(mw)		
1168(mw)	1168(w)	1168(w)
1092(mw)	1092(w)	1094(w)
1073(mw)	1071(mw)	1072(mw)
1067(mw)		
1039(w)	1035(w)	1035(vw)
1010(mw)	1004(sh)	
996(ms)	996(m)	
963(mw)	962(vw)	961(vw)
889(mw)		
874(ms)	877(mw)	880(mw)
817(w)		
780(s)	778(s)	
775(s)		
746(mw)		
687(sh)		
680(ms)	681(mw)	681(mw)
659(w)		649(w)
611(m)		
538(m)		
439(mw)		
403(w)		
398(sh)		
352(mw)		
307(vw)		

Table 41. Observed absorption frequencies of m-chloroacetanilide

KBr disk (cm^{-1})	CH_2Br_2 solution (cm^{-1})	CCl_4 solution (cm^{-1})
	3419(ms)	3444(m)
	3383(vvw)	3393(vvw)
3299(m)	3330(var)	3309(var)
3254(m)	3280(var)	3273(var)
3183(mw)	3188(vw)	3193(w)
3120(mw)	3124(vw)	3129(w)
3077(w)		3087(vw)
3060(sh)		3065(sh)
3023(vw)		3025(vvw)
2986(vvw)		
2940(vvw)	2933(vw)	2940(w)
2850(vvw)	2853(vw)	2856(vw)
2797(vw)		
1931(vw)	1932(vw)	1931(vw)
1848(vw)	1848(vw)	
1817(vw)		
1765(vw)	1758(vw)	1759(vw)
1682(sh)		
1671(vs)	1698(vs)	1713(vs)
	1688(var)	1671(var)
1655(sh)		
1608(sh)		1608(sh)
1592(vs)	1594(vs)	1597(vs)
	1535(var)	1540(var)
1540(vs)	1517(vs)	1517(vs)
1529(sh)		
1474(ms)	1482(vs)	1483(vs)
1430(sh)		
1420(s)	1419(s)	1420(s)
1403(sh)	1403(ms)	1402(m)
1370(mw)	1371(mw)	1371(m)
1331(mw)		
	1306(var)	1305(sh)
1310(m)	1299(ms)	1299(ms)
		1284(var)
1281(s)	1272(ms)	1271(m)
		1257(var)
1260(m)	1248(ms)	1246(mw)

Table 41. (Continued)

KBr disk (cm^{-1})	CH_2Br_2 solution (cm^{-1})	CCl_4 solution (cm^{-1})
1229(mw)		1231(w)
1217(sh)		
1165(w)	1165(vw)	1167(vw)
1126(vw)		
1091(mw)	1099(mw)	1099(mw)
	1093(sh)	1094(var)
1074(mw)	1077(mw)	1077(mw)
1039(w)	1035(w)	1037(vw)
1012(mw)	1006(m)	1013(mw)
998(mw)	998(sh)	1000(w)
987(vvw)		
962(mw)	965(vw)	962(vw)
954(sh)		
903(mw)	898(mw)	899(mw)
884(w)	879(mw)	883(w)
870(ms)		875(var)
784(s)	781(s)	
752(mw)		
705(m)	708(mw)	706(mw)
681(m)	683(m)	684(m)
658(w)		661(w)
610(mw)		612(mw)
565(w)		
536(m)		
438(m)		
428(mw)		
392(mw)		
344(mw)		
295(mw)		

Table 42. Observed absorption frequencies of m-chloroacetanilide-d

KBr disk (cm^{-1})	CH_2Br_2 solution (cm^{-1})	CCl_4 solution (cm^{-1})
	3419(*)	3444(*)
3299(*)	3330(*)	3309(*)
3259(*)		
3187(*)		
3129(w)		3120(vw)
3076(vw)		3076(vw)
3058(sh)		
3026(vvw)		3010(vw)
2964(vvw)		
2931(vw)	2933(vw)	
2858(vw)	2853(vw)	
2588(vvw)		
2540(vvw)		
	2542(mw)	2559(w)
	2513(vvw)	2531(vvw)
2516(vw)	2482(sh)	2489(sh)
2470(vw)		
2408(ms)	2425(var)	2419(var)
2377(sh)	2379(sh)	2373(sh)
2173(vvw)		
2150(vvw)		
1932(w)	1931(vw)	1931(vvw)
1871(vw)		
1848(vw)		
1828(vvw)		
1799(vw)		
1760(vw)	1753(vw)	1754(vw)
1734(w)		
1671(*)		
1653(vs)	1688(vs)	1706(vs)
		1685(sh)
	1670(var)	1658(var)
1634(sh)		
1594(s)	1596(vs)	1597(vs)
1572(sh)	1580(sh)	1582(vw)
1541(*)	1518(*)	1516(*)
1485(vs)	1483(vs)	1485(vs)
1442(ms)	1456(ms)	1455(ms)

Table 42. (Continued)

KBr disk (cm^{-1})	CH_2Br_2 solution (cm^{-1})	CCl_4 solution (cm^{-1})
	1439(sh)	
	1416(*)	
		1408(sh)
1401(vs)	1390(vs)	1390(vs)
1363(vw)	1356(sh)	1355(mw)
1330(*)		
1313(*)	1299(*)	1299(*)
1298(vw)		
1282(*)		
1272(ms)	1220(m)	1271(mw)
1261(*)	1248(*)	
1237(sh)		
1228(mw)	1229(mw)	1229(mw)
1215(sh)		
1165(mw)	1167(w)	1167(vw)
1113(vw)	1100(mw)	1100(mw)
1100(vw)		
1075(mw)	1077(m)	1078(mw)
1039(w)	1035(w)	1037(vw)
998(ms)	998(mw)	999(mw)
		985(sh)
977(m)	971(w)	975(w)
967(*)		964(*)
941(mw)		935(vw)
934(sh)	922(w)	917(vvw)
893(m)	890(sh)	891(mw)
881(vw)	878(mw)	884(sh)
		877(var)
783(s)	781(s)	
701(s)	702(mw)	703(w)
682(s)	681(ms)	681(m)
658(mw)		659(vw)
		653(w)
611(*)		
576(m)		
548(ms)		
534(ms)		
437(m)		
427(mw)		
392(mw)		
344(mw)		
295(mw)		

Table 43. Observed absorption frequencies of m-hydroxyacetanilide

KBr disk (cm^{-1})	CH_2Br_2 solution (cm^{-1})
	3421(mw)
3328(m)	
3269(w)	
3207(vw)	
3159(w)	
3061(vw)	
3050(ms)	
2926(vw)	
2806(vw)	
2776(w)	
2716(vvw)	
2650(vw)	
2563(vvw)	
1919(w)	
1828(vw)	
1735(vvw)	
1703(vvw)	
1670(sh)	
1658(ms)	1693(vs)
	1671(m)
1615(vs)	1612(sh)
	1604(vs)
	1543(sh)
1569(ms)	1530(vs)
1525(w)	
1495(vs)	1492(m)
1450(w)	
	1445(vs)
1426(mw)	
1378(ms)	
1349(s)	
1319(sh)	
1283(ms)	1281(mw)
	1269(w)
1250(mw)	
1177(s)	
1159(ms)	
1078(mw)	

Table 43. (Continued)

KBr disk (cm^{-1})	CH_2Br_2 solution (cm^{-1})
1038(sh)	
1032(m)	1015(mw)
998(mw)	999(vw)
962(vw)	966(vw)
918(m)	909(vw)
878(mw)	873(w)
867(mw)	
845(m)	
797(vw)	
778(sh)	
771(m)	770(mw)
734(mw)	
693(w)	695(mw)
683(m)	
666(mw)	
631(vw)	
593(mw)	
558(sh)	
555(w)	
532(m)	
491(vw)	
468(w)	
459(mw)	
374(m)	
351(mw)	
306(vw)	

Table 44. Observed absorption frequencies of m-methylacetanilide

KBr disk (cm^{-1})	CH_2Br_2 solution (cm^{-1})	CCl_4 solution (cm^{-1})
	3421(m)	3447(ms)
	3370(vvw)	3401(vvw)
3291(ms)	3332(var)	3312(var)
3258(sh)	3284(sh)	3281(var)
3195(w)	3218(var)	3219(var)
3144(w)	3148(var)	3149(var)
3113(vw)		
3089(vw)		3085(var)
3055(vw)		3055(w)
3046(sh)		3041(sh)
3004(vvw)		
2985(vvw)		2987(vw)
2933(sh)		2952(sh)
2921(w)	2924(vw)	2928(m)
2861(vw)	2862(vvw)	2860(vw)
2812(vw)		2824(vvw)
2735(vvw)		
1946(w)		1931(vw)
1867(vvw)		1858(vvw)
		1833(vvw)
1774(vw)		1762(vvw)
1664(vs)	1689(vs)	1705(vs)
		1689(sh)
		1677(var)
1651(sh)		
1617(vs)	1612(s)	1615(s)
	1592(ms)	1597(ms)
1569(ms)		
		1558(var)
1547(m)	1530(vs)	1530(s)
1518(vw)		
1492(s)	1488(s)	1489(s)
1445(w)	1450(sh)	1448(sh)
1431(w)		
1422(mw)	1428(ms)	1429(s)
1407(ms)	1405(sh)	1404(sh)
1368(ms)	1368(m)	1367(ms)
1327(ms)	1307(ms)	1307(ms)

Table 44. (Continued)

KBr disk (cm^{-1})	CH_2Br_2 solution (cm^{-1})	CCl_4 solution (cm^{-1})
	1294(ms)	1295(ms)
		1260(var)
1262(ms)	1245(ms)	1240(ms)
1223(vw)		
1169(m)		1169(mw)
1088(w)	1090(vw)	1090(w)
1039(mw)	1035(sh)	1037(w)
1029(sh)	1021(mw)	1021(mw)
1007(mw)	998(w)	998(w)
973(w)	971(vvw)	975(vvw)
968(sh)		962(w)
903(sh)		
894(mw)	896(w)	894(w)
878(ms)	874(sh)	870(vw)
	862(w)	856(vw)
784(ms)	786(ms)	
755(m)	760(mw)	
695(ms)	693(ms)	690(ms)
664(w)		
612(m)		
556(sh)		
551(mw)		
523(mw)		
447(mw)		
421(vw)		
354(w)		
295(w)		

Table 45. Observed absorption frequencies of m-methylacetanilide-d

KBr disk (cm^{-1})	CH_2Br_2 solution (cm^{-1})	CCl_4 solution (cm^{-1})
	3421(*)	3446(*)
3295(*)		3315(*)
3266(*)		
3203(*)		
3145(*)		
3115(*)		
3074(vvw)		3081(*)
3055		3052(sh)
3047		3039(mw)
3030(vvw)		3022(sh)
3003(vvw)		
2983(vvw)		2986(vw)
		2951(sh)
2923(mw)	2925(w)	2926(mw)
2861(w)	2862(vw)	2865(w)
2733(vvw)	2730(vw)	2735(vvw)
	2541(w)	2561(w)
2555(vw)		2553(sh)
2478(sh)		2490(sh)
2446(sh)		
2409(ms)	2450(vw)	2426(var)
2376(sh)		2387(sh)
2344(sh)		
1947(w)		1932(vw)
1872(vvw)		1857(vvw)
		1830(vvw)
1774(vw)		1762(vvw)
1749(vw)		
1709(sh)		
1665(*)		
1640(vs)	1685(vs)	1697(vs)
		1680(sh)
		1657(var)
1655(sh)		
1613(s)	1613(ms)	1613(s)
1586(ms)	1592(m)	1593(ms)
1557(*)		1558(*)
1532(*)	1530(*)	1530(*)
1492(s)	1492(s)	1493(s)
1485(s)	1468(mw)	1469(ms)
1431(*)	1428(*)	1429(*)

Table 45. (Continued)

KBr disk (cm^{-1})	CH_2Br_2 solution (cm^{-1})	CCl_4 solution (cm^{-1})
1419(w)		
		1408(var)
1390(s)	1401(s)	1395(vs)
	1388(sh)	1382(sh)
1361(w)	1361(sh)	1357(mw)
1324(*)	1307(*)	1308(*)
1310(w)		
1297(vw)		
1263(*)		1255(*)
1230(vvw)		
1178(vvw)		
1170(m)		1169(mw)
1149(vw)		
1110(vw)		1108(vvw)
1090(mw)	1090(vw)	1092(w)
1085(sh)		
1040(mw)	1036(w)	1037(w)
1005(*)		
1002(w)		1002(w)
984(w)	968(w)	971(mw)
973(vw)		964(sh)
950(vw)		942(sh)
943(w)		
897(mw)	895(w)	895(w)
891(sh)		
878(ms)	872(sh)	872(vw)
	860(w)	856(vw)
784(vs)	785(ms)	
766(ms)		
695(s)	692(m)	692(ms)
663(w)		
574(m)		
547(sh)		
540(m)		
521(mw)		
447(mw)		
419(vw)		
354(w)		
293(w)		

Table 46. Observed absorption frequencies of m-nitroacetanilide

KBr disk (cm^{-1})	CH_2Br_2 solution (cm^{-1})	CCl_4 solution (cm^{-1})
	3417(m)	3443(w)
	3372(vvw)	
3305(mw)	3344(var)	
3265(mw)	3301(sh)	
3194(w)	3220(vvw)	
3131(w)		
3098(w)		
3080(sh)		
3037(vvw)		
2940(vvw)		
2862(vw)		
2817(vw)		
1969(vw)		
1903(vw)		
1871(vvw)		
1840(vvw)		
1807(vw)		
1777(vw)		
1722(vvw)		
1675(vs)	1706(vs)	1718(vs)
	1686(sh)	
1646(w)		
1611(sh)	1621(mw)	
1601(s)	1593(mw)	
1551(vs)		
1530(vs)	1532(vvs)	
1480(m)	1484(m)	1485(mw)
1432(sh)		1434(mw)
1427(m)	1428(m)	1422(mw)
1415(sh)		
1371(m)		1379(mw)
1352(s)	1353(vs)	1351(s)
1328(ms)	1320(mw)	
1296(ms)	1298(m)	1295(m)
1278(mw)	1278(mw)	
1268(sh)		
1261(ms)	1248(ms)	
1169(sh)		

Table 46. (Continued)

KBr disk (cm^{-1})	CH_2Br_2 solution (cm^{-1})	CCl_4 solution (cm^{-1})
1164(w)		
1105(vw)		
1093(vvw)		
1079(m)	1083(w)	1082(s)
1035(w)	1035(vw)	1035(w)
1018(mw)	1009(mw)	
999(mw)	997(vvw)	
984(mw)	979(vw)	
963(mw)		963(vw)
951(vvw)		953(vw)
934(w)		933(vvw)
919(vw)	912(vvw)	
887(ms)	893(mw)	892(vvw)
	879(mw)	
824(ms)	825(m)	
806(s)		
761(mw)		
743(s)	740(s)	
712(vw)	712(vw)	
692(mw)	694(vw)	
672(m)	677(vw)	
658(vvw)		
648(w)		
608(mw)		
537(m)		
527(sh)		
417(mw)		
377(mw)		
328(w)		

Table 47. Observed absorption frequencies of m-nitroacetanilide-d

KBr disk (cm^{-1})	CH_2Br_2 solution (cm^{-1})
	3417(*)
3306(*)	
3267(*)	
3140(mw)	
3098(mw)	
3081(sh)	
2940(vvw)	
2864(vw)	
2817(vvw)	
	2673(w)
2551(vvw)	
	2540(w)
2500(vvw)	
2475(sh)	
2410(s)	
2378(sh)	
2355(sh)	
2203(vvw)	
2164(vvw)	
2047(vvw)	
1969(vw)	
1904(vw)	
1871(vvw)	
1840(vw)	
1805(vw)	
1777(vw)	
1767(sh)	
1722(vvw)	
1675(*)	
1658(vs)	1697(vs)
1619(mw)	1619(mw)
1603(*)	
1583(mw)	1583(w)
1552(*)	
1530(vs)	1532(vs)
1482(ms)	1484(ms)
1469(mw)	
1458(mw)	1460(mw)
	1438(*)
1403(s)	
1391(s)	1391(m)

Table 47. (Continued)

KBr disk (cm^{-1})	CH_2Br_2 solution (cm^{-1})
1349(s)	1353(vs)
1330(*)	1319(*)
1314(w)	
1298(*)	1298(*)
1289(mw)	1293(w)
1277(mw)	1278(mw)
1264(*)	1249(*)
1234(vvw)	
1169(sh)	
1164(w)	
1097(mw)	
1079(mw)	1082(vw)
1038(w)	1035(vw)
1020(*)	1009(*)
1000(mw)	1000(vvw)
983(m)	978(w)
960(*)	
951(vvw)	
942(vvw)	
927(mw)	930(vw)
918(sh)	912(vw)
889(ms)	892(mw)
	879(mw)
820(ms)	
815(ms)	
804(s)	
744(s)	740(m)
710(vw)	711(vw)
689(mw)	692(vw)
672(ms)	
658(vvw)	
648(w)	
608(*)	
571(m)	
530(ms)	
416(mw)	
376(mw)	
327(w)	

Table 48. Observed absorption frequencies of o-bromoacetanilide

KBr disk (cm^{-1})	CH_2Br_2 solution (cm^{-1})	CCl_4 solution (cm^{-1})
	3408(ms)	3416(m)
3280(ms)		
3257(sh)		
3192(sh)		
3152(vw)		
3105(vw)		
3068(vw)		3075(vw)
3036(vw)		3020(vw)
2992(vvw)		
2934(vvw)	2935(vvw)	2929(w)
		2855(vw)
2825(vvw)		
2777(vvw)		2804(vvw)
1965(vw)		
1923(vw)		
1884(vvw)		
1842(vvw)		
1801(vw)		
1662(vs)	1699(vs)	1713(vs)
1641(sh)		
1591(mw)	1593(s)	1595(ms)
1578(m)	1578(mw)	1579(mw)
1531(s)	1518(vs)	1518(vs)
1510(sh)		1505(sh)
1470(m)	1463(mw)	1464(mw)
1439(ms)	1433(vs)	1433(vs)
1425(mw)	1415(sh)	1408(vw)
1367(m)	1368(mw)	1367(mw)
1298(s)	1299(vs)	1298(vs)
1255(mw)	1241(m)	1239(sh)
1232(w)	1231(m)	1228(mw)
1161(w)	1162(vw)	1162(vvw)
1126(vw)	1124(vw)	1124(vvw)
1121(sh)		
1046(m)	1048(mw)	1048(w)
1029(ms)	1025(s)	1024(ms)
1010(mw)	1002(mw)	998(w)
967(w)	955(vw)	

Table 48. (Continued)

KBr disk (cm^{-1})	CH_2Br_2 solution (cm^{-1})	CCl_4 solution (cm^{-1})
943(mw)	940(w)	938(vw)
861(w)	860(vw)	
848(vw)		
763(s)	756(vs)	
715(m)	710(w)	
676(ms)	686(mw)	686(w)
641(mw)		645(w)
604(ms)		614(w)
544(ms)		
528(mw)		
445(ms)		
437(sh)		
377(ms)		
299(w)		

Table 49. Observed absorption frequencies of o-chloroacetanilide with frequency shifts produced by ^{15}N substitution

KBr disk		CH_2Br_2 solution		CCl_4 solution	
Frequency (cm^{-1})	Shift (cm^{-1})	Frequency (cm^{-1})	Shift (cm^{-1})	Frequency (cm^{-1})	Shift (cm^{-1})
		3417(m)	-9	3430(ms)	-9
				3399(vvw)	-7
				3351(mw)	-10
3271(sh)	-5				
3242(m)	-4				
3197(sh)	-3				
3163(sh)	<1				
3109(w)	-7			3110(vvw)	+5
3077(vw)	+4			3076(w)	<1
3065(vw)	-4			3066(sh)	-3
3044(w)	-12			3037(vw)	-13
2999(vw)	-6				
2935(vw)	+7			2934(vw)	-2
2890(vvw)	-5				
2840(vw)	-2				
2796(vw)	-16				
1950(vw)	-2			1948(vw)	<1
1914(vw)	<1			1912(vw)	<1
1882(vw)	<1			1876(vvw)	<1
1853(vvw)	-5				
1836(vvw)	<1			1835(vw)	-3
1813(vvw)	<1				
1802(vw)	-4			1792(w)	<1
1682(sh)	<1				
1664(vs)	-1.5	1701(vs)	-1.2	1712(vs)	-1.7
1587(s)	-2.4	1594(s)	<1	1596(s)	<1
		1584(sh)	-1.6	1584(sh)	-1.2
1545(sh)	-5				
1531(vs)	-7.6	1520(vs)	-11.4	1519(vs)	-6.9
				1506(sh)	<1
1475(m)	<1	1467(mw)	<1	1467(mw)	<1
1440(s)	-1.2	1436(vs)	-2.5	1436(vs)	-2.5
1420(mw)	<1	1420(sh)	<1	1413(sh)	<1
1368(m)	<1	1368(mw)	<1	1368(m)	+1.8
1302(vs)	-4.0	1303(vs)	-5.7	1303(vs)	-5.6

Table 49. (Continued)

KBr disk		CH_2Br_2 solution		CCl_4 solution	
Frequency (cm^{-1})	Shift (cm^{-1})	Frequency (cm^{-1})	Shift (cm^{-1})	Frequency (cm^{-1})	Shift (cm^{-1})
1281(sh)	-2.0	1281(sh)	<1	1284(sh)	<1
1258(mw)	-1.2	1244(m)	-2.0	1242(ms)	-2.4
1235(vw)	<1			1227(ms)	<1
1161(vw)	<1			1161(vw)	<1
1128(mw)	<1	1130(vw)	<1	1130(w)	<1
1061(s)	<1	1058(m)	<1	1057(ms)	<1
1036(ms)	<1	1036(m)	<1	1036(ms)	<1
1011(mw)	-1.8	1002(mw)	<1	1000(mw)	-1.4
967(w)	-11.0	955(vw)	-[a]	953(vw)	-[a]
941(mw)	<1	940(w)	<1	939(w)	<1
861(mw)	<1			860(vw)	<1
849(w)	-7.5				
756(vs)	<1	757(vs)	+2.7		
726(ms)	<1	720(w)	<1		
710(mw)	<1	704(w)	<1	707(mw)	-2.3
698(mw)	-1.4				
651(mw)	-1.0			652(w)	-1.6
606(mw)	-2.5				
550(ms)	-1.8				
534(w)	<1				
465(mw)	<1				
451(m)	<1				
413(m)	<1				
342(w)	<1				
298(vw)	-2.0				

[a]Probably obscured by 940 cm^{-1} band.

Table 50. Observed absorption frequencies of o-chloroacetanilide-d with frequency shifts produced by ^{15}N substitution

KBr disk		CH_2Br_2 solution		CCl_4 solution	
Frequency (cm^{-1})	Shift (cm^{-1})	Frequency (cm^{-1})	Shift (cm^{-1})	Frequency (cm^{-1})	Shift (cm^{-1})
		3417(*)	-	3430(*)	-
3283(w)	-8				
3197(*)					
3163(*)					
3077(vw)	-5			3076(vw)	<1
3065(vw)	-2			3066(sh)	-3
3048(vw)	-			3037(vw)	-13
2934(vw)	-6	2933(vvw)	<1	2935(vvw)	-3
2853(vw)	<1				
2581(vw)	-9				
		2536(mw)	-13	2542(mw)	-9
				2512(vvw)	-
2502(sh)	-16				
2464(sh)	-10				
2424(ms)	-15			2440(w)	-
2397(sh)	-9				
2355(vw)	-14				
2323(vw)	-9				
1964(vw)	<1			1948(vw)	<1
1924(vw)	<1			1912(vw)	<1
1878(vw)	-3			1876(vvw)	<1
1846(vvw)	-4			1830(vw)	-2
1802(vw)	-2			1793(vw)	<1
1649(vs)	<1	1695(vs)	<1	1706(vs)	<1
1592(ms)	<1	1592(ms)	<1	1594(ms)	<1
1573(ms)	<1	1583(sh)	<1	1585(sh)	<1
				1577(w)	<1
1529(*)	-	1518(*)	-	1518(*)	-
1488(vs)	-3.6	1486(vs)	-2.4	1487(vs)	-3.6
1448(m)	<1	1449(mw)	-1.9	1451(mw)	<1
1441(*)	-	1437(*)	-	1438(*)	-
1404(vs)	-15.4	1384(vs)	-8.0	1382(vs)	-8.0
1390(sh)					
1344(w)	-10	1357(m)	-7.4	1356(m)	-10.1
1303(*)	-	1303(*)	-	1304(*)	-
1283(vw)	+6.2	1291(mw)	<1	1291(mw)	<1

Table 50. (Continued)

KBr disk		CH_2Br_2 solution		CCl_4 solution	
Frequency (cm^{-1})	Shift (cm^{-1})	Frequency (cm^{-1})	Shift (cm^{-1})	Frequency (cm^{-1})	Shift (cm^{-1})
1273(mw)	-2.0	1279(sh)	<1		
1264(*)	-	1243(*)			
1233(w)	-1.4			1229(mw)	-1.1
1161(mw)	<1			1162(vw)	<1
1130(mw)	<1	1131(vvw)	<1	1131(vw)	<1
1094(m)	-2.5	1087(mw)	-1.6	1086(mw)	-2.2
1048(m)	<1				
1036(m)	<1	1035(m)	<1	1035(mw)	<1
979(m)	-2.4	969(w)	-3.9	966(mw)	-3.8
943(mw)	<1	941(w)	<1	939(w)	<1
932(w)	-7.9				
860(mw)	<1			860(vw)	<1
832(mw)	-7.2				
761(vs)	<1	757(s)	<1		
724(m)	<1	718(w)	<1		
693(ms)	-1.6				
648(mw)	-1.2			651(w)	-1.3
612(sh)	<1				
607(mw)	-3.7				
545(ms)	-2.2				
502(ms)	-1.5				
460(m)	<1				
449(m)	<1				
408(m)	<1				
338(w)	<1				
298(vw)	<1				

Table 51. Observed absorption frequencies of o-fluoroacetanilide

KBr disk (cm^{-1})	CH_2Br_2 solution (cm^{-1})	CCl_4 solution (cm^{-1})
	3424(ms)	3450(ms)
	3378(vvw)	3396(vvw)
3285(sh)	3321(var)	3333(var)
3249(ms)	3280(sh)	
3195(sh)	3212(vvw)	
3136(mw)	3125(var)	3129(var)
3069(mw)		3075(w)
3051(sh)		3048(w)
3033(sh)		
2997(sh)		
		2967(sh)
2938(vw)	2935(vvw)	2936(w)
2867(vw)		2851(vw)
2820(vw)		
1944(vw)		1940(vw)
1908(vw)	1906(vw)	1900(vw)
1877(vvw)		
1794(vw)	1790(vw)	1784(vw)
	1752(vw)	1752(vw)
1685(sh)		
1666(vs)	1696(vs)	1712(vs)
		1694(var)
1617(s)	1619(s)	1622(s)
1606(sh)	1594(mw)	1596(s)
1573(vvw)	1565(vw)	1565(vw)
1547(vs)	1523(vs)	1523(vs)
1506(mw)		
1492(ms)	1481(ms)	1481(ms)
1457(s)	1453(vs)	1453(vs)
1442(sh)	1439(sh)	1439(sh)
1430(sh)	1427(sh)	1422(sh)
1370(ms)	1369(m)	1370(ms)
1320(s)	1321(s)	1320(s)
	1307(sh)	1307(sh)
1286(mw)	1285(mw)	1286(m)
1282(sh)		
1268(ms)	1258(s)	1257(s)
1248(mw)	1235(m)	1232(ms)

Table 51. (Continued)

KBr disk (cm^{-1})	CH_2Br_2 solution (cm^{-1})	CCl_4 solution (cm^{-1})
1212(vw)		
1197(ms)		1192(m)
1155(w)	1156(vw)	1156(vw)
1129(vvw)		
1109(sh)		
1102(ms)	1100(ms)	1100(ms)
1062(vw)	1057(vw)	1057(vw)
1035(m)	1033(m)	1034(m)
1018(mw)	1002(mw)	1000(mw)
968(mw)	956(vw)	953(vw)
961(sh)		
938(mw)	935(w)	933(mw)
880(vvw)		
853(mw)	841(vw)	842(w)
801(mw)	800(m)	
783(sh)		
756(vs)	757(vs)	
714(mw)		
656(w)		655(w)
611(mw)		
564(w)		
522(w)		
534(mw)		
473(ms)		
462(mw)		
412(vw)		
378(vw)		
359(w)		
316(vw)		

Table 52. Observed absorption frequencies of o-hydroxyacetanilide

KBr disk (cm^{-1})	CH_2Br_2 solution (cm^{-1})
3403(ms)	3405(mw)
3086(mw)	3096(m)
2980(w)	
2935(vw)	2933(vw)
2885(w)	
2854(sh)	2856(vw)
2744(mw)	
2719(sh)	
2618(w)	
2492(vw)	
1954(vw)	
1906(vw)	
1784(vw)	
1660(vs)	1664(vs)
1632(vvw)	
1614(mw)	
1595(ms)	1601(s)
1545(s)	1524(s)
1529(sh)	
	1497(vs)
1456(s)	1453(w)
1433(sh)	
1393(sh)	
1383(m)	
1371(sh)	
1333(m)	1317(m)
1286(s)	
1253(ms)	
1242(ms)	
1204(mw)	
1182(vw)	
1162(vw)	
1107(m)	1097(mw)
1040(m)	1042(w)
1019(mw)	1012(w)
968(mw)	962(vw)
933(w)	930(w)
881(vw)	881(vw)

Table 52. (Continued)

KBr disk (cm^{-1})	CH_2Br_2 solution (cm^{-1})
862(vvw)	
844(mw)	836(mw)
812(w)	808(w)
768(vs)	757(s)
724(vw)	
667(m)	
598(mw)	
575(m)	
558(vw)	
544(mw)	
485(w)	
459(mw)	
373(mw)	
336(vvw)	
320(vvw)	

Table 53. Observed absorption frequencies of o-methoxyacetanilide

KBr disk (cm^{-1})	CH_2Br_2 solution (cm^{-1})	CCl_4 solution (cm^{-1})
	3419(ms)	3439(m)
		3387(vvw)
3282(sh)		
3251(ms)		
3193(vw)		
3136(w)		3132(vvw)
3087(vw)		3092(vvw)
3061(mw)		3071(vw)
3023(vw)		3016(w)
2967(w)	2967(vw)	2966(w)
2946(vw)	2943(w)	2948(w)
2935(sh)		2937(sh)
2908(vw)	2908(vw)	2907(vw)
2837(vw)	2838(w)	2839(vw)
2818(vvw)		
2621(vvw)		
2568(vvw)		
2506(vvw)		
2038(w)		
1929(vw)		
1887(vw)		
1845(vw)		
1804(vvw)		
1763(vvw)	1775(vw)	
1659(vs)	1688(vs)	1701(vs)
1649(sh)		
1603(sh)		
1596(m)	1600(s)	1601(ms)
1547(ms)	1525(vs)	1527(vs)
1523(sh)		1521(sh)
1496(m)	1484(s)	1483(m)
1467(m)		
1460(m)	1460(vs)	1460(vs)
1449(sh)		
1435(mw)	1433(s)	1434(s)
1369(m)	1368(m)	1367(mw)
1324(m)	1333(m)	1332(mw)
1291(m)	1290(ms)	1291(mw)

Table 53. (Continued)

KBr disk (cm^{-1})	CH_2Br_2 solution (cm^{-1})	CCl_4 solution (cm^{-1})
1272(mw)		
1253(s)	1254(s)	1252(s)
	1238(mw)	1233(mw)
1223(mw)		1218(ms)
1180(mw)	1177(w)	1177(mw)
1161(w)		
1145(vvw)		
1119(ms)	1117(s)	1118(ms)
1049(mw)	1048(ms)	1050(mw)
1026(s)	1030(s)	1033(ms)
	1004(w)	
965(mw)	957(w)	955(vw)
960(sh)		
925(mw)	928(w)	926(vw)
857(w)		
843(w)		
784(mw)	782(mw)	
752(s)	753(vs)	
711(m)		
658(mw)		
610(mw)		
583(w)		
556(vw)		
527(m)		
511(sh)		
467(w)		
356(w)		
325(vw)		

Table 54. Observed absorption frequencies of o-methylacetanilide

KBr disk (cm^{-1})	CH_2Br_2 solution (cm^{-1})	CCl_4 solution (cm^{-1})
	3435(sh)	3461(mw)
	3418(mw)	3439(sh)
	3371(sh)	3398(vw)
3253(sh)	3312(var)	3332(var)
3225(mw)		
3186(vw)		
3117(sh)		
3065(sh)		3065(w)
3033(w)		3029(w)
2983(vw)		2983(vw)
2956(vw)		
2930(vw)	2938(vw)	2933(w)
2858(vw)	2859(vw)	2862(vw)
2808(vw)		
2735(vvw)		
1957(vw)		
1913(vw)		
1872(vvw)		
1835(vvw)		
1791(vvw)		
1657(vs)	1691(vs)	1705(vs)
	1678(var)	1692(var)
1628(sh)		
1604(mw)	1604(vw)	
1587(w)	1588(ms)	1592(mw)
1538(s)	1517(vs)	1520(s)
1529(sh)		
1499(sh)		
1490(ms)	1495(sh)	1486(sh)
1459(mw)	1452(vs)	1452(s)
1439(m)		
1427(sh)		
1380(sh)	1379(sh)	1380(sh)
1367(m)	1368(ms)	1366(mw)
1308(sh)	1330(w)	1321(vw)
1301(s)	1304(ms)	1304(ms)
1284(mw)	1292(sh)	1294(sh)
1274(ms)	1257(s)	1256(m)

Table 54. (Continued)

KBr disk (cm^{-1})	CH_2Br_2 solution (cm^{-1})	CCl_4 solution (cm^{-1})
1237(vw)	1231(w)	1229(mw)
1198(w)		
1120(mw)	1116(mw)	1116(w)
	1047(mw)	1050(w)
1041(m)	1036(mw)	1036(w)
		1015(sh)
1013(mw)	1002(mw)	1003(w)
972(mw)	955(vw)	
965(sh)		
939(w)	939(vw)	938(vw)
935(sh)		
872(vw)	864(vw)	
856(w)	856(vw)	
779(m)	775(sh)	
753(vs)	758(s)	
714(mw)	714(mw)	714(w)
657(mw)		
617(mw)		
575(m)		
534(m)		
520(ms)		
455(ms)		
353(mw)		
294(w)		

Table 55. Observed absorption frequencies of o-methylacetanilide-d

KBr disk (cm^{-1})	CH_2Br_2 solution (cm^{-1})	CCl_4 solution (cm^{-1})
	3418(*)	3461(*)
3230(*)		
3105(vw)		
3066(sh)		3068(sh)
3031(mw)		3033(w)
2985(vw)		2982(sh)
2957(w)		
2930(w)	2932(vw)	2934(mw)
2858(vw)	2862(vw)	2858(w)
2814(vvw)		
2732(vvw)		
	2553(sh)	2565(w)
	2540(mw)	2554(sh)
	2496(w)	2518(vw)
2406(sh)	2445(var)	
2385(s)		
2355(sh)		
2330(sh)		
2157(w)		
2065(vw)		
2017(vw)		
1957(vw)		
1918(vw)		
1870(vvw)		
1845(vvw)		
1786(vvw)		
1658(*)		
1641(vs)	1686(vs)	1699(vs)
		1685(sh)
1615(sh)		
1603(sh)	1603(m)	1605(mw)
1580(mw)	1584(mw)	1592(sh)
1534(*)	1517(*)	1520(*)
1499(sh)		
1492(ms)	1495(s)	1496(ms)
1466(ms)	1462(sh)	1465(sh)
	1446(m)	1451(ms)
1438(*)		

Table 55. (Continued)

KBr disk (cm^{-1})	CH_2Br_2 solution (cm^{-1})	CCl_4 solution (cm^{-1})
	1397(sh)	
1407(s)	1388(vs)	1382(vs)
1380(sh)		
	1358(m)	1356(mw)
1303(*)	1304(*)	1304(*)
1280(mw)	1291(mw)	1293(mw)
1276(*)	1256(*)	1256(*)
1237(*)		
1197(w)		
	1127(w)	1125(vvw)
1119(w)	1120(w)	1116(vw)
1078(w)	1065(sh)	
	1047(m)	1049(w)
1040(m)	1036(m)	1035(w)
	1002(*)	1003(*)
	974(sh)	
990(mw)	968(mw)	964(w)
	939(w)	937(vw)
933(m)	919(vw)	
868(w)	864(vw)	
852(vw)		
778(ms)	773(sh)	
749(vs)	757(vs)	
712(mw)	713(mw)	
657(mw)		
620(w)		
574(m)		
545(mw)		
520(s)		
454(s)		
350(w)		
294(w)		

Table 56. Observed absorption frequencies of o-nitroacetanilide with frequency shifts produced by ^{15}N substitution

KBr disk		CH_2Br_2 solution		CCl_4 solution	
Frequency (cm^{-1})	Shift (cm^{-1})	Frequency (cm^{-1})	Shift (cm^{-1})	Frequency (cm^{-1})	Shift (cm^{-1})
3372(ms)	-9	3374(mw)	-11	3371(ms)	-9
3089(vw)	-1	3088(vw)	-13		
2935(vvw)	+4				
2001(vw)	-1				
1965(vvw)	-4				
1925(vvw)	-2				
1875(vvw)	-1				
1835(vw)	-4				
1798(vw)	<1				
1701(vs)	-1.5	1708(vs)	<1	1717(vs)	<1
1668(vw)	-4.0				
1610(s)	<1	1609(ms)	<1	1611(s)	<1
1585(s)	-2.4	1587(ms)	-2.4	1588(vs)	-2.4
1555(vw)	-2.6				
1541(w)	-6.8	1525(sh)	+3	1532(mw)	+3.7
1530(vw)	-				
				1510(sh)	-2.8
1507(s)	-6.0	1498(vs)	-4.3	1501(vs)	-1.7
1456(mw)	<1	1456(mw)	-2.1	1457(ms)	-1.7
1434(sh)	<1				
1426(mw)	-2.3	1433(ms)	-5.3	1432(ms)	-5.4
1371(mw)	<1	1367(mw)	<1	1368(mw)	<1
1344(ms)	-2.0	1339(s)	-2.7	1338(s)	-3.1
1319(vw)	<1	1316(w)	<1	1316(mw)	<1
1307(vvw)	-5.2				
1279(sh)	<1				
1274(m)	-3.3	1279(ms)	-4.4	1278(ms)	-4.6
1234(m)	-1.3	1231(m)	-2.0	1227(ms)	-3.0
1228(sh)	-4				
1180(vw)	<1				
1163(mw)	<1	1165(w)	-1.8	1165(mw)	<1
1149(ms)	<1	1148(mw)	<1	1149(ms)	<1
1084(w)	-1.7	1084(w)	-1.8	1082(w)	<1
1041(m)	<1	1043(w)	<1	1042(w)	<1
1003(mw)	<1	1001(w)	<1	1001(mw)	-3
967(vw)	<1	958(vw)	<1	957(vw)	<1

Table 56. (Continued)

KBr disk		CH_2Br_2 solution		CCl_4 solution	
Frequency (cm^{-1})	Shift (cm^{-1})	Frequency (cm^{-1})	Shift (cm^{-1})	Frequency (cm^{-1})	Shift (cm^{-1})
872(w)	<1			872(vw)	<1
859(ms)	-1.8	858(mw)	-2.0	858(m)	-1.8
836(mw)	-7.4	836(vw)	-	837(vw)	-
795(ms)	<1				
789(ms)	<1	784(mw)	<1		
752(vs)	<1	748(s)	-4.0		
707(ms)	<1				
689(w)	-1.7				
668(sh)	<1				
661(ms)	-2.5				
652(mw)	-1.5				
596(m)	-3.0				
533(sh)	<1				
528(ms)	<1				
418(m)	<1				
351(w)	<1				
341(sh)	<1				

Table 57. Observed absorption frequencies of o-nitroacetanilide-d

KBr disk (cm^{-1})	CH_2Br_2 solution (cm^{-1})	CCl_4 solution (cm^{-1})
3372(*)	3373(*)	3371(*)
2505(ms)	2510(mw)	2508(m)
2002(w)		
1965(vw)		
1928(vvw)		
1875(vvw)		
1833(vw)		
1798(w)		
1696(vs)	1707(vs)	1710(vs)
1657(sh)		
1612(ms)	1610(ms)	1612(s)
1585(*)	1587(*)	1588(*)
1574(m)	1575(mw)	1575(w)
1540(sh)		
1519(s)	1515(vvs)	1522(vs)
1508(*)	1499(*)	1501(*)
1480(mw)	1483(mw)	1485(ms)
1455(*)	1456(*)	1456(*)
1445(vw)	1448(vw)	1447(vw)
1426(*)	1432(*)	1432(*)
1382(m)	1378(s)	1375(vs)
1361(vvw)	1360(mw)	1358(mw)
1339(ms)	1337(ms)	1336(vs)
1306(m)	1306(ms)	1307(m)
1277(m)	1276(s)	1275(vs)
1229(mw)	1234(w)	1230(m)
1168(mw)		1168(mw)
1151(mw)	1151(mw)	1151(mw)
1093(w)	1093(vw)	1091(w)
1043(m)	1046(mw)	1046(mw)
970(mw)	970(w)	968(w)
917(w)		
873(w)		873(vvw)
857(ms)	858(mw)	857(mw)
826(vw)		
793(s)		
790(s)	784(mw)	
750(vs)	746(ms)	

Table 57. (Continued)

KBr disk (cm^{-1})	CH_2Br_2 solution (cm^{-1})	CCl_4 solution (cm^{-1})
706(m)		
686(vw)		
665(sh)		
660(*)		
652(mw)		
598(mw)		
533(m)		
487(ms)		
418(m)		
351(mw)		
340(sh)		

Table 58. Observed absorption frequencies of 2,6-dibromoacetanilide

KBr disk (cm^{-1})	CH_2Br_2 solution (cm^{-1})	CCl_4 solution (cm^{-1})
	3402(m)	3432(mw)
	3368(sh)	3393(vw)
3223(ms)	3289(var)	
3182(sh)	3194(sh)	
3120(sh)		
3073(w)		
3053(sh)		
3019(mw)		
2975(vw)		
2947(vvw)	2932(vvw)	
2847(vvw)		
2801(vw)		
1945(vw)	1937(vw)	
1875(vw)	1865(vw)	
1807(vw)	1788(vw)	
1664(vs)	1702(vs)	1722(vs)
		1707(sh)
	1625(vw)	
1583(vw)		
1567(sh)		
1559(ms)	1555(m)	
1520(s)	1481(s)	1474(s)
1481(vvw)	1460(sh)	1458(sh)
1446(ms)	1446(mw)	
1430(ms)	1430(ms)	1426(mw)
1371(ms)	1368(mw)	1367(mw)
	1316(mw)	1307(mw)
1290(ms)	1237(m)	1227(ms)
1283(sh)	1264(mw)	1258(m)
1252(w)		
1243(sh)		
1212(vvw)		
1197(mw)		
1168(vvw)		
1148(w)	1149(w)	1150(vw)
1074(sh)		
1070(mw)	1073(mw)	1074(w)
1040(w)	1036(w)	
1015(mw)	1001(mw)	

Table 58. (Continued)

KBr disk (cm^{-1})	CH_2Br_2 solution (cm^{-1})	CCl_4 solution (cm^{-1})
978(sh)		
970(mw)	968(vw)	
902(vvw)		
861(w)		
777(vs)	776(s)	
732(ms)	728(s)	
719(m)		
689(mw)		
669(mw)		
611(mw)		
558(mw)		
526(vw)		
496(vw)		
430(vvw)		
387(mw)		
329(vw)		
306(vw)		

Table 59. Observed absorption frequencies of 2,6-dibromoacetanilide-d

KBr disk (cm^{-1})	CH_2Br_2 solution (cm^{-1})
	3400(*)
3227(*)	
3184(*)	
3073(vw)	
3019(*)	
2960(sh)	2960(vw)
2927(mw)	2928(mw)
2855(w)	2854(w)
2559(vvw)	
	2526(mw)
2496(vvw)	
2459(vvw)	
2397(sh)	
2372(ms)	2420(var)
2198(vvw)	
1945(vw)	1936(vvw)
1874(vvw)	1865(vvw)
1806(vvw)	1789(vvw)
1658(vs)	1701(vs)
1649(sh)	
1624(sh)	1629(vw)
1585(vw)	
1568(mw)	
1553(m)	1554(mw)
1520(*)	1481(*)
1457(s)	1452(ms)
1433(m)	1434(m)
1397(s)	1377(ms)
1360(vw)	
	1348(mw)
	1317(w)
1289(*)	1237(*)
	1265(mw)
1257(vw)	
1244(w)	
1197(mw)	
1164(vvw)	
1148(w)	1151(w)

Table 59. (Continued)

KBr disk (cm^{-1})	CH_2Br_2 solution (cm^{-1})
1100(w)	
1074(w)	1073(w)
1041(w)	1037(vw)
1015(*)	1001(*)
992(mw)	979(vw)
973(vw)	
933(w)	
904(vvw)	
845(w)	
804(vvw)	
776(vs)	775(s)
730(ms)	727(s)
718(m)	
663(ms)	
615(mw)	
556(m)	
538(mw)	
508(mw)	
478(mw)	
387(mw)	
329(w)	
305(w)	

Table 60. Observed absorption frequencies of 2,6-dimethylacetanilide

KBr disk (cm^{-1})	CH_2Br_2 solution (cm^{-1})
	3416(m)
	3371(w)
3237(ms)	3310(var)
3189(sh)	
3135(vw)	
3049(mw)	
2982(w)	
2956(vw)	
2923(w)	2928(w)
2854(vw)	2857(w)
1921(vw)	
1856(vw)	
1817(vvw)	
1783(vw)	
1674(sh)	
1651(vs)	1681(vs)
1626(sh)	1628(vvw)
1601(w)	
1591(w)	1593(w)
1575(vvw)	
1540(s)	1490(sh)
1475(m)	1479(s)
1468(sh)	
1443(mw)	1441(mw)
1430(sh)	
1385(vvw)	1375(m)
1373(m)	1370(sh)
	1332(mw)
1305(ms)	1248(m)
1289(w)	1297(vvw)
1272(vw)	1268(mw)
1257(vw)	
1212(w)	
1166(w)	
1098(w)	1096(w)
1045(mw)	1037(w)
1014(w)	1004(w)
996(vvw)	

Table 60. (Continued)

KBr disk (cm^{-1})	CH_2Br_2 solution (cm^{-1})
973(w)	
964(mw)	968(vvw)
917(w)	917(vw)
893(vvw)	
853(vw)	853(vw)
770(ms)	777(s)
732(mw)	
702(mw)	701(w)
620(w)	
612(sh)	
546(vw)	
519(mw)	
513(sh)	
480(vvw)	
368(w)	
347(vvw)	
316(w)	
282(vw)	